Florida A & M University - Florida State University
College of Engineering
Department of Civil and Environmental Engineering

ACCELRATED CURING OF SILICA FUME CONCRETE

Final Report
Contract No. BD-488
CFDA No. 52009

Submitted By
Nur Yazdani, Ph.D., P.E.
Saif Haroon, Ph.D.
Martine Fils-Aime, M.S.

Submitted to the

Florida Department of Transportation

May 2005

DISCLAIMER

The opinions, findings, and conclusions expressed in this publication are those of the authors and not necessarily those of the State of Florida Department of Transportation or the USDOT.

Technical Report Documentation Page

1. Report No.	2. Government Accession No.	3. Recipient's Catalog No.
BD-488		

4. Title and Subtitle	5. Report Date
Accelerated Curing of Silica Fume Concrete	April 30, 2005
	6. Performing Organization Code 6120-591-39
7. Author(s) Nur Yazdani, Ph.D., P.E., Martine Fils-Aime	8. Performing Organization Report No. 6120-591-39
9. Performing Organization Name and Address FAMU-FSU College of Engineering Civil and Environmental Engineering Department 2525 Pottsdamer St. Tallahasse FL 32310	10. Work Unit No. (TRAIS) 11. Contract or Grant No. BD-488
12. Sponsoring Agency Name and Address Florida Department of Transportation 605 Suwannee Street Tallahassee, FL 32399-0450	13. Type of Report and Period Covered 14. Sponsoring Agency Code

15. Supplementary Notes
Prepared in cooperation with the US Department of Transportation and Federal Highway Administration

16. Abstract
Silica fume is a common addition to high performance concrete mix designs. The use of silica fume in concrete leads to increased water demand. For this reason, Florida Department of Transportation (FDOT) currently allows only a 72-hour continuous moist cure process for concrete containing silica fume. Accelerated curing has been shown to be effective in producing high-performance characteristics at early ages in silica-fume concrete. However, the heat greatly increases the moisture loss from exposed surfaces, which may cause shrinkage problems. This experimental study was undertaken to determine the feasibility of steam curing of FDOT concrete with silica fume in order to reduce precast turn around time. Steam curing durations of various lengths were utilized. The concrete compressive strength, surface resistivity and shrinkage (both in small samples and full scale samples) were determined for various durations of steam curing. Results indicate that steam cured concrete silica fume concrete met all FDOT requirements for the 12, 18 and 24 hours of curing periods. All steam cured samples demonstrated excellent durability up to 1 year age. No shrinkage cracking was observed in any samples up to one year age. It is recommended that FDOT allow the first 12 – 24 hours duration steam curing for silica fume concrete, followed by continuous curing for the remaining period of 72 hours.

17. Key Word	18. Distribution Statement
Silica fume, microsilica, accelerated curing, steam curing, bridge piles, shrinkage, durability	No restriction This report is available to the public through the National Technical Information Service, Springfield VA 22161

19. Security Classif. (of this report)	20. Security Classif. (of this page)	21. No. of Pages	22. Price
Unclassified	Unclassified	128	

ACKNOWLEDGEMENTS

The project investigators would like to appreciate the FDOT for providing them with research grant to conduct this important research work. Mr. Ghulam Mujtaba, Mr. Micheal Bergin and Mr. Charles Ishee of the State Materials Office deserves special acknowledgement for the extensive technical advice during the course of the research work. Thanks are also due to Mr. Mario Paredes for assistance with the Surface Resistivity testing at the State Corrosion Laboratory. The assistance provided by Dr. Saif Haroon, Mr. Badre Enam and Mr. Mike Pratt during the experimental phase of this study are gratefully acknowledged.

EXECUTIVE SUMMARY

Silica fume (SF) is probably the most common addition to concrete mixtures to produce high-performance concrete. This material, also called microsilica, is a finely powdered amorphous silica that is highly pozzolanic. It contains large amounts of silicon dioxide and consists of extremely fine particles. The extremely fine particles can fill spaces between cement particles, which results in a more refined microstructure and a more dense cement paste. Due to its high specific surface area, the use of silica fume in concrete leads to increased water demand. For this reason, Florida Department of Transportation (FDOT) only allows a 72-hour continuous moist cure process for concrete containing silica fume.

Accelerated curing has been shown to be effective in producing high-performance characteristics at early ages in silica-fume concrete (PCI Committee on Durability 1994). However, the heat greatly increases the moisture loss from exposed surfaces, which tends to cause more shrinkage problems. Since silica fume has shown to accelerate cement hydration, when using accelerated curing with silica-fume concrete, the minimum amount of heat necessary for the required strength gain should be used, and the concrete should be allowed to attain initial setting prior to commencing accelerated curing.

The proposed study was geared towards experimental verification of the feasibility of steam curing of FDOT concrete with SF. The study investigated the possibility of speeding up the curing process of such concrete through steam curing. The effects of such curing on the desired properties of hardened concrete were also investigated. In this study, concrete containing SF was mixed at the laboratory and at Gulf Coast Prestress, Inc. in Mississippi. They were steam cured for 12, 18, and 24 hours above the allowable temperatures, and then moist cured for 60, 54, and 48 hours, respectively. The laboratory specimens were tested for compressive strength,

surface resistivity, and shrinkage. While the field specimens were tested for compressive strength and shrinkage. The experimental results indicated that silica fume concrete that was steam cured for 12 hours and then moist cured for 60 hours would meet the desired strength and permeability, with the least amount of shrinkage occurring within the concrete. Therefore, if the silica fume concrete is steam cured for 12 hours at temperatures below the allowable stated in FDOT specification 450-10-7, and then cured for additional 60 hours using the methods described in FDOT specification 450-10-6, all strength and durability requirements will be met. Also, if the ideal steam curing cycle is followed, steam curing for times exceeding 12 hours would also be feasible and economical.

By replacing the current 72-hour moist curing cycle with a 12-hour steam curing cycle on a precast bed and an additional 60–hour curing period off the precast bed as specified in FDOT specification 450-10-6, the concrete precast industry can increase the rate of production of concrete elements containing silica fume by six times.

TABLE OF CONTENTS

LIST OF TABLES

LIST OF FIGURES

LIST OF ABBREVIATIONS

The following abbreviations are used in this report:

$(CF)_H$ = humidity correction factor

d = cylinder diameter

H = relative humidity, %

L = shrinkage at age x

L_i = initial micrometer reading of specimen at time of removal from mold

L_x =micrometer reading of specimen at age x

M_s = surface moisture of aggregate, %

R = resistance

t = time in days after initial curing

V = resultant potential difference between to inner electrodes

W'_a = weight of aggregate to weigh out, kg (lb)

W'_{ssd} = saturated-surface-dry weight of aggregate, kg (lb)

W'_w = weight of total water, kg (lb)

$(\varepsilon_{sh})_t$ = shrinkage strain at anytime t after the recommended ages

$(\varepsilon_{sh})_u$ = ultimate shrinkage strains

ρ = cell constant for resistivity measurements of concrete cylinders

Chapter 1

Introduction

1.1 Brief History of Silica Fume

Silica fume, also known as microsilica, has been used as a concrete property enhancing material and as a partial replacement for portland cement for over twenty-five years. Before the mid-1970's, nearly all silica fume was discharged into the atmosphere. Due to environmental concerns, it became economically justified to use silica fume in various applications. Norcem, a cement production group in Norway, performed the first major placement of ready-mixed silica fume concrete in the United States for chemical attack resistance in 1978. The Corps of Engineers undertook the first major project using silica fume concrete in 1983. Investigations on the performance of silica fume in concrete began in the Scandinavian countries, particularly in Iceland, Norway, and Sweden, with the first paper being published by Bernhardt in 1952 (ACI 1997).

Silica fume is a byproduct in the production of silicon metal or ferrosilicon alloys. Silicon metal and alloys are produced in electric furnaces using raw materials such as quartz, coal, and woodchips. The smoke, condensed gases, that results from the furnace is known as silica fume. Silica fume for use in concrete is available in slurry or dry forms (ACI 1997). The wet form of silica fume is known as *slurried silica fume*. Slurried silica fume contains 42 to 60 percent silica fume by mass. The dry forms of silica fume are available as-*produced* silica fume, *densified* silica fume, and *pelletized* silica fume. As-produced silica fume is the fine powder collected directly from the furnace. Densified silica fume is also known as compacted silica fume. This form is normally used in place of the as-produced silica fume, since the dust

associated with as-produced silica fume is reduced due to the densification process of the silica fume. Pelletized silica fume is the least used form of silica fume. The as-produced silica fume is pelletized by mixing the silica fume with a small amount of water on a disk pelletizer. Pelletized silica fume is used with portland cement clinker to form a blended cement. In either form, silica fume is a very reactive pozzolan when used in concrete due to its fine particles, large surface area, and the high silicon dioxide content (ACI 1997).

There are many effects on the properties of fresh and hardened concrete when silica fume is used along with fly ash and chemical admixtures such as the high range water-reducing admixture and sulfonated melamine formaldehyde condensate. In fresh concrete, silica fume affects the water demand and slump. The water demand of concrete containing silica fume increases with the increased amounts of silica fume, due primarily to the high surface area of the silica fume (Scali, Chin, and Berke 1987). Fresh concrete containing silica fume is more cohesive and less prone to segregation than concrete without silica fume (ACI 1997). Since silica fume is used with other admixtures, such as water-reducing or high-range water-reducing admixtures, the slump loss is actually due to the change in chemical reactions. Silica fume is also known to affect the time of setting and bleeding of fresh concrete. When concrete containing silica fume hardens, the mechanical properties differ from concrete not containing silica fume. Mechanical properties of silica fume concrete, such as creep and drying shrinkage, have been known to be lower then that of concrete without silica fume (ACI 1997). Silica fume plays a significant role in the compressive strength of concrete. At 28 days, the compressive strength of silica fume concrete is significantly higher than concrete without silica fume. Silica fume is also linked to the decrease of permeability, chemical attack resistance, and enhancement of the chloride ion penetration resistance of concrete (ACI 1997).

1.2 Problem Statement

Silica fume concrete normally has low water-to-cementitious material ratios and experiences little bleeding. The surface of silica fume concrete tends to dry quickly, subsequently causing shrinkage and cracking prior to final setting. This is one reason why early-age moist curing of silica fume-concrete is important. Immediately after placement, steps must be taken to prevent drying of the surface (Ozyildirim 1991).

For a given concrete, the curing conditions play a major role in the strength development of the concrete as it matures over time. Curing requirements are established to provide the necessary moisture and temperature conditions in the field for adequate strength development after concrete placement. ACI Committee 308 on Curing of Concrete (ACI 2000) simply states that curing is necessary for the development of both strength and durability. There are no special curing requirements for low water-to-cementitious ratio concretes.

There are several ways to cure concrete in the field. One form of curing that has become popular at precast prestressed concrete plants is accelerated curing. This type of curing is advantageous where early strength gain in concrete is important or where additional heat is required to accomplish hydration, as in cold weather (CAC 2004). Accelerated curing reduces costs and curing time in the production of precast members resulting in economic benefits (Theland 2003).

A primary concern with accelerated curing is the potential for increased moisture loss during the curing process, as mentioned in the ACI 517.2R (1992). Another concern is the possible detrimental effect on long-term concrete properties from high temperatures. There is limited available information on how accelerated curing affects silica fume concrete. Some problems in strength gain have been noted in precast silica fume concrete members cured under

accelerated conditions (Holland 1989). These problems were resolved, however, simply by allowing the concrete to attain initial setting prior to beginning the accelerated curing process. Accelerated curing has been shown to be effective in producing high-performance characteristics at early ages in silica fume concrete (PCI Committee on Durability 1994). However, the heat from the high temperatures greatly increases the moisture loss from exposed surfaces, which tends to cause more shrinkage problems and a reduction in the ultimate strength (Memphis 2004). Therefore, when using accelerated curing with silica fume concrete, the minimum amount of heat necessary for the required strength gain should be used, and the concrete should be allowed to attain initial setting prior to commencing accelerated curing.

Prolonged curing of silica fume concrete has been recommended to ensure optimum results. Over curing has been advocated because of the importance of curing in these silica fume mixtures in which the water-to-cementitious ratio is typically quite low (Holland 1989). The Prestressed Concrete Institute (PCI) specifically recommends over curing high-performance concrete that contains silica fume (PCI Committee on Durability 1994). There has also been a tendency to be on the safe side, since the body of knowledge on how to cure silica fume concrete most effectively and efficiently is limited (Ayers and Khan 1994).

The Florida Department of Transportation (FDOT) Standard Specifications 346 allows the use of silica fume in concrete as 7 to 9% replacement of cementitious material, together with the usage of high range water reducing admixture (FDOT 2004). The silica fume must meet the requirements of ASTM C 1240 specifications (ASTM 1240). Typically, silica fume is used in FDOT higher concrete classes such as Class V and VI for increased strength and durability. These FDOT concrete classes have been tested and approved to meet specified strength, workability, durability, and several other requirements to be considered as high strength concrete

classes. Stated in ACI Report 363R, high strength concrete has economic advantages when used in columns of high-rise buildings, parking garages, bridge decks, and other installations requiring improved density, lower permeability, and increased resistance to freeze-thaw and corrosion (ACI 1997).

FDOT Specifications 450-10.8 modifications, effective January 2004, specify extended moist curing requirements for silica fume concrete. Immediately after finishing, curing blankets must be applied to all exposed surfaces and saturated with water. The moist curing must continue for a minimum of three days. Immediately afterwards, two coats of curing compound must be applied and the surfaces kept undisturbed thereafter for a minimum of seven days. This extensive curing procedure means extra expense and delays on the part of the precast yards. Although not allowed by FDOT, the process may be sped up through employing accelerated curing techniques. ASTM C-684 accelerated curing methods involving elevated temperature water use or high temperature and pressure method are not convenient for large precast prestressed elements (ASTM 684). However, use of steam curing for silica fume concrete is convenient, and would mean significant economic savings and convenience for precasters and FDOT. With a maximum probable steam curing time of 24 hours, the precast concrete products could be turned around at a significantly faster rate, resulting in economic benefits. It is known that steam curing results in more complete hydration of the pozzolanic materials, resulting in increased strength gain of concrete. The increased cost of the curing process is more than offset by the savings in curing time and extra productivity.

1.3 Goals and Objectives

The objective of this study was to verify the feasibility of steam curing of FDOT concrete with silica fume. The study investigated the possibility of speeding up the curing process of such concrete through steam curing. The effect of such curing on several desired properties of hardened concrete were also investigated.

The following objectives were accomplished during this study:

- Review of published information on silica fume and high performance concrete, various relevant standards, steam-curing technology, various properties of silica fume concrete, and their relationship to the curing process.
- Steam curing of various laboratory samples and representative full-scale pile samples of silica fume concrete for various durations using an FDOT approved mix design.
- Determination of the relevant properties of the steam cured silica fume concrete at various ages.
- Determination of whether steam curing allows silica fume concrete to attain or surpass the compressive strength, permeability, shrinkage and cracking properties of currently practiced moist cured silica fume concrete.
- Determination of the effect of the duration of steam curing on the properties of silica fume concrete.
- Examine any physical effect of accelerated curing on FDOT silica fume concrete, such as potential shrinkage cracking at early ages.
- Proposition of modifications/revisions to current FDOT standards.

Chapter 2

Background Review

2.1 Introduction

Since its introduction to concrete in the late 1970's, silica fume has played a major role in the advancement of high performance concrete. Silica fume has been attributed to enhance the compressive strength and other significant properties of concrete. ACI Committee 234 report "Guide for the Use of Silica Fume in Concrete" contains the following:

- The physical and chemical properties of silica fume.
- Interaction of silica fume with portland cement.
- Effect of silica fume on the properties of fresh and hardened concrete.
- Recent typical applications of silica fume concrete.
- How silica fume concrete is proportioned, specified, and handled in the field.
- Areas where additional research is needed.

2.2 Effect of Silica Fume on the Chemical and Physical Properties of Concrete

The article "Benefits of Silica Fume in High Performance Concrete (HPC)" states that silica fume is a highly reactive material, which is used in relatively small amounts to enhance the properties of fresh and hardened concrete (Holland 2001). The article outlines the physical and chemical contributions silica fume have on concrete. Silica fume fills in the spaces between cement grains, a process called particle packing or micro filling, and provides concrete with high silicon dioxide content. The article also notes that silica fume is used to increase mechanical properties, improve durability, enhance constructability, modulus of elasticity and flexural strength.

The article "High Strength Concrete Containing Natural Pozzolan and Silica Fume," documents the advantages of using pozzolans and silica fume in concrete (Shannag 2000). The article observed that the addition of 15% pozzolan to the mix containing 15% silica fume resulted in a 26% increase of the 28-day compressive strength, relative to the strength of the control mix containing 15% silica fume only. Most of the concretes mixes had a high slump value and were workable. The mix containing 15% natural pozzolan and 15% silica fume (by weight of cement) was of optimal workability. For mixes with a water-to-cementitious materials ratio of 0.35, the strength of the silica fume concrete was found to be higher than the strength of the concretes without silica fume; the difference increased with the silica fume content. The relative increase in the strength of concrete became smaller with higher contents of silica fume, that is, beyond 15-20%. This led to the conclusion that the mix containing 15% natural pozzolan and 15% silica fume may be considered an optimum mix for producing high to very high strength concrete at a lower cost.

"Durability Performance of Concrete Containing Condensed Silica Fume," described a short-term study to examine the durability performance of various condensed silica fume concrete in comparison to portland cement (PC) and PC/ground granulated blast furnace slag (GGBS) controls up to the age of 28 days (Alexander and Magee 1999). Three durability index tests were developed to produce reliable results using simple and inexpensive test methods: oxygen permeability, water absorptivity, and chloride conductivity. Alexander and Magee showed that concrete durability dramatically improved with the use of silica fume. Optimum performance was achieved through the use of silica fume as a 10% addition by mass to the initial binder content, slightly less than the 15% considered by Shannag. The study confirmed the effectiveness of silica fume when used in ternary binder blends with PC and GGBS.

"Effect of Silica Fume on Mechanical Properties of High Strength Concrete," presented results of experimental work on short- and long-term mechanical properties of high-strength concrete containing different levels of silica fume (Mazloom, Ramezanianpour, and Brooks 2003). The mechanical properties evaluated were compressive strength, secant modulus of elasticity, and strain due to creep, shrinkage, swelling and moisture movement. As the proportion of silica fume increased, the workability of concrete decreased. However, the short-term mechanical properties, such as the 28-day compressive strength and secant modulus, improved. In addition, the percentage of silica fume replacement did not have a significant influence on total shrinkage. However, the autogenous shrinkage of concrete increased as the amount of silica fume increased. The basic concrete creep decreased at higher silica fume replacement levels, and the drying creep of the specimens was negligible. The results of the swelling tests after shrinkage and creep indicated that increasing the proportion of silica fume lowered the amount of expansion.

The article "Effect of Silica Fume and Fly Ash on Heat of Hydration of Portland Cement," documents the main benefits of utilizing silica fume to the hydration in concrete, which includes: (1) Substantial increase in the compressive strength of concrete; (2) Reduction in the required cement content for specific target strength; and (3) Durability increase for hardened concrete when added in optimum amounts (Langan, Weng, and Ward 2002). The study concluded that the effect of silica fume on hydration varies depending on the w/c ratio. Addition of silica fume alters the hydration process in the period of 2 to 20 hours after the start of hydration. For the low w/c ratios, silica fume prolongs the dormant period, reduces the rate of heat of hydration during the acceleration period, and increases the rate after the acceleration period. The acceleration effect of silica fume begins earlier as the w/c ratio increases. At low

w/c ratios, silica fume retards cement hydration and prolongs the dormant period, followed by enhanced hydration of the cement.

Another article that discusses the effect of silica fume on the water/cement ratio of concrete is "Modified Water-Cement Ratio Law for Silica-Fume Concretes" (Bhanja and Sengupta 2003). The article documents the difference in w/c ratios of silica fume concrete to concrete containing only cement. The study noted that Abram's Law, originally formulated for conventional concrete containing cement as the only cementitious material, is not directly applicable to new-generation concrete containing pozzolan materials, such as silica fume and fly ash. Abram's formulation of the w/c ratio law in 1918 is still considered a milestone in the history of concrete technology, and, until now, was accepted that the largest single factor that governs the strength of concrete is the w/c ratio. The results found that the optimum silica fume replacement percentage was not constant at all the w/c ratios, but was dependent on the water content of the mix. The variables most influential in the strength development of concrete were water-cementitious material ratio, total cementitious material content, and the cement admixture ratio.

The article "Tensile and Compressive Strength of Silica-Fume Cement Pastes and Mortars," documented a test where 16% and 25% of the cement used in the paste and mortar, measured by mass, was replaced by silica fume (Toutanji and El-Korchi 1996). Four different w/c ratio mixtures were tested: 0.22, 0.25,0.28, and 0.31. The superplasticizer content was adjusted for each mixture to provide a sufficient amount of efficient dispersion of the cement and silica fume particles, and to make sure there would be no silica fume excess that might lead to bleeding. Results showed that the partial replacement of cement by silica fume increased the compressive strength of mortar, but had no effect on the compressive strength of the paste. The

partial replacement of portland cement by silica fume decreases the tensile strength of both paste and mortar. The ratios of tensile to compressive strength of paste and mortar were decreased with the increasing silica fume content.

An experimental study on the autogenous shrinkage of portland cement concrete and concrete incorporating silica fume was presented in the article "Effect of Water-to-Cementitious Materials Ratio and Silica Fume on the Autogenous Shrinkage of Concrete" (Zhang, Tam, and Leow 2003). The results confirmed the autogenous shrinkage increased with decreasing w/c ratio and increasing silica fume content. Autogenous shrinkage strains in concrete with a low w/c ratio and silica fume developed rapidly at early ages. About 60% or more of the autogenous shrinkage strain up to 98 days occurred in the first two weeks after concrete casting. The results indicated most of the total shrinkage of the concrete specimens with a low w/c ratio and silica fume exposed to 65% relative humidity after an initial moist curing of 7 days did not seem to be due to the drying shrinkage, but due to the autogenous shrinkage.

In the article "Influence of Silica Fume Replacement of Cement on Physical Properties and Resistance to Sulfate Attack, Freezing and Thawing, and Alkali-Silica Reactivity," data was presented on the permeability and resistance to sulfate attack and alkali-aggregate reactivity for silica fume replacements of 5% to 20% by mass of the cement (Hooton 1993). Cement pastes consisting of sulfate-resisting portland cement, partially replaced with 0%, 10%, and 20% by volume silica fume, were tested for strength development, permeability, and other tests pertaining to the mortar. The tests found that at all ages, the paste containing 20% silica fume exhibited higher strengths than the one containing 10%. The paste containing 20% silica fume replacement was more effective in minimizing permeability at 28, 91, and 182 days of age. It was observed that, in most cases, the compressive strengths increased more than that of the

portland cement control mix even at 1-day age. The control mix continued to gain strength, and after 182 days, it caught up to the silica fume mixes. At ages greater than 56 days, the silica fume concrete nearly stopped developing strength, most likely due to self-desiccation effects. The shrinkage differences for the two mix types were negligible up to 16 weeks of drying. At 32 and 64 weeks, all silica fume mixes demonstrated almost 22% higher shrinkages than the control concrete. The concrete with 10% silica fume did not shrink as much as those with the higher percentages.

2.3 Use of Silica Fume Concrete in Field Practice

The article "Silica Fume Concrete Proves to be an Economical Alternative," documented why silica fume is an essential pozzolan in the field (Rocole 1993). The article determined silica fume concrete was less than half the cost of a traffic membrane and offered several advantages. Special techniques and equipment had to be acquired during the placement of the concrete. One topic addressed was the floating and brooming of silica fume concrete. Since silica fume concrete is more cohesive than conventional concrete, specific techniques and proper precautions were necessary to prevent plastic shrinkage cracking. To address this issue, a resin-based curing compound was applied immediately after brooming the surface. The most valuable lesson learned during the initial pours was the importance of coordinating each step and the roles of those involved.

The article "High Performance (HP) Concrete Flexes its Muscles," describes the role silica fume plays in high performance concrete used on bridge decks (Kojundic 1997). Silica fume was initially applied in concrete bridge decking in 1984 to help extend the life of the decks. One reason for the increased durability is that silica fume acts as a pozzolan, which reacts with water and cement to form compounds with cementitious properties. The article documents that

silica fume reacted with the calcium hydroxide, a weak by-product found in concrete due to cement/water hydration, converting it into good strength-producing product C-S-H, calcium silicate hydrate. Other benefits of silica fume concrete include prevention of chloride-induced corrosion of reinforcing steel, filling of gaps between cement particles due to its fine size, and enhancement of the concrete's electrical resistance that determines the rate of corrosion in rebars.

"In-service Performance of High-Performance Concrete Bridge Decks," is a survey conducted by the New York State DOT on the placement of bridge decks containing fly ash and silica fume. Earlier NYDOT bridge decks frequently exhibited spalling caused by rebar corrosion, which was directly attributable to excessive permeability and ingress of deteriorating soluble such as deicing salts. A task force determined that significant improvement would result from a concrete mixture that reduced permeability and the potential for cracking. Designated as high-performance (HP) or Class HP concrete, this mix had two pozzolanic substitutions, fly ash and silica fume, for cement. It had workability characteristics, lower permeability, and greater resistance to cracking. Effective April 12, 1996, Class HP concrete was implemented as the standard for all New York State bridge decks. By June 1998, more the 80 bridge decks had been constructed with HP Concrete. The results of the survey indicated that the Class HP concrete has improved bridge deck performance. Nearly half of the bridge decks inspected exhibited no cracking at all. Of the Class HP decks that were inspected, 80% were reported as performing as well as or better than earlier Class E and H decks (Alampalli and Owens 1996).

2.4 Effect of Different Curing Procedures on Silica Fume Concrete

The article "Curing Concrete- Normal, Hot, and Cold Weather," published by Pennsylvania State University, discussed the effects of weather conditions on the curing process of concrete (PSU 1999). The article concluded that under normal weather, the key concerns in

curing would be the maintenance of a moist environment around the concrete. Under hot weather conditions, the high temperatures are likely to result in excessive moisture loss. The biggest concern for curing in cold weather is the maintenance of an adequate and conducive temperature for hydration.

The article "Effect of Curing Procedures on Properties of Silica Fume Concrete" presents the effect of curing procedures on hardened silica fume concrete (Toutanji and Bayasi 1999). Three different curing methods were evaluated: steam, moist, and air curing. Steam curing was found to enhance the properties of silica fume concrete, whereas air curing exhibited adverse effects as compared to moist curing. Enhancement in the mechanical properties of silica fume concrete caused by steam curing was manifested by strength increase and permeable void volume decrease. On the other hand, air curing increases the volume of permeable voids as compared with moist curing. Under steam and moist curing, the compressive strength of concrete was practically unaffected by increasing the silica fume content beyond 10%. The only exception were specimens with 30% and exposed to moist curing, which exhibited significant increase in strength as compared to specimens with lower silica fume content under the same curing environments. Air curing had detrimental effect on the strength, particularly on specimens with 10% and 30% silica fume. With the addition of silica fume beyond 15%, the flexural strength was significantly decreased, regardless of curing condition. Specimens with lower silica fume content of 10% and exposed to moist curing exhibited higher flexural strength as compared to those exposed to steam and air curing. Specimens exposed to steam curing and 15% silica fume exhibited higher strength than those exposed to air and moist curing. The effect of steam curing becomes more significant as silica fume content increases.

2.5 Steam Curing

Steam Curing is advantageous where early strength gain in concrete is important or where additional heat is required to accomplish hydration, such as in cold weather (Kosmatka and Panarese 1994). Two methods of steam curing are used: live steam at atmospheric pressure (for enclosed cast-in-place structures and large precast concrete units) and high-pressure steam in autoclaves (for small manufactured units).

A steam-curing cycle, as shown in Fig. 2.1, consists of (1) an initial delay prior to steaming, (2) a period for increasing the temperature, (3) a period for holding the maximum temperature constant, and (4) a period for decreasing the temperature (Kosmatka and Panarese 1999). In field practice, steam curing at atmospheric pressure is generally done in an enclosure to minimize moisture and heat loss. Part (1) of the cycle is considered to be the initial set period of the concrete. The initial set time is determined according to ASTM Standard C 403 (ASTM 1999). The time of initial set varies depending on the admixtures used in the concrete (ACI 1997). Part (2) is the time through which the temperature of the enclosure rises to the maximum temperature. During part (3) of the cycle, the concrete specimens are cured at the maximum temperature for the needed amount of time. Part (4) is the time when the temperature of the concrete is decreased to ambient conditions.

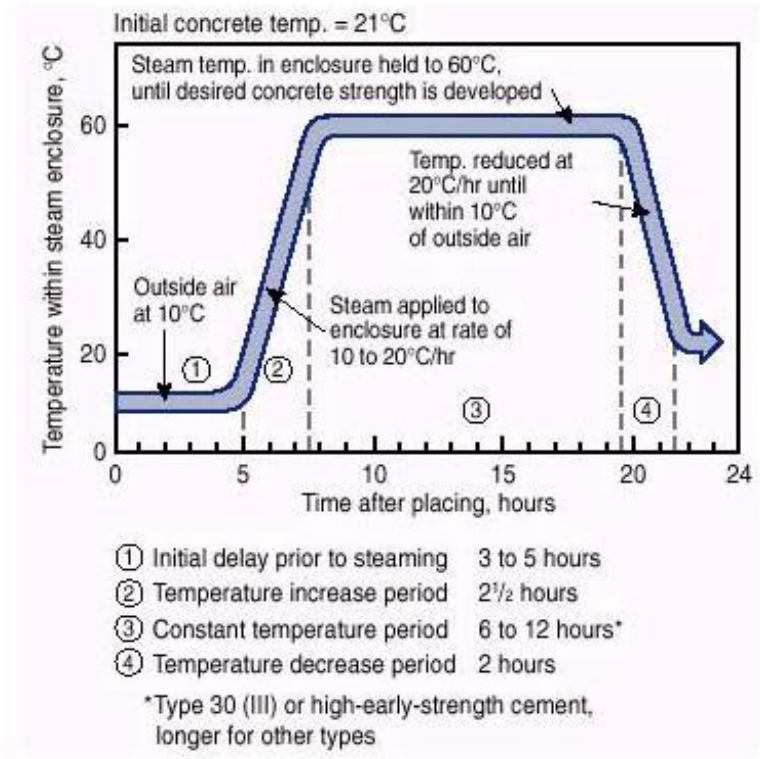

Figure 2.1. A Typical Atmospheric Steam Curing Cycle (http://www.cement.ca/cement.nsf)

When accelerated curing is used as the curing method, the steam temperature primarily determines the quality of the concrete. The desired maximum temperature within the enclosure and the concrete is approximately 66°C (150°F). It has been shown that strength will not increase significantly if the maximum steam temperature is raised from 66°C (150°F) to 79°C (175°F). Steam temperatures above 82°C (180°F) should be avoided because of wasted energy and potential reduction in ultimate concrete strength (Kosmatka and Panarese 1999). The advantage of steam curing around 66°C (150°F) is the potential reduction of concrete drying shrinkage and creep. Also, excessive rates of heating and cooling should be avoided during curing to prevent damaging volume changes. Temperatures in the enclosure surrounding the concrete should not be increased or decreased more then 4°C (40°F) to 16°C (60°F) per hour depending on the size and shape of the concrete element being cured.

Accelerated curing has become widely used in field practices and has been proven economical. Many contractors find the advantages to outweigh the disadvantages of accelerated curing.

2.6 Concrete Shrinkage

Shrinkage is the volume change with time in concrete that is unrelated to load application (Wang and Salmon 1998). Shrinkage is a complex phenomenon which is influenced by many factors, including the concrete constituents, the ambient temperature and relative humidity, the age when the concrete is subjected to the drying environment and the size of the structure or member (Barr, Hoseinian, and Beygi 2001). Approximately 80 percent of shrinkage takes place during the first year of life of a concrete structure (Nawy 2003). Two types of shrinkage occur in concrete: plastic shrinkage and drying shrinkage. Plastic shrinkage occurs during the first few hours after placing fresh concrete in the forms. Drying shrinkage is the decrease in the volume of a concrete element when it loses moisture by evaporation. Drying shrinkage occurs after the concrete has already attained its final set, and a good portion of the chemical hydration process in the cement gel has been achieved. Shrinkage represents water movement out of the gel structure of a concrete specimen due to the difference in humidity or saturation levels between the specimen and the surroundings. Since shrinkage is not a completely reversible process, if a concrete member is saturated with water after completely shrinking, the member will not expand to its original volume. For this reason, the effects of shrinkage are very important for field practices.

Several factors affect the magnitude of drying shrinkage: aggregates, w/c ratio, size of the concrete element, median ambient conditions, amount of reinforcement, admixtures, and type of cement. The coarse aggregates restrain the shrinkage of the cement paste; therefore, concrete

with high aggregate content is less likely to shrink. The shrinkage of concrete increases with increasing w/c ratio. With an increase in the volume of the concrete element, the rate and the total magnitude of shrinkage decreases. Also, the shrinkage duration is longer for larger members since more time is needed for drying to reach the internal regions.

One of the most important factors affecting concrete shrinkage is the median ambient conditions. The relative humidity greatly affects the level of concrete shrinkage; the shrinkage rates are lower at higher levels of relative humidity. The ambient temperature also affects concrete shrinkage; shrinkage stabilizes at low temperatures. Reinforced concrete shrinks less than plain concrete; the relative difference is a function of the reinforcement percentage (Wang and Salmon 1998). The effect of admixtures and cements on the shrinkage of concrete varies depending on the types used. Admixtures used to accelerate the hardening and setting process of the concrete increase shrinkage, however, air-entraining agents have negligible effect. Rapid-hardening cement concrete shrinks somewhat more than other types, while shrinkage-compensating cement minimizes shrinkage cracking if used with restraining reinforcement.

To determine the shrinkage strain, ε_{sh} (Fig. 2.2), ACI committee 209 recommends the use of the expression developed by Dan E. Branson, published in his book *Deformations of Concrete Structures* (Branson 1977):

For any time t after age 7 days for moist-cured concrete,

$$(\varepsilon_{sh})_t = \left(\frac{t}{35+t}\right)(\varepsilon_{sh})_u \qquad (2.1)$$

For anytime after 1 to 3 days for steam-cured concrete,

$$(\varepsilon_{sh})_t = \left(\frac{t}{55+t}\right)(\varepsilon_{sh})_u \qquad (2.2)$$

where,

$(\varepsilon_{sh})_t$ = shrinkage strain at anytime *t* after the recommended ages

t = time in days after initial curing

$(\varepsilon_{sh})_u$ = ultimate shrinkage strains; average value suggested is

800 x 10^{-6} mm/mm (in/in) at 40% humidity.

For conditions other than the standard 40% ambient humidity, a correction factor (CF) is applied to the standard value from Eqs. 2.1 and 2.2:

$$(CF)_H = 1.40 - 0.010H,\ 40 \leq H \leq 80\%) \quad (2.3)$$

$$(CF)_H = 3.00 - 0.030H,\ H \geq 80\% \quad (2.4)$$

where H is the relative humidity in percent (Nawy 2002).

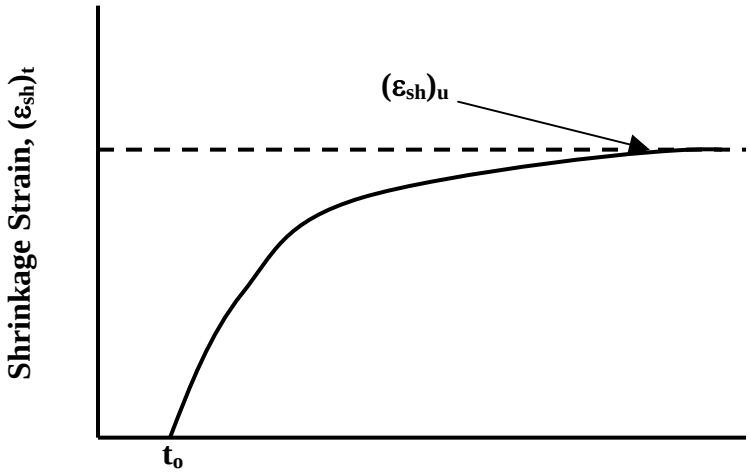

t_o = time at which concrete is subjected to drying environment

Figure 2.2. Shrinkage - Time Curve

2.7 Concrete Durability Evaluation

According to the ACI Committee 234 Report: "Guide for the Use of Silica Fume in Concrete", the permeability of concrete is determined by the measurement of the liquid or vapor flow rate through the medium (ACI 1997). High concrete permeability is closely linked to poor durability. High concrete permeability has been associated with freezing and thawing damage, and corrosion of embedded steel reinforcement by ingress of chloride ions.

It was observed in previous studies (Mehta and Gjorv 1982, and Huang and Feldman 1985) that silica fume makes the pore structure of cement paste and mortar more homogeneous by decreasing the number of large pores. The permeability to liquids and vapors is reduced by the addition of silica fume with the smaller capillary pores. Sellevold and Nilsen (1987) concluded that silica fume is more effective in reducing permeability than it is in enhancing strength (ACI 2000). The low permeability of silica fume concrete led the concrete construction industry to believe that it is the best type of concrete to use in chloride environments.

In a study conducted by Byfors (1987), the addition of 20% of silica fume by mass of cement considerably reduced the diffusion rate of chloride ion, compared with the performance of ordinary portland cement paste with the same w/c ratio. Although these studies proved valuable, a more practical method of specifying and evaluating the resistance of concrete to chloride ion penetration was needed for transportation usage.

In 1983, the American Association of State Highway and Transportation Officials (AASHTO) approved the Rapid Chloride Permeability Test (RCP) (AASHTO 1983) to evaluate the resistance of concrete to chloride ions. The test measures electrical charges passed through concrete, which is then related to the chloride penetration. Based on experimental results,

guidelines were set to qualitatively classify concrete mixtures in different chloride permeability categories (Wee, Suryavanshi, and Tin 2000). Being the only approved test, engineers considered the RCP test method to be fast and economic.

However, through the years, the RCP test has actually been found to be labor intensive and costly (Chini, Muszynski, and Hicks 2003). Another concern is that the RCP data reflects the electrical resistance of concrete rather than the resistance to chloride penetration (Wee, Suryavanshi, and Tin 2000). For these reasons, a Non Destructive Test (NDT) alternative, the Surface Electrical Resistivity Test, was evaluated by FDOT (FDOT FM 5-578) as a possible replacement of the RCP Test. In the study "Determination of Acceptance Permeability Characteristics for Performance-Related Specification for Portland Cement Concrete," the correlation between the RCP and Surface Resistivity test was investigated (Chini, Muszynski, and Hicks 2003).

The Surface Electrical Resistivity Test was developed by geologists to measure resistivity of soil when investigating soil strata by test probes (Ewins 1990). Several configurations of the test probes are possible. The Werner 4-probe array is exclusively used for concrete resistivity studies (Millard 1991). The Wenner array utilizes four equally spaced surface contacts. The resultant potential difference between the two inner electrodes, *V*, is measured with a digital voltmeter (Broomfield and Millard 2002). The resistance, *R*, is given by the ratio of voltage to current. Figure 2.3 illustrates the device and the electrical set-ups.

The resistivity is obtained by multiplying the measured resistance by a conversion factor, called the cell constant (Polder 2001). The cell constant, ρ, commonly used for the application of taking resistivity measurements of concrete cylinders, is as follows:

$$\rho = \left(\frac{\pi d^2}{4L}\right)\left(\frac{V}{I}\right) \qquad (2.5)$$

where L is the cylinder length and d is the diameter of the cylinder (Morris, 1996). Several factors may affect the accuracy of the resistivity measurements, such as the spacing of the test probes, the different surface layers of concrete, w/c ratio, and ambient conditions.

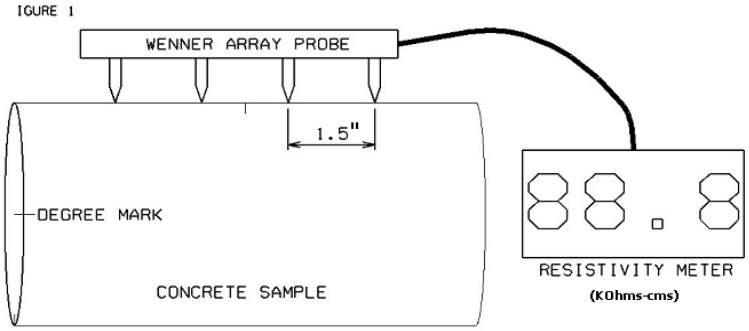

(a) Surface Resistivity Device

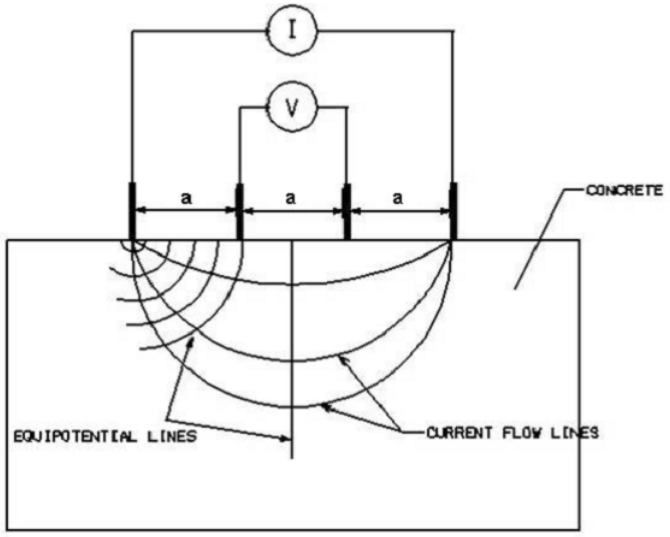

(b) Surface Resistivity Current Flow

Figure 2.3. Surface Resistivity Test Set-Up

Chapter 3

Laboratory Test Procedure

3.1 Introduction

Experiments conducted in laboratories are conducted under a controlled environment and properly monitored. Such controlled conditions do not exist for actual structures in practice. In precast plants, several tests, such as slump and air content, are conducted in environments different than in laboratory conditions. Temperature at the time of testing, mixing procedures, and quality are some of the factors that may affect the results of tests performed in the laboratory and in the field.

Many of the ASTM standards, such as ASTM C 157, are structured to be performed on non-reinforced concrete specimens. Results obtained from laboratory tests performed on non-reinforced concrete are assumed to be valid for reinforced concrete structures in the field. In many cases, this may not be true due to the different behavior of non-reinforced and reinforced concrete, and also due to the varying ambient conditions.

3.2 Mix Design

The concrete ingredients used in this study were selected through consultation with the FDOT quality control personnel to be a representative of the material types typically used in FDOT concrete. The concrete mix design used for the laboratory testing part of this research was an FDOT Class V (Special) mix design with silica fume (Appendix A, Table A.1). The mix design, which was issued in 1998, is the most current mix design used by precast plants in northern Florida. The mix ingredients were cement, mineral admixtures, chemical admixtures, and coarse and fine aggregates. The FDOT Class V (Special) mixes are primarily intended for use in structures requiring high performance concrete, such as piles.

A Type II portland cement, conforming to AASHTO M-85 specifications was utilized in this mix design. The mix design involved two mineral admixtures, densified silica fume and Class F fly ash. The densified silica fume, Rheomac SF 100 dry, is formulated to produce extremely strong, durable concrete or mortar possessing special performance qualities. It maximizes concrete service life by providing superior resistance to attack from damaging environmental forces. Other benefits of using the densified silica fume include adding cohesiveness to the concrete, increasing the modulus of elasticity, reducing permeability, and increasing resistance to sulfate attack and alkali-silica reactivity. Chemical and physical analysis on samples of the cement and fly ash from the same manufacturer were performed at the FDOT State Materials Office as a part of a previous study, as presented in Tables 3.1 and 3.2 (Yazdani 2002). These test results are typical and do not represent data for the batched material from the current study. Some information not available from FDOT was obtained from the manufactures. The chemical admixtures used in the chosen mix were an air entrainer conforming to AASHTO M-154, Type D retarder conforming to AASHTO M-194, and Type F water reducer conforming to ASTM C 494. The air entrainer, MBVR (neutralized Vinsol Rensin solution), has several benefits when used in production of high-quality normal or lightweight concrete. The benefits include increasing resistance to damage from freezing and thawing, improved plasticity and workability, and reduced permeability. The Type D retarder, Pozzolith 100 XR, reduces segregation, controls retardation, and reduces water content required for a given workability. The water reducer, Glenium 3200 HES, is a new generation of admixture based on polycarboxylate chemistry, very effective in producing concrete mixtures with different levels of workability and very high early strength requirements. The coarse and fine aggregates were

Grade 67 Brooksville lime rock from Brooksville, FL, and silica sand from Chattahoochee, FL, respectively.

Table 3.1: Chemical and Physical Analysis Results of Type II Cement

Parameter	**Value**
Chemical Analysis	
Silicon Dioxide (SiO_2) (%)	20.45
Aluminum Oxide (Al_2O_2) (%)	5.60
Ferric Oxide (Fe_2O_2) (%)	4.33
Calcium Oxide (CaO) (%)	63.97
Magnesium Oxide (MgO) (%)	0.78
Sulfur Trioxide (SO_3) (%)	2.81
Alkalis as Na2O equivalent (%)	0.60
Insoluble Residue (%)	0.19
Loss on Ignition (%)	1.30
Dicalcium Silicate (C_2S) (%)	18.80
Tricalcium Silicate (C_3S) (%)	53.19
Tricalcium Aluminate (C_3A) (%)	7.50
Tetracalcium Aluminoferrite (C_6AF) (%)	13.18
Physical Analysis	
Blaine Fineness m^2/kg (ft^2/lbm)	385 (1880)
Autoclave Expansion (Soundness) (%)	+0.03
Gilmore Setting Time - Initial (min)	140
Gilmore Setting Time - Final (min)	202
Compressive Strength - 3 days MPa (psi)	24.89 (3610)
Compressive Strength - 7 days MPa (psi)	33.16 (4810)

Table 3.2: Chemical and Physical Analysis Results of Fly Ash

Parameter	Value	ASTM C 618 Class F Specifications
Chemical Analysis		
Sum of SiO2, Al2O3, & Fe2O3 (%)	88	min 70.0
Sulfur Trioxide (SO3) (%)	0.5	max 5.0
Moisture Content (%)	0.2	max 3.0
Loss of Ignition (%)	3.4	max 6.0
Alkalis as Na2O equivalent (%)	1.89	max 1.5
Calcium Oxide (CaO) (%)	4.54	N/A
Physical Analysis		
Fineness, amount retained on No. 325 sieve (%)	24	max 34
Strength Activity Index - 7 days (%)	77	min 75
Strength Activity Index - 28 days (%)	…	min 75
Water Requirement (%)	100	max 105
Autoclave Expansion (Soundness) (%)	-0.01	max 0.8
Specific Gravity	2.08	N/A

In early June of 2003, the manufacturer discontinued the production of silica fume slurry. In order to accommodate the replacement of the silica slurry, 28.98 kg (63.9 lbs) of dry powder silica fume and 31.62 kg (69.7 lbs) of water were included in the mix design. Also, due to unavailability, Grade 67 Brooksville lime rock with a specific gravity of 2.5 was used instead of the specified Grade 67 with a specific gravity of 2.43. The FDOT personnel at the State Materials Office approved the changes.

3.3 Test Matrix

The test matrix yielded four mix combinations for each steam curing time frames and control curing; steam curing for 12, 18, 24 hours and moist curing. The precast industry typically uses a curing duration of about 10 – 18 hours as current practice. In some cases, if the precast elements do not meet the design strength within this time span, the steam curing can be continued for as long as 24 hours. As will be discussed later, the laboratory testing included the Compressive Strength Test (ASTM C-39), Shrinkage Test (ASTM C-157), and the FDOT Surface Resistivity Test. These tests involved 3 – 152 mm x 305 mm (6 in x 12 in) cylindrical, 3

– 102 mm x 102 mm x 254 mm (4 in x 4 in x 10 in) prism, and 3 – 102 mm x 203 mm (4 in x 8 in) cylindrical specimens, respectively. The compressive strength test was destructive in nature, whereas the shrinkage and surface resistivity tests were non-destructive. This means that the same sets of samples were utilized at various time intervals for the last two tests. Each curing combination was tested at five different concrete ages: 7, 28, 56, 90, and 365 days. Therefore a total of 75 large cylinders, 15 small cylinders, and 15 prisms were prepared, as shown in Table 3.3. The steam curing method nomenclature used herein contains 4 characters, as shown in Table 3.3. The first two characters represent the steam curing duration in hours. The third letter designates the fact that the specimens were steam cured, and the fourth letter represents the curing method used for the balance of the 72-hour total continuous curing requirement (FDOT 2004). To determine the effect of dry post-steam curing, an alternate 24-hour steam cured batch of samples was kept dry during the post-steam curing phase. The control non-steam moist cured specimens are designated as "MC."

Table 3.3: Laboratory Test Matrix

Curing Method*	Specimens		
	Cylinder		Prism
	Large	Small	
12SM	15	3	3
18SM	15	3	3
24SM	15	3	3
24SD	15	3	3
MC (control)	15	3	3
Total	**75**	**15**	**15**

*12SM: 12 hr. steam + 60 hr. moist
*18SM: 18 hr. steam + 54 hr. moist
*24SM: 24 hr. steam + 48 hr. moist
*24SD: 24 hr. steam + dry curing
*MC: 72 hr moist

Table 3.3: Laboratory Test Matrix (cont.)

	Testing Age (days)					
Specimens	**7**	**28**	**56**	**90**	**365**	**Total**
Large Cylinder	15	15	15	15	15	**75**
Small Cylinder	3	3	3	3	3	**15**
Prism	3	3	3	3	3	**15**

3.4 Concrete Mixing and Casting

Identical procedures were used for mixing and casting of the steam and moist cured specimens.

3.4.1 Absorption and Moisture Content: The absorption of the coarse and fine aggregate is the amount of water retained within the pores of the aggregates after saturation and removal of the excess surface moisture. The suppliers performed absorption and specific gravity tests for the fine and coarse aggregates according to ASTM specifications, ASTM C 127 and ASTM C 128, respectively (ASTM 2001 and 1997). The coarse and fine aggregates had absorption rates of 3.5% and 1.5%, respectively, as supplied by the manufacture. Accurate determination of the aggregate moisture contents were needed, due to additional water being added to accommodate the substitution of silica slurry with silica fume powder. The aggregates were maintained in a saturated condition and the moisture content of the aggregates were determined 24 hours prior to mixing (ASTM 1997). The absorptions of the aggregates were subtracted from the total water requirement to yield the surface moisture, which was counted as additional mixing water for the mix design. The actual weights of the wet aggregates and water to weigh out were determined as follows:

$$W'_a = W_{ssd} \cdot (1 + M_s) \quad (3.1)$$

$$W'_w = W_w - W_{ssd} \cdot M_s \quad (3.2)$$

where:

W'_a = weight of aggregate to weigh out, kg (lb)

W_{ssd} = saturated-surface-dry weight of aggregates, kg (lb)

W'_w = weight of total water, kg (lb)

M_s = surface moisture of aggregate (moisture minus absorption), %

3.4.2 Concrete Mixing: Concrete mixing was performed using a 0.17 m^3 (6 ft^3) Gilson HM-244 electric mixer according to ASTM standard C 192 (ASTM 2002). From observations conducted during the trial batch mixing, precautions were taken to achieve the proper workability and slump. The coarse aggregate, fine aggregate and water were divided into thirds and added to the mix in sequence. For convenience, one-third of the coarse aggregate, fine aggregate and mixing water were added to the mixer prior to the start of mixing. The air-entrained admixture was added to the initial mixing water. The mixer was started and the remaining coarse aggregate and fine aggregate were added to the mixture, followed by half of the required cement, silica fume powder, and fly ash. After a few revolutions of the mixer, the mixer was stopped, and another one-third of the water and the remaining admixtures, cement, and pozzolans were added to the mixture. The concrete was mixed for 3 minutes, followed by a 3-minute rest. The concrete was mixed for another 2 minutes. During this two-minute mixing, the remaining one-third of water was added to the mix incrementally to attain the consistency and slump. The time, sequence, and method of adding the aggregates, admixtures, and pozzolans for each batch remained unchanged and simulated good field practice.

3.4.3 Concrete Casting: Casting of the concrete was performed according to ASTM C 192 (ASTM 2002). Plastic lids were placed on the cylinder molds to maintain shape and prevent loss of water by evaporation. Concrete for the 102 mm x 102 mm x 254 mm (4 in x 4 in x 10 in) prisms was placed in two layers, and each layer was rodded separately. The prismatic specimens were rodded once for each 25.40 mm (1 in^2) of surface, for a total of 40 times. The prisms were covered with wet burlap to minimize surface moisture loss.

3.4.4 Temperature Recording Device: According to FDOT 2004 Specification 450-10-7, if accelerated curing (steam curing) is used as the curing procedure, the temperature of the concrete and enclosure must be continuously recorded (FDOT 2004). Additionally, accurate time-temperature recording is critical to conform to the requirements set forth in the FDOT Specifications for accelerated curing. The OM-CP-TEMP from Omega Corporation, a thermal data logger, was used to acquire accurate, continuous and permanent records of the time and temperature relationship in the concrete throughout the entire steam curing period. The data logger had eight-channels, through which T-type thermocouple wires from the Omega Corporation were connected. For each steam curing batch, sheathed thermocouples were placed within three randomly selected large cylinders, two small cylinders, and one prism. The thermocouples were placed horizontally at the center of the specimens, and vertically at mid-height of each specimen immediately after casting. With thermocouples plugged into the data logger, software installed in a laptop computer was used to record the time and temperature in the concrete specimens and enclosure at every 10-minute interval (Fig. 3.1). The data was subsequently formatted into spreadsheets.

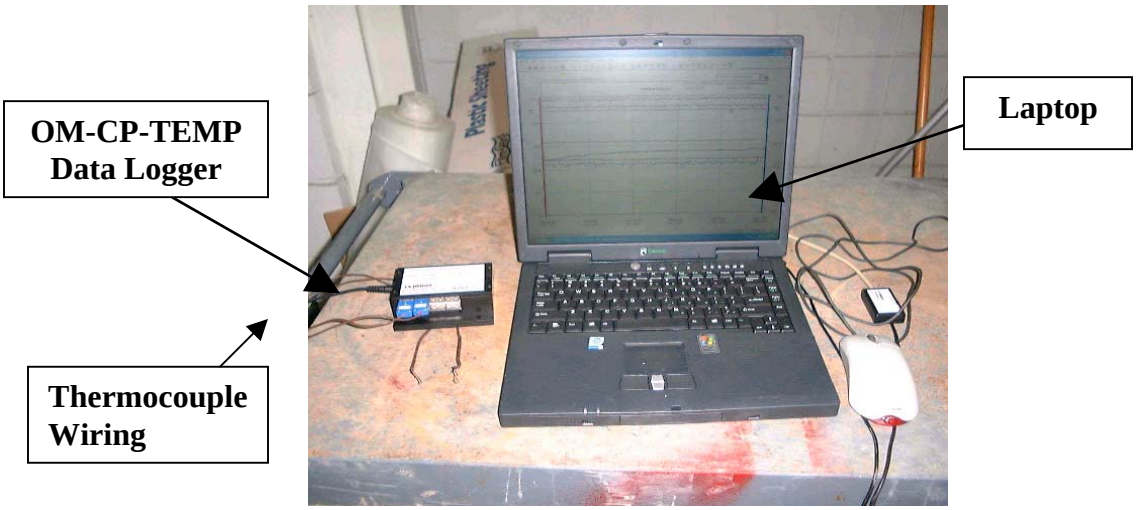

Figure 3.1. Thermal Data Acquisition Set-Up

3.5 FDOT Accelerated Curing Specifications

FDOT Specification 450-10.7 contains the requirements for accelerated curing of prestressed members, and is used for non-prestressed members also (FDOT 2004). Section 450-10-7.1 states that if accelerated curing is used, temperature-recording devices that will provide accurate, continuous, and permanent records of the time and temperature relationship of the enclosure and concrete throughout the entire curing period should be provided. Using the data logger and thermocouple set-up, as mentioned in the previous section, the time and temperature of the enclosure and concrete were properly monitored. The specifications require that the temperature recording sensors be placed at a minimum of two locations, spaced approximately at or near the third point of the bed length, to measure the temperature of the enclosure and concrete. The sensors should be placed at the center of gravity of the cross sections, normal to pile length for solid piles.

FDOT specifications provide separate temperature requirements for the steam curing when the ambient temperature is above or below 10º C (50º F). During this study, since the ambient temperature was always above 10º C (50º F) during the time of mixing and curing, only

the specifications for the higher temperature is mentioned herein. When the ambient air temperature is equal to or higher then 10º C (50º F), the accelerated curing should be initiated by supply or retaining of moisture and the application of the heat, following the initial set period of the concrete. The initial set period of the concrete was determined herein using ASTM C 403 procedures (ASTM 1999). The FDOT specification also states that during the application of heat, the temperature rise in the concrete should not exceed 20º C (36º F) per hour. The maximum curing temperatures of the enclosure and concrete must not exceed 71º C (160º F). The maximum curing temperature has to be uniformly maintained throughout the enclosure, with variation of no more than 11º C (20º F) from the maximum peak temperature until the concrete reaches the required release strength. The concrete should be allowed to cool gradually at the maximum cooling rate of 27.8º C (50º F) per hour. The cooling rate needs to be continued until the concrete temperature is 22º C (40º F) or less than the ambient temperature outside the curing enclosure. If accelerated curing is completed before the minimum specified curing period of 72 hours has elapsed, curing needs to be continued for the remaining part of the curing period in accordance with one of the following curing methods: continuous moisture, membrane curing compound, or curing blankets.

3.6 Concrete Curing

3.6.1 Determination of Setting Time: The ACI Manual of Concrete Practice indicates that the time of setting of silica fume concrete is not significantly affected by the use of silica fume. Instead, additional admixtures in the concrete affect the time of setting (ACI 1997). FDOT Specification 450-10-7.1 indicates that accelerated curing is to begin through application of moisture and heat, only following the initial set period of the concrete. The time of initial set is the elapsed time after initial contact of cement and water required for the mortar sieved from the

concrete to reach a penetration resistance of at least 3.45 MPa (500 psi) (ASTM 403 1999). Based on information obtained from industry personnel, the initial set time of concrete containing silica fume in the field is around 6 hours, which has been confirmed by the results from this study reported herein . For purposes of the research, the concrete time of setting was determined in accordance with ASTM 403.

The time of setting was determined from three separate batches of concrete involving a total of 9 specimens. For each batch, the slump, air content, and temperature were determined to ensure that the mix met the mix design specifications. A mortar sample was obtained from the mixture by sieving a representative sample of fresh concrete through a No. 4 sieve onto a non-absorptive surface. The mortar was thoroughly remixed manually on the non-absorptive surface. The temperature of the mortar was measured and recorded. The mortar was placed in rigid, watertight, non-absorptive and non-oiled 152 mm x 152 mm (6 in x 6 in) cylindrical containers. To prevent excessive evaporation of moisture, the specimens were covered with a damp burlap for the duration of the test, except when bleeding water was being removed or penetration tests were conducted. The specimens were stored at a temperature within the range of 20˚ to 25˚ C (68˚ to 77˚ F). The temperature was measured and recorded throughout the test using the data logger set-up. Prior to making a penetration test, bleeding water was removed by means of a pipette. Because the test batches contained retarders, the initial test was deferred for an elapsed time of 4 hours, and subsequent test were performed at 1-hour intervals, until less time was required. The appropriate needle size was inserted in the specimens, depending on the degree of setting of the mortar, using an ACME Laboratory Penetrometer provided by ELE International. The needle was gradually and uniformly applied using a vertical force downward on the

apparatus until the needle penetrated the mortar to a depth of 26.99 mm (1.063 in). The penetration test was terminated when a minimum 3.45 MPa (500 psi) pressure was obtained.

3.6.2 Steam-Curing Chamber and Moisture Tank: A steam chamber for the accelerated curing part of the test was constructed at the FAMU-FSU College of Engineering (Fig. 3.2). The chamber was built with marine grade pressure treated plywood and 50 mm x 100 mm (2 in x 4 in) lumber. The dimension of the chamber was 100 mm x 100 mm x 200 mm (4 ft x 4 ft x 8 ft). The interior of the chamber was waterproofed with water sealant and the corners were sealed with silicon caulk to prevent loss of moisture or steam. The chamber contained a metal grate at 610 mm (2 ft) from the bottom to support the specimens during the accelerated curing process. The steam was produced by a total of six heaters, consisting of two different types. The Blue M Stainless Steel Sheathed Tubular Heater was obtained from Fisher Scientific Company. The other type was the Lindberg/Blue Laboratory Immersion Heater obtained from Gilson Company. The heaters were placed in three containers capable of holding 16 gallons of water each (Fig. 3.3). From several trial operations of the steam chamber, it was found that this heater combination produced the desired FDOT Specified temperature requirements. During the accelerated curing process, the tank was covered with plastic sheathing to provide further protection from heat and steam loss, and for protection from rain. As mentioned previously, the concrete specimens were steam cured for 12, 18, and 24 hours, which is less than the required 72-hour total curing by the FDOT Specifications. After the 12SM, 18SM, and 24SM specimens were steam cured for the desired time frames, they were placed in a moist curing tank, approximately 2.44 m x 610 mm x 610 mm (8 ft x 2 ft x 2 ft) in size, for the remaining 72 hours of the completion of the curing period, as specified by the FDOT. For comparison purposes, the

24SD specimens were left in the laboratory ambient conditions for the balance of the 72-hour period after the initial 24 hours steam curing.

3.6.3 Temperature Control: The temperature within the steam chamber was monitored using the data logger. Periodically, temperature readings were monitored to ensure that it was within the limits specified by the FDOT specifications. To maintain the efficiency of the heaters and the tubs, the heaters were cleaned every week and the tubs were replaced if any leakage was detected. The temperature of the moist curing tank was recorded manually using a thermometer. The temperature in the tank was maintained at approximately 23º C (73° F) by means of curing tank heaters if needed.

3.7 Plastic Property Testing of Fresh Concrete

After mixing, a portion of the concrete was placed in a damp mixing pan and the plastic properties of the fresh concrete were determined. The tests performed were slump, temperature, and air content.

3.7.1 Slump and Temperature: The slump of fresh concrete was measured according to ASTM C 143 Specifications (Fig, 3.4) (ASTM 143 2003). During the slump test, the temperature of the concrete was measured according to ASTM C 1064 Specification (Fig. 3.5). The thermometer was placed in the fresh concrete that remained in the tank and the temperature was recorded (ASTM 1999).

3.7.2 Air Content Test: The air content of the concrete was measured using the volumetric method in accordance with ASTM C 173 (ASTM 2001), as shown in Fig. 3.6.

Figure 3.2. Steam Curing Chamber

Figure 3.3. Set-up of Heaters Inside Steam Curing Chamber

Figure 3.4. Slump Test

Figure 3.5. Temperature Reading of Fresh Concrete

Figure 3.6. Air Content Test by Volumetric Method

3.8 Testing of Hardened Concrete

3.8.1 Compressive Strength Test: The compressive strength test was performed in accordance with ASTM C 39 (ASTM 2003). A sulfur compound from ELE Corporation, meeting ASTM C 167 Specifications was used for capping the cylinders (ASTM 1998). The diameter of each specimen was measured to ensure that no individual diameter differed from any other diameter of the same cylinder by more than 2 percent. Following the FDOT specifications, the specimens were tested in a dry condition, following the initial steam and/ or moist curing. A Forney compression machine using a load rate of 0.14 to 0.34 MPa/s (20 to 50 psi/s) was used for all compression strength testing. For each cylinder, the load was continuously applied without shock until the specimen failed (Fig. 3.7).

Figure 3.7. Cylinder Failure in Compression Testing

The average strength of the three cylinders for each batch and age combination was reported as the final compressive strength.

3.8.2 Shrinkage of Laboratory Specimens: This test method covers determination of the length changes of hardened concrete due to causes other than externally applied forces and temperature changes. The significance of the measurement of length change in concrete permits the assessment of the potential for volumetric expansion or contraction of concrete due to various causes other than applied force or temperature change.

The length change test was performed according to ASTM C 157 Specifications (ASTM 2003). Minor adjustments were made to conform closely to the ASTM C 490 Specifications (ASTM 2000). The molds used were prismatic in shape of 102 mm (4 in) square cross-section and approximately 254 mm (10 in) in length. There were no gage studs within the molds, because the standard length comparator was not used for the test. Instead, a micrometer was used to measure the length change of the concrete prisms. The micrometer, provided by Fisher Scientific Corporation, was graduated to read in 0.00254 mm (0.0001 in) units, matching the minimum accuracy of 0.00254 mm (0.0001 in) units specified in ASTM C 490.

After the curing process was completed, the specimens were removed from the molds and eight permanent markings were placed on the two ends of the prisms. The specimens were then placed in lime-saturated water maintained at approximately 23 ± 2˚ C (73 ± 3˚ F) for a minimum of 30 min. before length measurements to minimize length variations due to variations in temperature. The specimens were removed from the lime bath one at a time, wiped with a damp cloth, and length readings were taken. The micrometer was placed on each coinciding mark on both sides and the measurement was recorded (Fig. 3.8). After the initial reading, the specimens were restored in lime-saturated water until they reached an age of 28 days, including the period in the molds, when a second reading was taken. Weekly length change readings were taken thereafter. The shrinkage results were obtained as follows:

$$L = \frac{(L_x - L_i)}{L_i} \tag{3.3}$$

where:

L = shrinkage at age x

L_x = micrometer reading of specimen at age x

L_i = initial micrometer reading of specimen at the time of removal from mold

Figure 3.8. Prism Length Reading with Micrometer

3.8.3 Surface Resistivity Test: The Surface Resistivity Test was conducted at the FDOT State Materials Office (SMO) in Gainesville. The 102 mm x 203 mm (4 in x 8 in) cylindrical specimens were prepared at the FAMU-FSU College of Engineering as described previously. After the samples were cured according to the process described in Section 3.7, they were properly packaged and shipped to SMO for testing. The samples were tested for resistivity at ages 28, 56, 91 and 365 days.

As the samples arrived at the SMO, they were checked in and stored in a moist room sustaining 100% humidity until they were 26 days old. At that time, the samples were submerged in a holding tank. On day 28, the samples were removed from the holding tank in the morning, allowing surface air drying of the samples. After surface dry conditions were achieved, surface resistivity readings were taken longitudinally around the sample's circumference at eight different tangential points about the x-axis of the cylinders: 0˚, 90˚, 180˚, 270˚, and again at 0˚, 90˚, 180˚, 270˚. The readings were averaged using the Wenner array configuration (Fig. 3.9).

No readings were taken at the ends of the samples. After the readings were taken, the samples were returned to the holding tank to await future tests.

Figure 3.9. Surface Resistivity Test using Wenner Array

Chapter 4

Large Pile Test Procedure

4.1 Sample Procurement

Full-scale precast prestressed pile specimens were monitored for shrinkage behavior under ambient conditions. This allowed for shrinkage comparison between small-scale laboratory sample and full-scale samples described herein. The pile samples were obtained from Gulf Coast Prestress, Inc (GCP) located at Pass Christian, Mississippi. This supplier was selected because they produce a large number of precast prestressed piles using FDOT approved mix designs. GCP maintains 22 multi-project casting beds over 121.9 m (400 ft.) long each, a large concrete slab area for match-casting and miscellaneous precast items, and pile spinning and assembly areas. GCP also operates its own fully automated, computer controlled, twin turbine central mix batch plant capable of delivering up to 458.7 m^3 (600 cubic yards) of concrete per day. The plant has the ability to provide steam curing to allow faster production and delivery, or the traditional moist curing for sensitive projects.

A total of 8 full-scale prestressed piles were obtained from GCP in October 2003. They included 4 – 356 mm x 356 mm x 1.83 m (14 in x 14 in x 6 ft) and 4 – 610 mm x 610 mm x 1.83 m (24 in x 24 in x 6 ft) piles. They were cast and cured at GCP. The 14-in. square piles contained 8 - ½-in. diameter strands, and the 24 in. piles contained 16 - 1/2in diameter strands, as shown in Figs. 4.1 and 4.2. Also obtained were 152.4 mm x 304.8 mm (6 in. x 12 in.) cylindrical specimens for compressive strength.

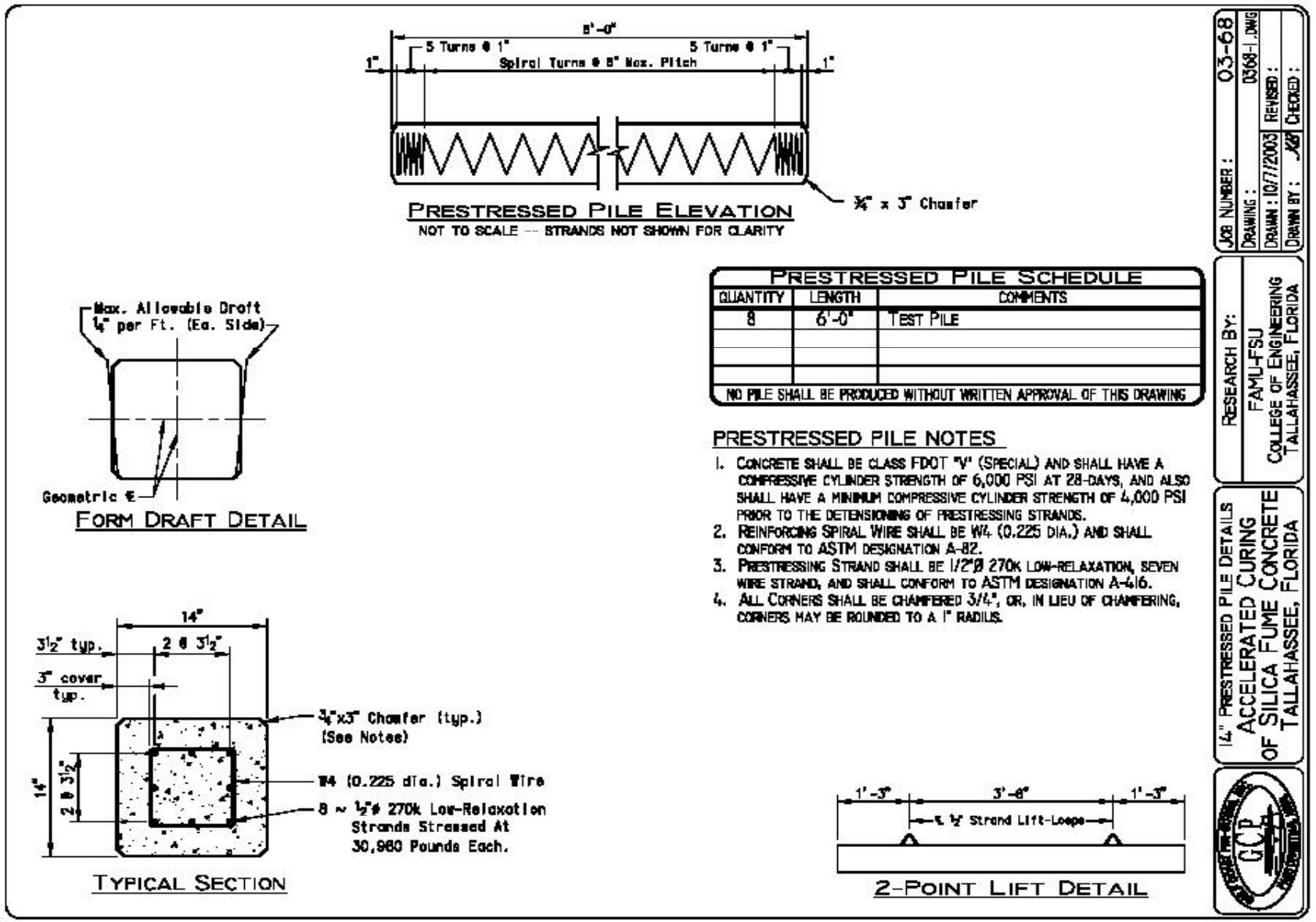

Figure 4.1. Design Details for GCP 356 mm x 356 mm x 1.83 m (14 in x 14 in x 6 ft) Pile

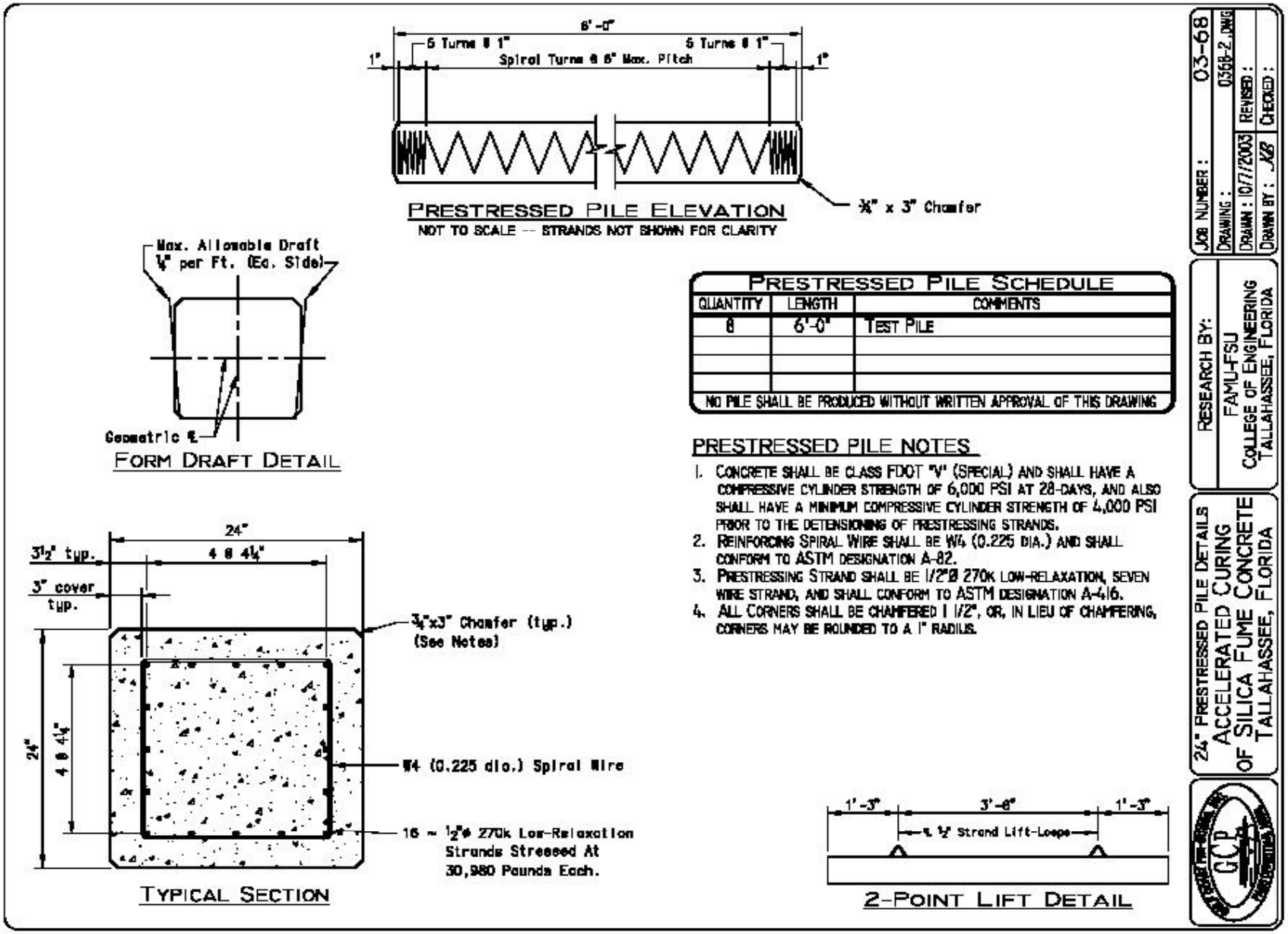

Figure 4.2. Design Details for GCP 610 mm x 610 mm x 1.83 m (24 in x 24 in x 6 ft)

4.2 Concrete Mix Design

The concrete mix used in the precast piles was selected through consultation with personnel from GCP and SMO, to be a representative of the typical FDOT Class V concrete. The chosen concrete mix design was an FDOT Class V (Special) mix design issued in 1995, with silica fume, as shown in Table A.2. The mix ingredients were cement, mineral admixtures, chemical admixtures, and coarse and fine aggregates.

The Type II portland cement conformed to ASTM C 1240 specification. The mineral admixtures in the mix design were densified silica fume and Class F fly ash. The densified silica fume, Force 10 000 D, conformed to AASHTO C 1240 specifications. The Class F fly ash conformed to ASTM C 618 specifications. The two mineral admixtures provided equivalent enhancements to the properties of plastic and hardened concrete, as did the mineral admixtures used for the laboratory specimens.

The chemical admixtures used were an air entrainer conforming to AASHTO M 154, Type D retarder conforming to AASHTO M 194, and Type F water reducer conforming to ASTM C 494 specifications. The air entrainer, known as Air-In, is an economical high quality agent for concrete, designed and controlled to a uniform concentration to ensure consistent performance. Essential purpose of the retarder, HPS-R, is to control retardation to allow more flexibility in scheduling the placing and finishing of the concrete. The water reducer, HPS-HRWR-SP, is composed of high-molecular-weight, condensed-naphthalene sulfonate, and rigidly controlled at each manufacturing step to ensure the appropriate reduction in mixing water. The

coarse aggregate, Gradation #67 river gravel, had a specific gravity of 2.52. The fine aggregate, silica sand with a fineness modulus of 2.57, had a specific gravity of 2.62. Due to the discontinuation of the silica slurry, minor changes were made to the water added to the mix. In place of the silica slurry, 27.3 kg (60.20 lbs) of dry silica fume powder and 27.99 kg (61.70 lbs) of additional water were included in the mix design.

4.3 Test Matrix

The test matrix for this portion of the study yielded four mix combinations, steam curing for 12, 18, 24 hours, and control moist curing. The tests included the Compressive Strength (ASTM C-39) and Shrinkage Tests (ASTM C-157). The compressive strength test was repeated at three different concrete ages: 28, 90, and 365 days. Table 4.1 shows the test matrix with sample designations and number of samples obtained from GPC.

Table 4.1: Pile Specimen Test Matrix

	Specimens		
Curing* Method	**Cylinders**	**Piles**	
Test	**152 mm x 305 mm (6 in. x 12 in.)**	**355 mm x 355 mm (14 in. x 14 in.)**	**610 mm x 610 mm (24 in. x 24 in.)**
12SM	9	1	1
18SM	9	1	1
24SM	9	1	1
MC (control)	9	1	1
Total	**36**	**4**	**4**

*****12SM: 12 hr. steam + 60 hr. moist
*18SM: 18 hr. steam + 54 hr. moist
*24SM: 24 hr. steam + 48 hr. moist
*MC: 72 hr moist cure

4.4 Mixing, Casting, and Curing

Several factors were determined by the quality control team at GCP prior to mixing. The absorption, moisture content, and the set time of the concrete were determined to adhere to all specifications.

4.4.1 Concrete Mixing: The concrete mixing was performed using the standard concrete plant-mixing facilities at GCP. All materials used in the mix were properly controlled and monitored by a field technician.

4.4.2 Concrete Casting: A lever arm concrete dispenser was used to cast the pile specimens (Fig. 4.3), while the cylindrical specimens were manually cast. The pile specimens were vibrated using a manual vibrator during casting. The cylinders were cast according to ASTM C 192 Specifications, as described in Section 3.5.3. Small metal plates were partially inserted into the piles prior to hardening, in order to facilitate subsequent shrinkage determination. Three embedded sets of two metal plates were placed near the ends and at the middle of each pile. The two plates in each set were spaced approximately 254 mm (10 in.) apart. The external end plate was placed approximately 75 mm (3 in.) from the pile end, as shown in Fig. 4.4. After casting, the cylindrical specimens were covered with caps and the piles were covered with burlap to prevent surface moisture loss.

4.4.3 Concrete Curing: As stated previously, when steam curing is used, FDOT requires the temperature of the enclosure and specimens to be continuously monitored. At GCP, thermocouples were inserted into the specimens and connected to a data logger for continuous temperature monitoring (Fig. 4.5). Two sets of

thermocouples were used to record the temperature in the piles. They were placed at the center of the piles before casting. After the initial set time, the 12SM, 18SM, and 24SM specimens were steam cured using low pressure steam pipes, for the proper curing times of 12, 18, or 24 hours, and then moist cured for 60, 54, and 48 hours, respectively, for the completion of the 72 hour total continuous curing period. The MC samples were moist cured for the entire 72-hour period.

The concrete piles were covered with burlap, which provided enclosure during the steam curing cycle. Because all pile specimens were cast on the same bed, the burlap was removed in sections, at the end of each steam curing period. The burlap was also used for the moist curing period, as required by FDOT.

Figure 4.3. Casting of GCP Piles

Figure 4.4. Cylinders and Finished Piles with Embedded Shrinkage Plates

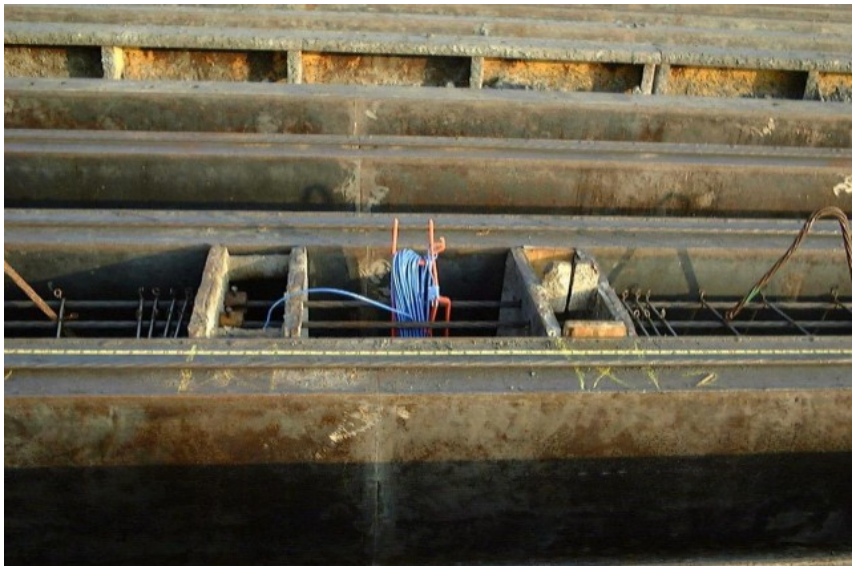

Figure 4.5. Thermocouple Wires for Concrete Piles

4.5 Plastic Property Testing of Fresh Concrete

After mixing, a portion of the concrete was placed in a barrel and the plastic properties of the fresh concrete were determined, during the casting of the concrete specimens. The tests performed were slump, temperature, and air content.

4.5.1 Slump and Temperature: The slump of the fresh concrete was measured according to ASTM C 143 (ASTM 143), and the temperature of the concrete was measured according ASTM C 1064 (ASTM 1064), as described in Section 3.8.1.

4.5.2 Air Content: The air content of the concrete was measured using the pressure method, in accordance with ASTM C 231 (ASTM 2003).

4.6 Transportation and Storage in Tallahassee

The time span between the initial construction of the piles and the delivery of the piles spanned 14 days. The specimens were delivered to the FAMU/FSU College of Engineering by means of a flat bed truck. Upon delivery the specimens were placed on a combination of concrete blocks and 2 x 4 lumbers. They were exposed to ambient conditions for the 364-day duration of the study.

4.7 Testing of Hardened Concrete

4.7.1 Compressive Strength Test: The compressive strength test was performed in accordance with ASTM C-39 Specification, as described in Section 3.9.1.

4.7.2 Shrinkage Test: Because the ASTM C 490 shrinkage specification is designed for small-scale samples, the procedure was slightly modified to make it applicable to large pile samples. As mentioned in Section 4.4.2, metal plates were inserted into the pile surfaces prior to concrete hardening. The outside distances between the pairs of embedded steel plates were measured weekly with a micrometer (Figs. 4.6 and 4.7).

A total of 3 readings were taken from each pair of shrinkage plates, and the average of the three readings was recorded as the gage length (L_x). It was also not possible to immerse the large pile samples continuously in lime solutions, as specified by ASTM C 490. Therefore, a humidity correction was applied to the basic shrinkage formulations, as expressed in Eq. 4.1. Equation 3.3 was then used to calculate the shrinkage occurring on the pile surface.

Because the piles were exposed to ambient conditions, the relative humidity and temperature changes over time were expected to affect the drying shrinkage. As described in Section 2.2, when the ambient humidity is greater than 40%, a correction factor is applied to the actual shrinkage of the concrete (Eqs. 2.3 and 2.4). The net shrinkage after humidity corrections was obtained as follows:

$$(\varepsilon_{sh})_{net} = (\varepsilon_{sh})_t * (CF)_H \quad (4.1)$$

Figure 4.6. GCP Piles with Embedded Metal Plates

Figure 4.7. Micrometer Measurement of Embedded Plate Distance

Chapter 5

Results and Analysis

5.1 Time of Setting of Laboratory Concrete Specimens

Prior to mixing the laboratory concrete specimens, the time of setting was determined in accordance with ASTM C 403 specification. A total of three concrete batches and three mortar samples from each batch were tested. The slump, temperature and air content for each batch are presented in Table 5.1. The results of the time of set test are shown in Tables 5.2 and 5.3. Based on the test results the average initial set time was determined to be approximately 6 hours and 16 minutes. This value was subsequently used in the steam curing time measurements.

Table 5.1: Plastic Property of Fresh Concrete For Time of Set Test

	Air Content (%)	Slump, mm (in.)	Temp., °C (°F)
Batch			
1	4.5	146 (5.75)	27 (81)
2	4.25	165 (6.50)	27 (81)
3	4.5	171 (6.75)	28 (82)

Table 5.2: Time of Set Test Readings

Reading No.	Dial Reading, kg (lb)	Needle Surface Area, mm (in^2)	Force, MPa (psi)	Reading Time
Batch 1				
1	9 (20)	0.16 (0.25)	0.55 (80)	9:45 PM
2	36 (79)	0.32 (0.50)	1.09 (158)	10:45 PM
3	26 (58)	0.16 (0.25)	1.60 (232)	11:23 PM
4	18 (40)	0.06 (0.10)	2.76 (400)	11:53 PM
5	20 (45)	0.06 (0.10)	3.10 (450)	12:23 AM
6	28 (62)	0.06 (0.10)	4.27 (620)	12:53 AM
Batch 2				
1	9 (20)	0.16 (0.25)	0.55 (80)	6:36 PM
2	13 (28)	0.16 (0.25)	0.77 (112)	7:28 PM
3	37 (81)	0.16 (0.25)	2.23 (324)	8:31 PM
4	39 (85)	0.16 (0.25)	2.34 (340)	8:44 PM
5	46 (102)	0.16 (0.25)	2.81 (408)	9:00 PM
6	56 (124)	0.16 (0.25)	3.42 (496)	9:10 PM
7	58 (127)	0.16 (0.25)	3.50 (508)	9:15 PM
Batch 3				
1	19 (42)	0.16 (0.25)	0.58 (84)	7:32 PM
2	36 (80)	0.16 (0.25)	2.21 (320)	8:33 PM
3	54 (118)	0.16 (0.25)	3.25 (472)	8:47 PM
4	54 (120)	0.16 (0.25)	3.31 (480)	8:59 PM
5	55 (122)	0.16 (0.25)	3.36 (488)	9:05 PM
6	57 (126)	0.16 (0.25)	3.48 (505)	9:10 PM

Table 5.3: Time of Set Test Results

	Start time	End time	Initial Set Time	
Batch			Hrs	Min.
1	6:12 PM	12:32 AM	6	20
2	3:23 PM	9:13 PM	5	50
3	3:31 PM	9:08 PM	6	37
		Average	6	16

5.2 Plastic Property of Fresh Concrete

5.2.1 Small Laboratory Specimens: The plastic properties were determined for all batches of concrete to assure that all specifications were met. The slump, temperature, and air content were determined in accordance with ASTM standards. Table 5.4 presents the plastics properties for the laboratory batches cast at the FAMU-FSU College of Engineering. The acceptable ranges for the plastic properties were as follows: slump range 140 – 216 mm (5.50 – 8.50 in) and air content 1.0 – 5.0 %. Table 5.4 shows that all 4 laboratory mixes satisfied the FDOT mix design plastic property requirements.

Table 5.4: Plastic Property Results for Small Laboratory Specimens

Curing Type	Slump, mm (in)	Air Content, %	Temperature, º C (ºF)
12SM	191 (7.5)	4.75	27 (80)
18SM	171 (6.75)	5.00	26 (78)
24SM	159 (6.25)	5.00	26 (78)
24SD	191 (7.5)	4.25	21 (70)
MC (control)	191 (7.5)	4.75	26 (79)

*12SM: 12 hr. steam + 60 hr. moist
*18SM: 18 hr. steam + 54 hr. moist
*24SM: 24 hr. steam + 48 hr. moist
*MC: 72 hr moist cure

5.2.2 Large Pile Specimens: The plastic properties of the large pile specimens were determined at GCP to assure that specifications were met. Only one batch of concrete was mixed at the yard to cast the cylinders and piles. Therefore, only one set of plastic property tests was performed. Table 5.5 presents the results of the tests.

Table 5.5: Plastic Property Results for Large Pile Mix

Curing Type	Slump, mm (in)	Air Content, %	Temperature, ° C (° F)
12SM	121 (4.75)	2.1	30 (86)
18SM			
24SM			
MC (control)			

*12SM: 12 hr. steam + 60 hr. moist
*18SM: 18 hr. steam + 54 hr. moist
*24SM: 24 hr. steam + 48 hr. moist
*MC: 72 hr moist cure

5.3 Steam Curing Temperatures

As mentioned in Sections 3.5.4 and 4.4.3, the temperatures of both the laboratory and field specimens were continuously monitored during the steam curing cycle. The temperatures of the laboratory specimens were monitored using the OM-CP-TEMP recording device with thermocouples from Omega Corporation. The temperatures of the field specimens were monitored using the GCP temperature-recording device.

5.3.1 Laboratory Specimens: Figure 5.1 displays the steam curing temperature variations inside the specimens for each steam curing batch. Complete output files are presented in Appendix Tables B.1- B.4, which include the ambient and enclosure temperature readings during the curing cycles. It may be observed that, for each batch, the maximum temperature reached beyond the maximum specified temperature of 71º C [160º F] by FDOT, with a variation no greater than 11º C [20º F] from the maximum peak temperature. The maximum specified temperature was deliberately exceeded, to enforce a worst case and conservative scenario of steam curing. The 12SM specimens were steam cured at the ideal steam curing cycle, as described in Section 3.6. The maximum temperature was maintained throughout the steam-curing period. For the specimens that were steam cured for longer than 12 hours, there was

minor drop in the maximum temperature. As described in Section 3.7.2, the steam was supplied through the use of six heaters submerged in three water tubs. Due to the length of required steam curing time, there was a time period where more water had to be supplied to the tubs by opening the steam chamber. The opening of the steam chamber allowed heat to escape the chamber while the water was supplied to the tubs. The minor temperature drops were not expected to significantly affect the steam cured concrete properties.

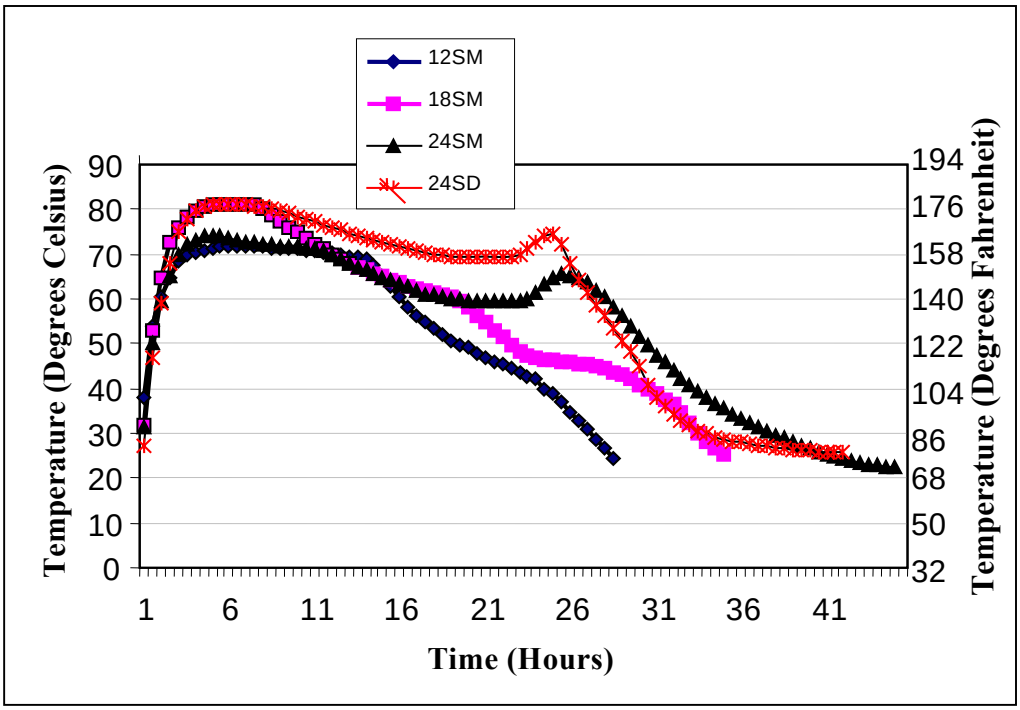

Figure 5.1. Steam Curing Temperature for the Laboratory Specimens

5.3.2 Pile Specimens: At the precast yard, major emphasis was placed on the continuous temperature reading of the specimens during curing, and less on the temperature in the specimens during the cooling period. Therefore, the temperature readings described in this section reflect the average temperature during the steam curing.

Figure 5.2 displays the temperature of the concrete specimens during periods 2 and 3 of the steam curing cycle described in Section 2.5. Channels 1 and 2 correspond to the temperature in

the 610mm (24 in.) specimens, and Channels 3 and 4 correspond to the 356mm (14 in.) specimens. As seen in Fig. 5.2, approximately a 10º C (50º F) temperature difference existed in the maximum curing temperatures for the two pile groups. This may be due to the size effect and specimen location during curing. The larger piles are expected to build up more heat at their cores. The larger pile casting bed was located nearest to the boiler used to heat the water, while the smaller piles were located further away. However, it is obvious that the GCP pile specimen steam curing temperature cycles satisfied the FDOT requirements.

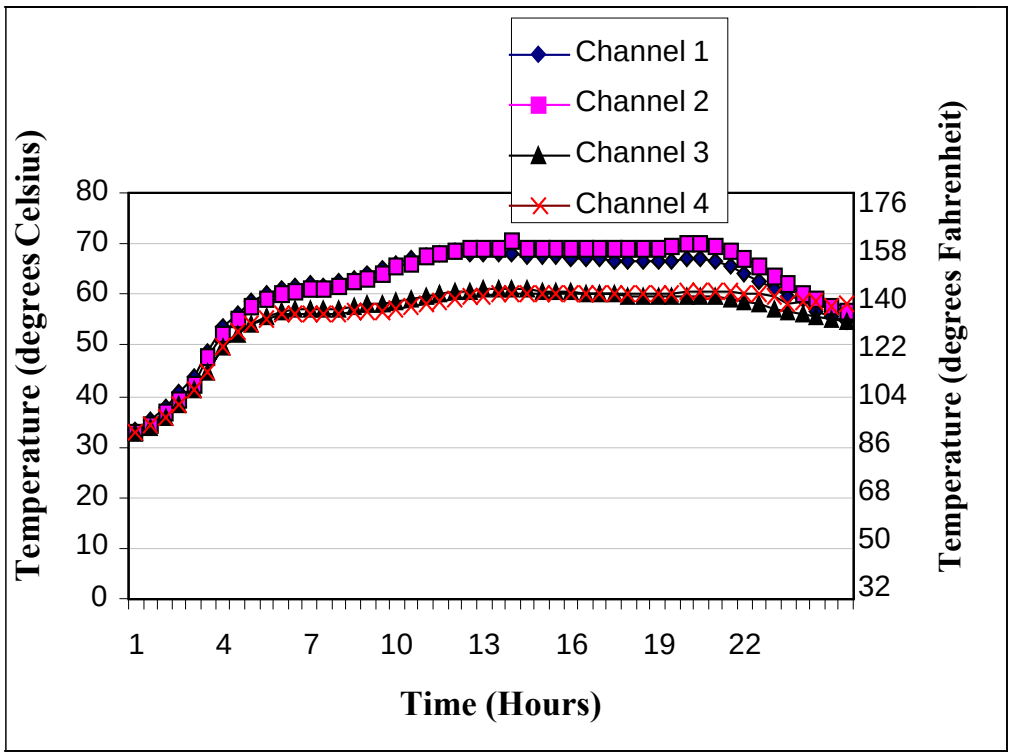

Figure 5.2. Steam Curing Temperature of the Field Specimens

5.4 Compressive Strength Results

5.4.1 Small Laboratory Specimens: The compressive strength results for the laboratory specimens are presented in Table 5.6 and Fig. 5.3. Samples12SM, 24SM and MC reached the target 41.37 MPa (6,000 psi) minimum required compressive strength for the Class V Special mix at 28 days. At 56 days and beyond, as seen from Table 5.7, all laboratory samples reached

the minimum specified compressive strength. All sample sets continued to gain compressive strength with age. In the initial stages, the 24SD samples displayed high early strength gain; however, the strength gain in these samples slowed with time. By 365 days, the 24SD samples displayed the smallest strength, which may be due to the lack of continued moist curing for the remainder of the 72-hour requirement, after the initial 24-hour steam curing. As expected, at 365-day age, the MC sample set displayed the highest average compressive strength. As discussed in Section 2.2, concrete containing silica fume displays very high compressive strengths when moist cured. The 12SM sample set displayed higher compressive strength at latter stages, as compared to the other samples that were steam cured for a longer period of time.

The 18SM and 24SD specimens that were steam cured at higher temperatures showed the least compressive strength at 28 days. The average compressive strengths at 365 days show that the moist cured and the 12SM specimens attained the most strength, respectively. In comparison to the 24SM specimens, the 24SD specimens had lower strength at 28 days and beyond.

5.4.2 Pile Specimens: The compressive strength results for the cylindrical specimens collected at GCP during the pile casting are shown in Table 5.7 and Fig. 5.4. It is observed that all field samples reached the target compressive strength of 41 MPa (6000 psi) at 28 days. The field samples continued to gain strength with age beyond 28 days. The MC specimens demonstrated the specified 28-day strength, and this trend continued for future ages. The 12SM specimens were the highest strength producers among the steam cured specimens at 365 days, followed by the 18SM samples, as shown in Fig. 5.4.

Table 5.6: Laboratory Specimen Compressive Strength Results

	Average Compressive Strength, MPa (psi)				
Curing Type	**14 Day**	**28 Day**	**56 Day**	**91 Day**	**365 Day**
12SM	32 (4666)	41 (6051)	45 (6505)	48 (7023)	50 (7303)
18SM	32 (4692)	33 (4842)	44 (6388)	44 (6399)	45 (6544)
24SM	33 (4775)	44 (6402)	48 (6903)	48 (6957)	48 (6995)
24SD	35 (5087)	40 (5734)	42 (6127)	44 (6356)	44 (6312)
MC (control)	32 (4659)	45 (6510)	52 (7503)	58 (8427)	60 (8726)

*12SM: 12 hr. steam + 60 hr. moist
*18SM: 18 hr. steam + 54 hr. moist
*24SM: 24 hr. steam + 48 hr. moist
*MC: 72 hr moist cure

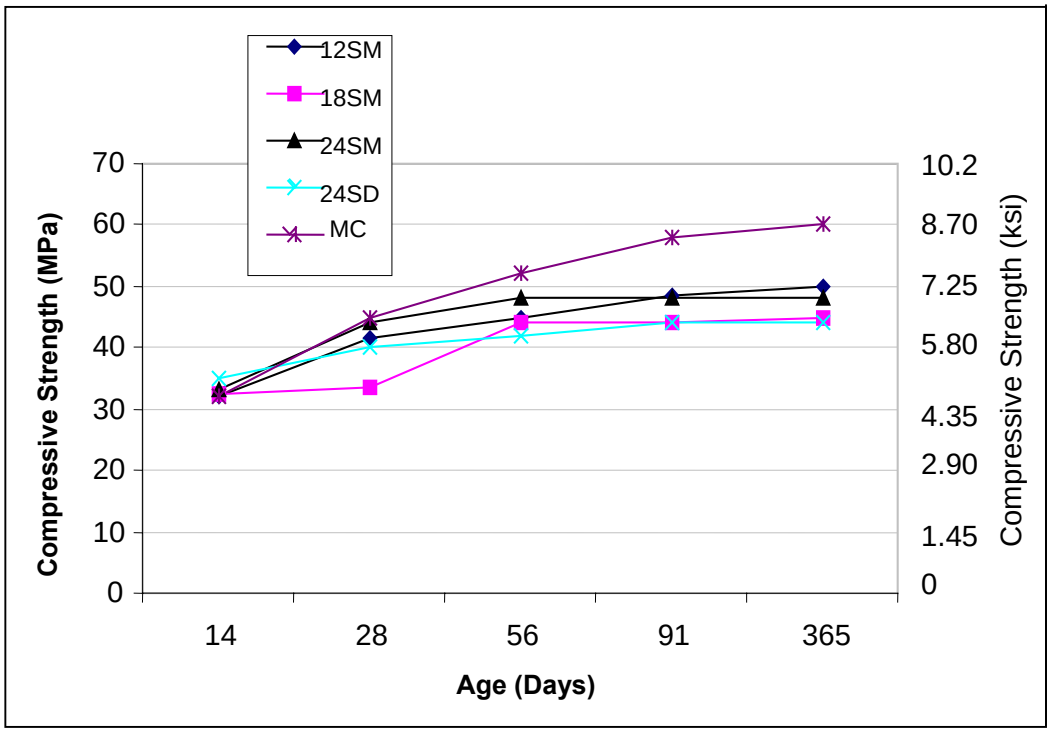

Figure 5.3. Laboratory Specimen Compressive Strength Results

Table 5.7: Pile Specimen Compressive Strength Results

	Average Compressive Strength, MPa (psi)		
Curing Type	**28 Day**	**91 Day**	**365 Day**
12SM	46 (6651)	52 (7538)	54 (7778)
18SM	44 (6352)	50 (7228)	52 (7576)
24SM	45 (6463)	51 (7409)	51 (7423)
MC* (Control)	47 (6884)	53 (7615)	55 (7924)

*12SM: 12 hr. steam + 60 hr. moist
*18SM: 18 hr. steam + 54 hr. moist
*24SM: 24 hr. steam + 48 hr. moist
*MC: 72 hr moist cure

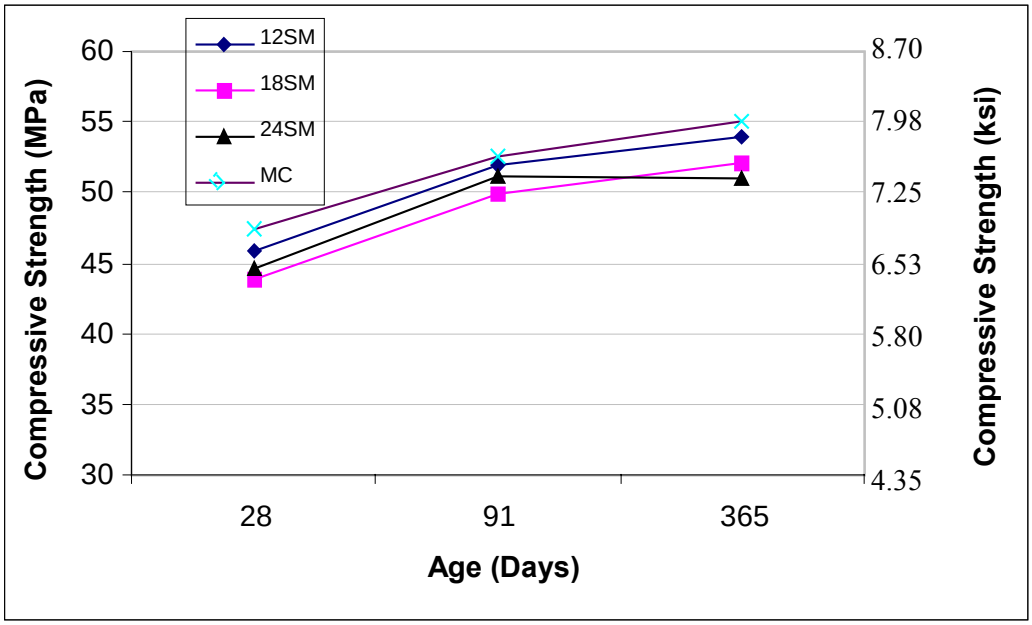

Figure 5.4. GCP Compressive Strength Results

5.4.3 Analysis of the Compressive Strength Results: Comparison of Tables 5.6 and 5.7 shows that the average compressive strength for the field specimens was higher than the laboratory specimens at 28 days. The moist cured MC specimens displayed high compressive strengths at 28 days and consistently at all other ages. At 91-days, the 12SM samples for both the laboratory and pile specimens displayed the second highest compressive strengths, followed

by the 24SM specimens. In both the laboratory and field specimens, the 18SM specimens displayed the least compressive strengths.

5.5 Surface Resistivity Test Results

As mentioned previously, the surface resistivity tests were conducted at the FDOT State Materials Office in Gainesville, Florida. Assurance was received that all standards were followed accordingly, and the results presented herein are accurate.

Interpretive guidelines for the Surface Resistivity test results are presented in Table 5.8 in terms of the test data, correlation with ASTM C 1202 RCP test output and levels of chloride ion permeability (Chini, Muszynski, and Hicks 2003), regardless of the class of concrete. Although Table 5.8 provides surface resistivity thresholds for only 28 and 91 day concrete, this table is used as the basis for all concrete types at any age if the same curing conditions were used. Greater surface resistivity indicates lower permeability and increased long-term durability of concrete.

Table 5.8: Correlation of Surface Resistivity and RCP Test Results

Chloride Ion Permeability	**RCP Charge Passed (Coulombs)**	**Surface Resistivity**	
		28 Day (kΩ.cm)	91 Day (kΩ.cm)
High	>4000	<11.8	<10.6
Moderate	2000-4000	11.8 - 21.0	10.6 - 19.7
Low	1000-2000	21.0 - 37.4	19.7 -36.9
Very Low	100-1000	37.4 - 253.7	36.9 - 295.3
Negligible	<100	>253.7	>295.3

Table 5.9: Average Surface Resistivity Results (kΩ.cm)

	Concrete Age (days)					
Curing Type	**14**	**28**	**56**	**91**	**182**	**364**
12SM	16.2	25.7	45.6	69.7	79.5	101.5
18SM	27.8	35.6	51.5	54.1	85.4	103.3
24SM	20.3	32.8	48.2	60.0	81.5	116.5
24SD	30.1	33.9	44.1	59.5	80.5	103.1
MC (control)	7.8	20.7	43.8	55.4	90.1	143.2

*12SM: 12 hr. steam + 60 hr. moist
*18SM: 18 hr. steam + 54 hr. moist
*24SM: 24 hr. steam + 48 hr. moist
*MC: 72 hr moist cure

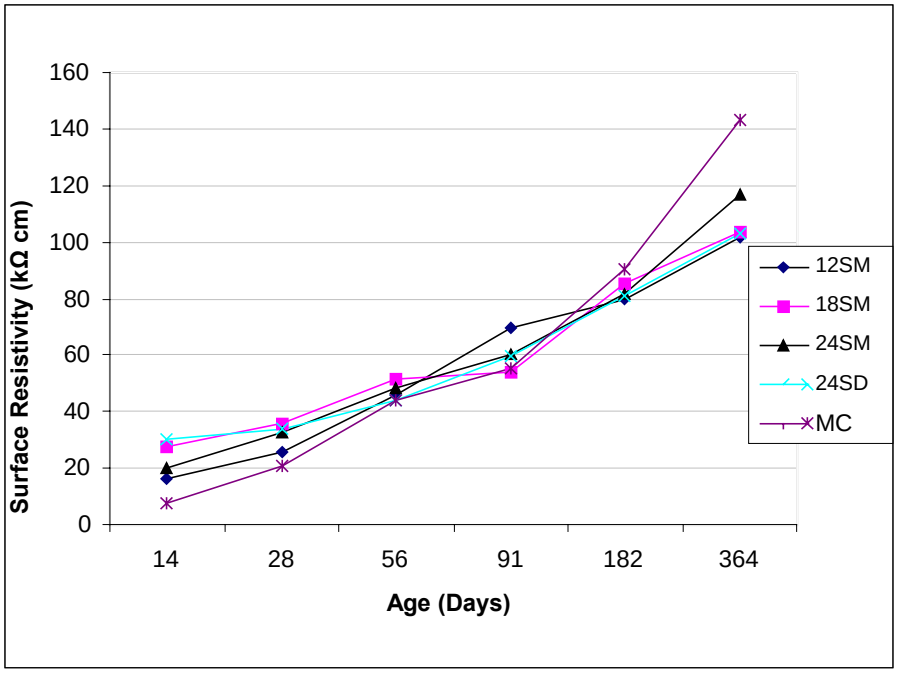

Figure 5.5. Surface Resistivity Results

The average surface resistivities obtained for the 102 mm x 203 mm (4 in x 8 in) cylindrical specimens for various concrete ages are shown in Table 5.9 and displayed in Fig. 5.5. The actual resistivity data is presented in Appendix C.

Table 5.9 and Fig. 5.5 show that the average Surface Resistivity values of all test cylinders increased significantly with time. Initially at 14 days, the 24SD dry specimens showed the most resistivity, and the MC specimens showed the least. At 28-day age, the 18SM specimens were the most surface resistive, and the MC samples were still the least. By 91-day age, the 12SM and the 18SM samples demonstrated the greatest and the lowest resistivity, respectively. The MC samples gained in surface resistivity at a much higher rate than the steam cured samples, and by the age of 364 days, the MC samples outperformed all steam cured samples. Among the steam cured specimens, the 24SM samples demonstrated the greatest resistivity at 364-day age. However, all the steam cured samples displayed resistivities at 364 days that were relatively close to each other.

It is observed from Tables 5.8 and 5.9 that at 28 day age, all steam cured specimens demonstrated low permeability, while the MC specimens demonstrated moderate permeability. At 91-day age, all the specimens, including those that were moist cured, demonstrated very low chloride ion permeability, indicating that all samples represented concrete that are durable and corrosion resistant.

5.6 Shrinkage Test Results

5.6.1 Laboratory Shrinkage Results: Actual drying shrinkage results for the small prism samples are presented in Appendix D, Table D.1. Graphical representations of the results are shown in Fig. 5.6 as dotted lines. The graphs display small inconsistencies due to the variation in the micrometer readings. All data sets show a general increase in shrinkage with time. Each

graph contains a best-fit trend line for non-linear functions produced in EXCEL. A regression analysis was performed on the data to produce the trend lines shown on the graphs. The data for the predicted shrinkage from the regression analysis are located in Appendix D, Table D.2. At early ages, the 24SM samples showed the least amount of shrinkage, followed by the MC, 12SM, 24SD, and 18SM samples, respectively. At age of 364 days, the MC samples showed the least shrinkage, followed in order by the 12SM, 24SD, 24SM, and 18SM samples, respectively. Comparison of the best-fit trend lines in Fig. 5.7 shows that at later stages, the 18SM samples are expected to experience the greatest shrinkage, while the 24SD and 12SM samples may experience the least shrinkage. No humidity correction to the shrinkage data is needed because the laboratory samples were continuously immersed in a lime bath as per ASTM specifications.

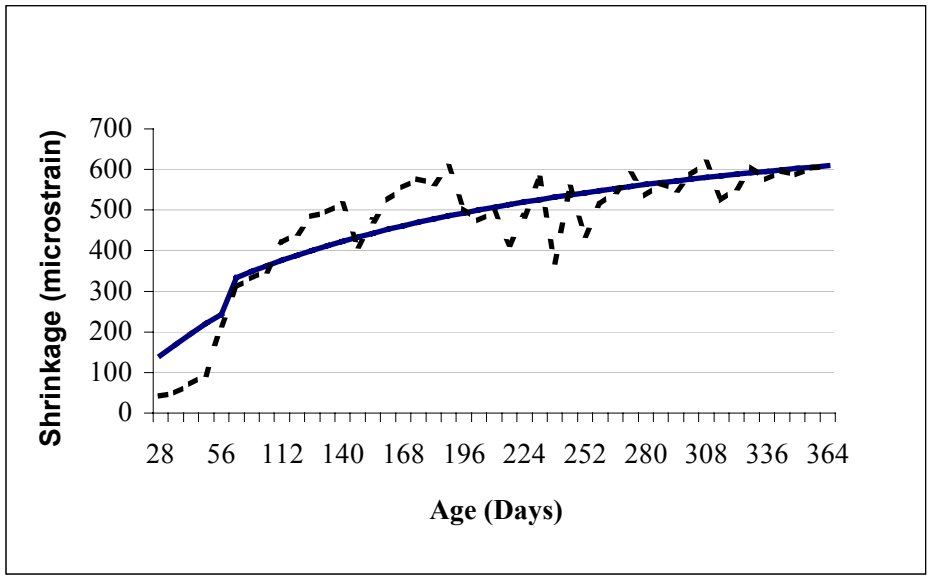

(a) 12SM Specimens

Figure 5.6: Small Prism Sample Shrinkage Results

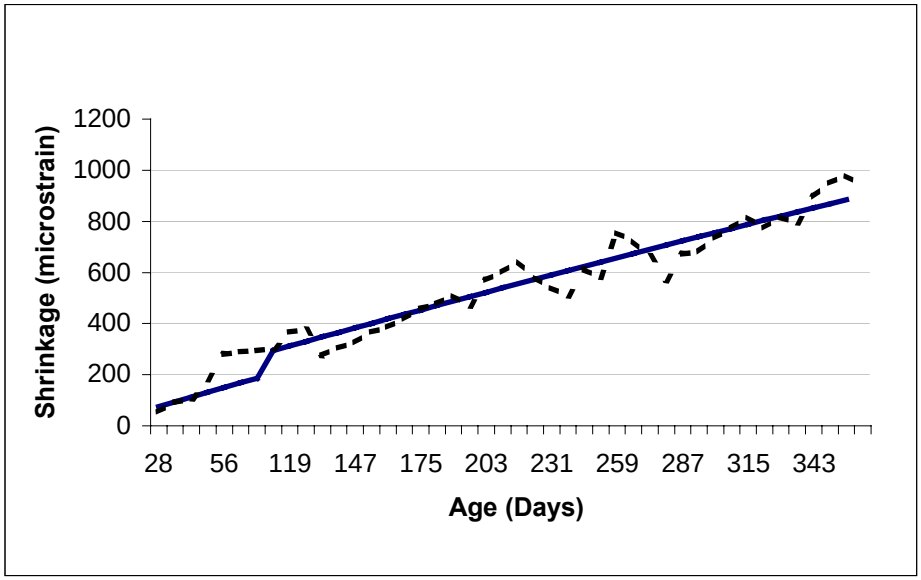

(b) 18SM Specimens

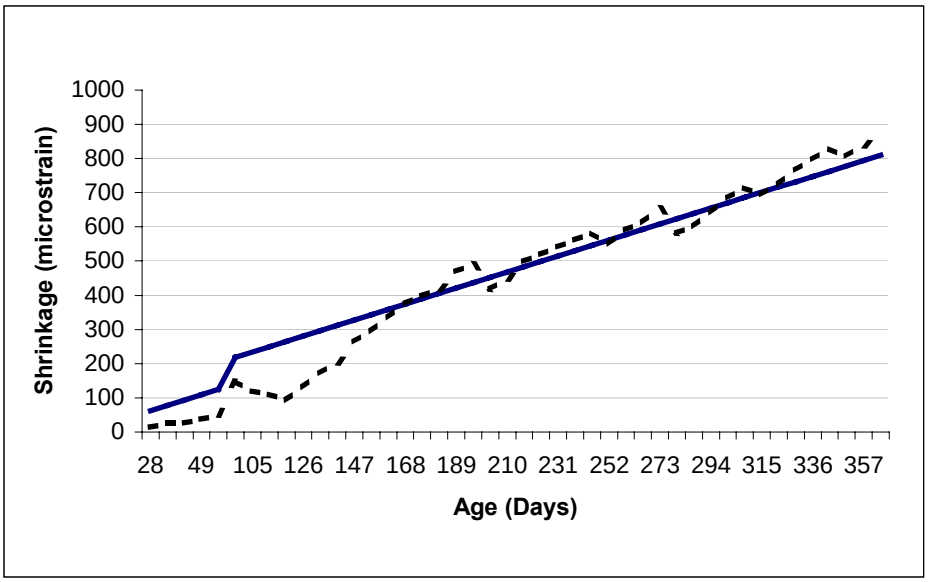

(c) 24SM Specimens

Figure 5.6: Small Prism Sample Shrinkage Results (cont.)

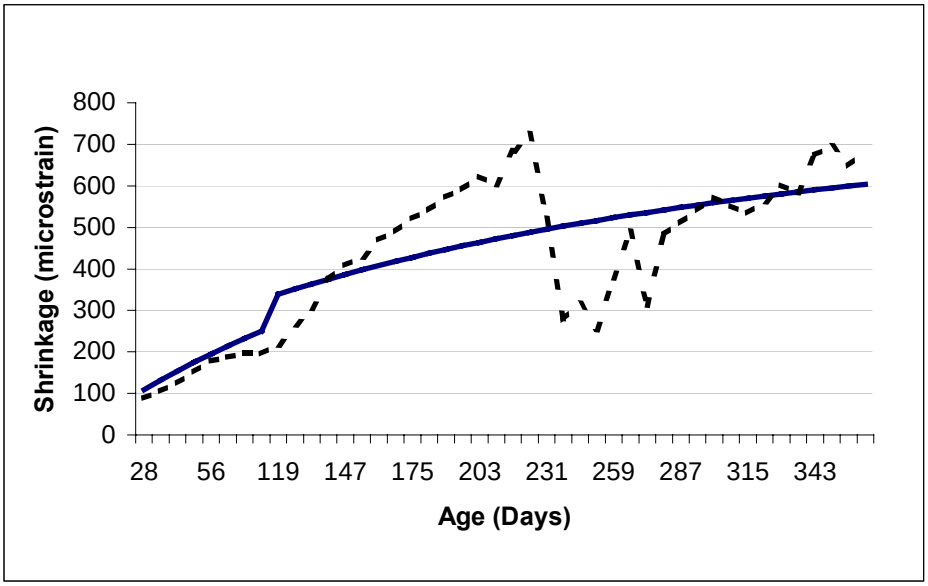

(d) 24SD Specimens

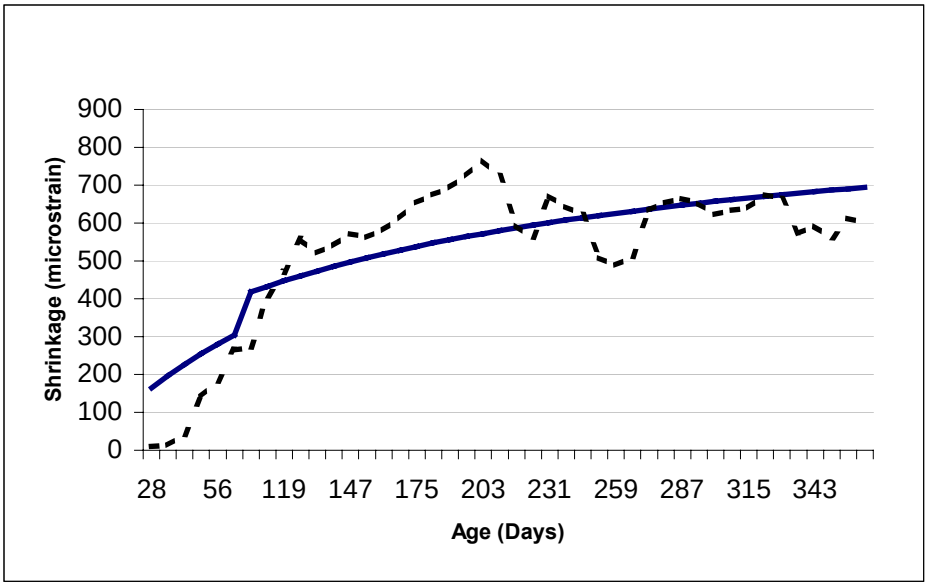

(e) MC Specimens

Figure 5.6. Small Prism Sample Shrinkage Results (cont.)

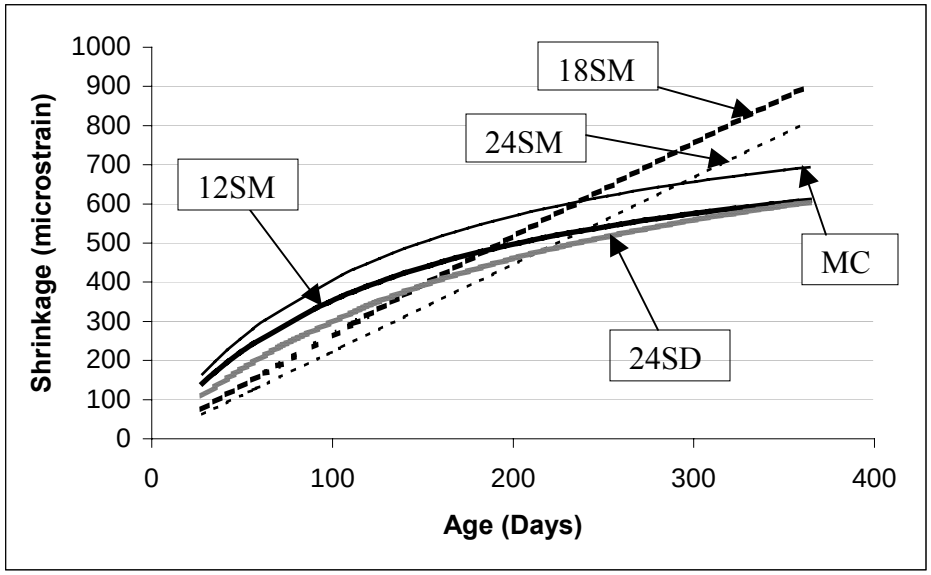

Figure 5.7. Comparison of Best-Fit Shrinkage Trendlines for Laboratory Prisms

5.6.2 Pile Shrinkage Results: The shrinkage results for the small and large piles are presented in Appendix D, Table D.3. The results were corrected for ambient humidity by using Eqs. 2.3 and 2.4. Graphical representations of the modified shrinkage for the small and large pile specimens are shown in Fig. 5.8 and 5.10, respectively. Figures 5.9 and 5.11 display the best-fit regression trendlines for the small and large pile shrinkage data, respectively. The trendline shrinkage prediction values are presented in Appendix D., Tables D.4 and D.5.

Based on the shrinkage results, the least amount of shrinkage occurred in the moist cured specimens for both the small and large pile specimens at 350 days. Among the steam cured specimens, the least shrinkage occurred within the 18SM specimens followed by the 12SM specimens for the small piles, as evident from the Fig. 5.9 trendlines. The greatest amount shrinkage occurred within the 24SM samples. For the larger piles, the moist cured samples again performed best for shrinkage at 350 days, followed in order by the 24SM, 12SM, and 18SM samples.

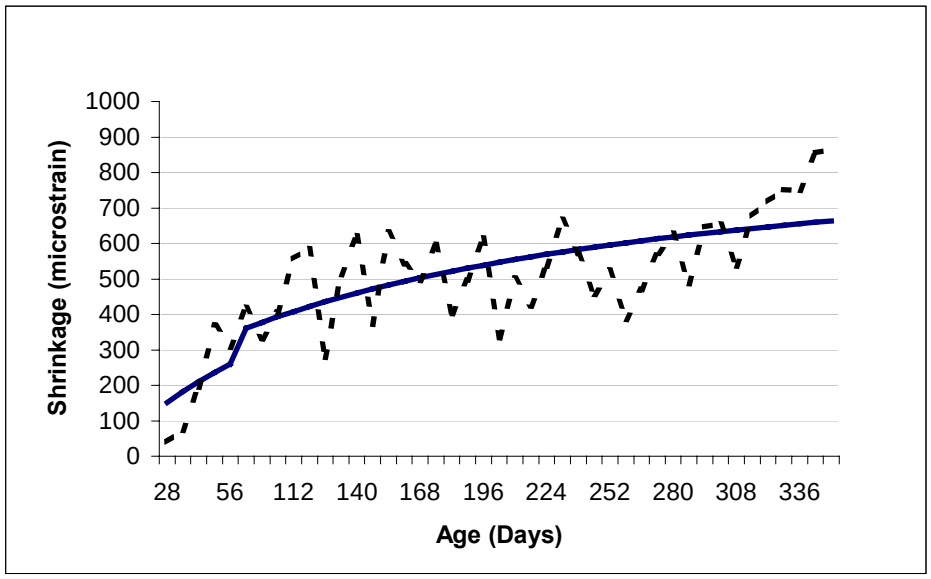

(a) 12SM Specimens

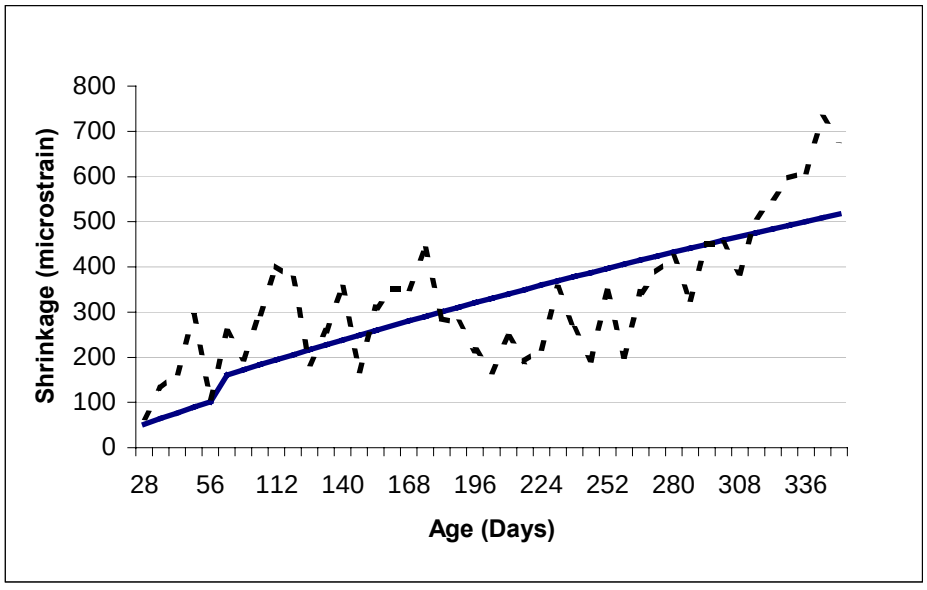

(b) 18SM Specimens

Figure 5.8 Humidity Modified Shrinkage Results for Small Pile Specimens

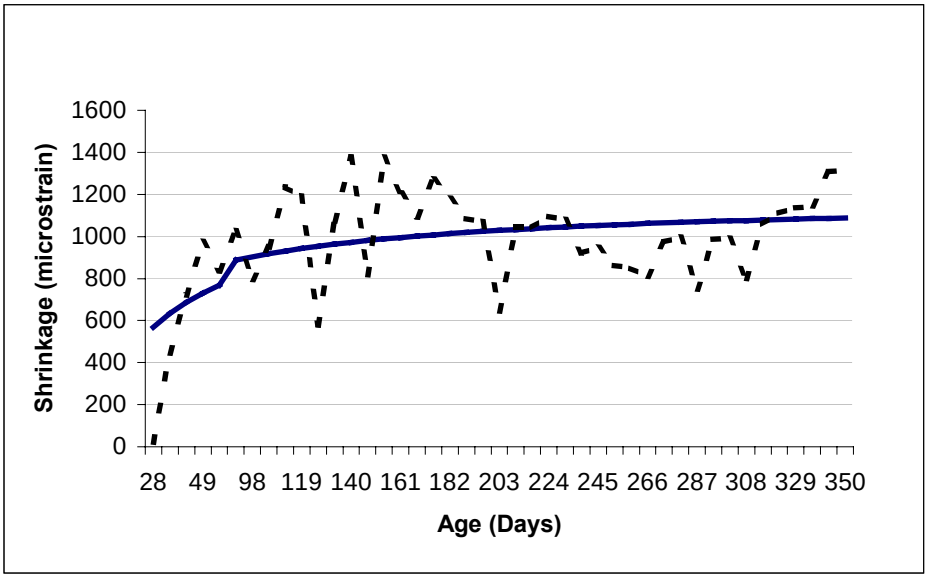

(c) 24SM Specimens

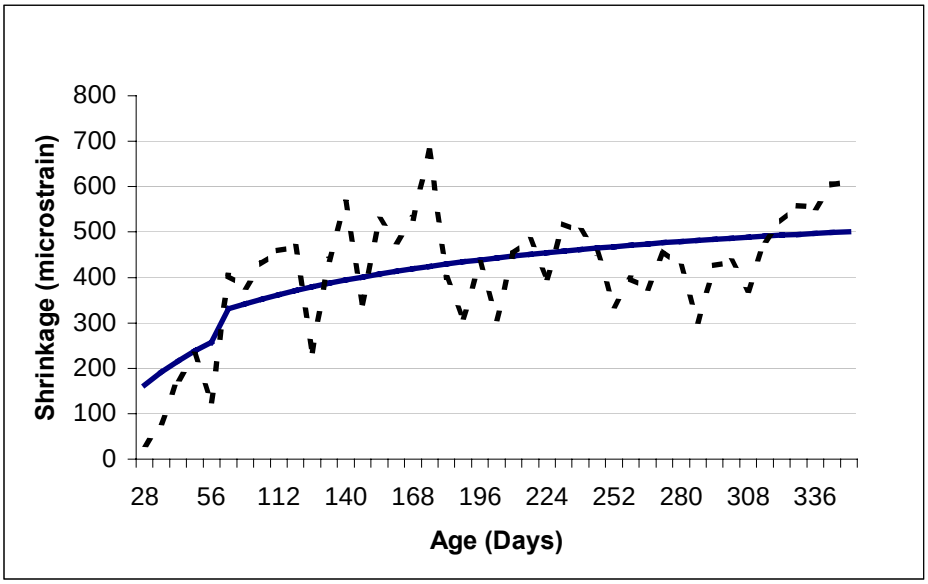

(d) MC Specimens

Figure 5.8. Humidity Modified Shrinkage Results for Small Pile Specimens (cont.)

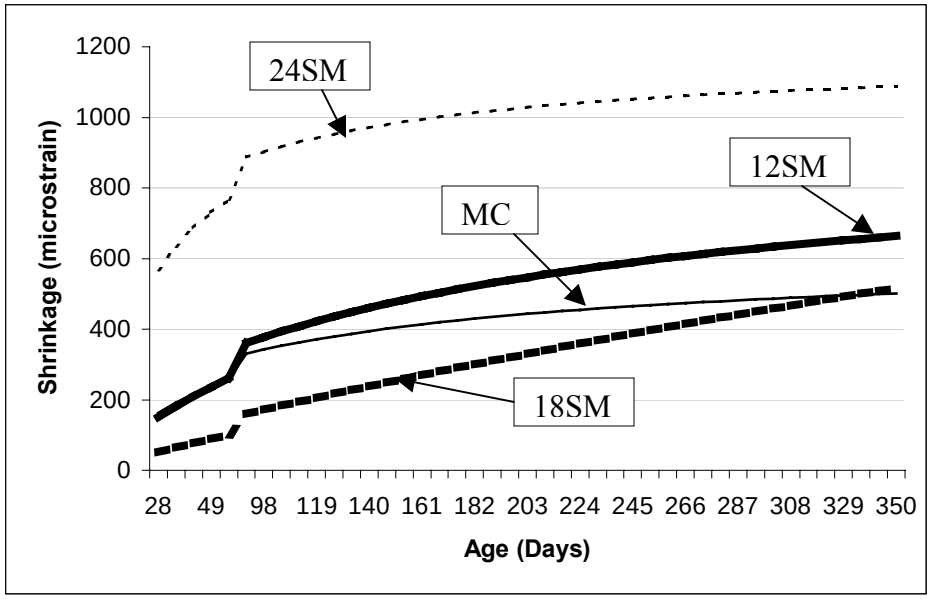

Figure 5.9. Best-Fit Shrinkage Trendlines for Small Pile Samples

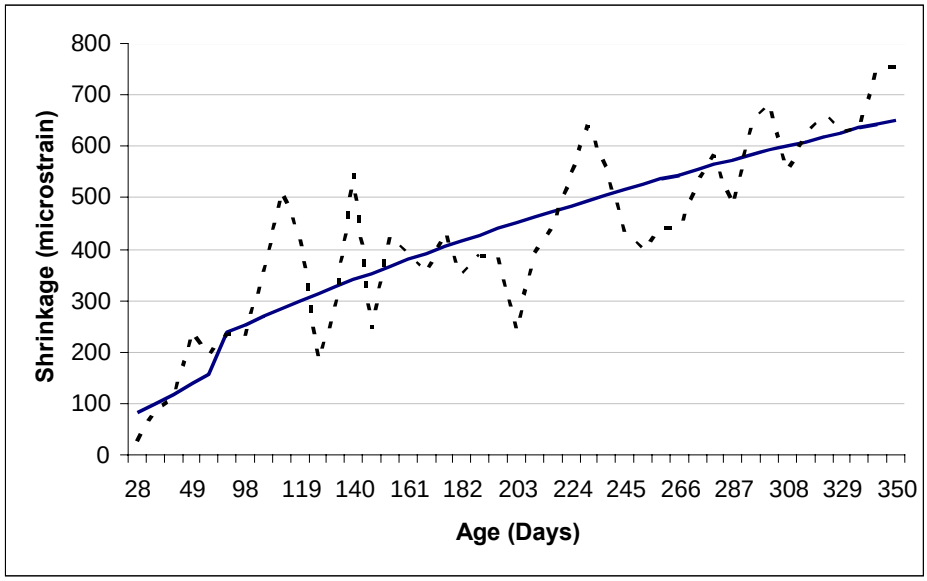

(a) 12SM Specimens

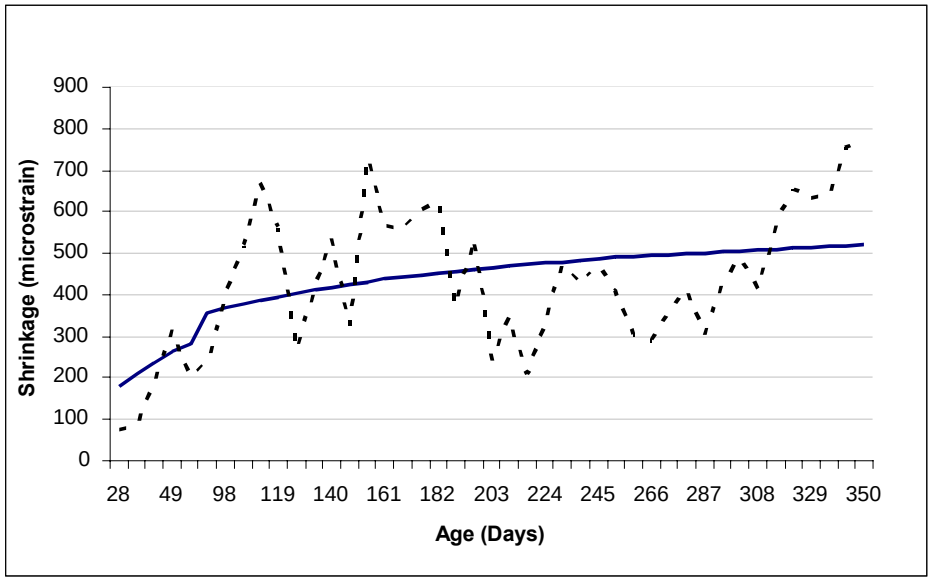

(b) 18SM Specimens

Figure 5.10: Humidity Modified Shrinkage Results for Large Pile Specimens

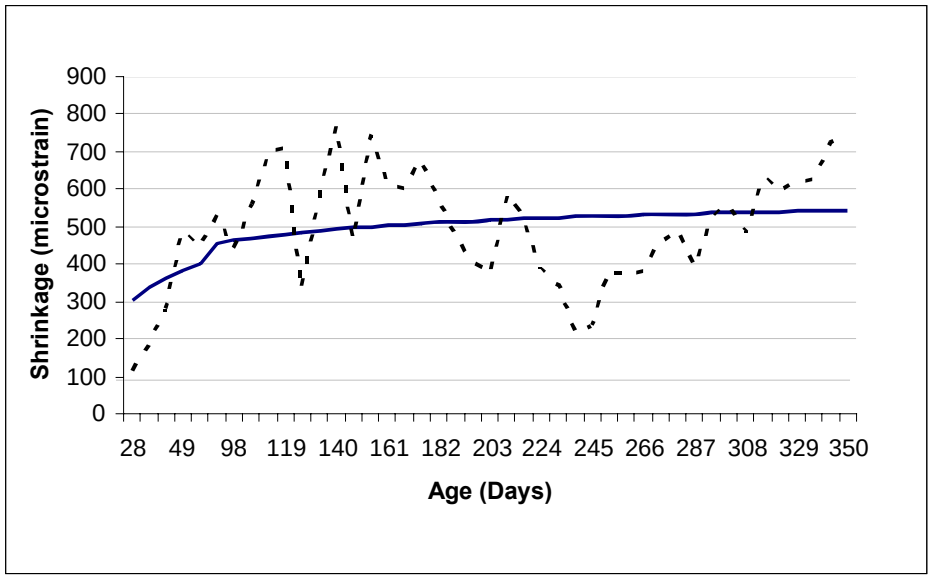

(c) 24SM Specimens

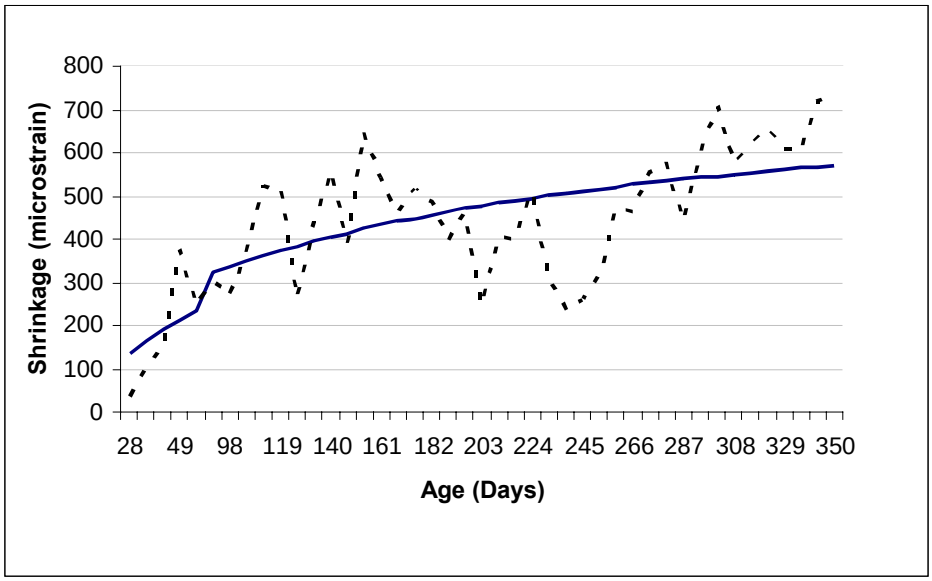

(d) MC Specimens

Figure 5.10. Humidity Modified Shrinkage Results for Large Pile Specimens (cont.)

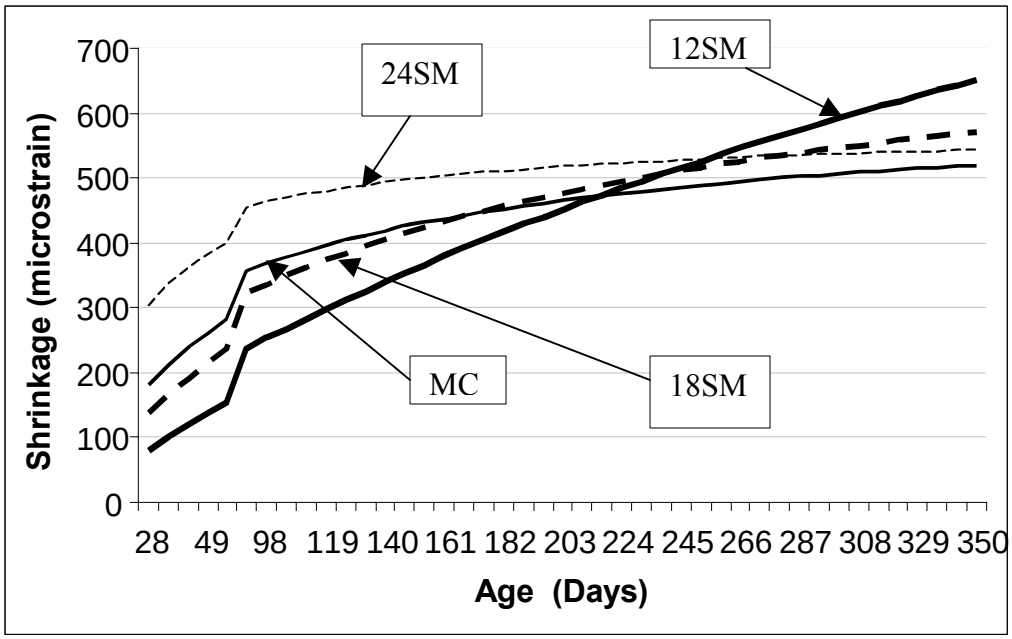

Figure 5.11. **Best-Fit Shrinkage Trendlines for Large Pile Specimens**

5.6.3 Size Effect on Shrinkage: Comparison between the shrinkage trend lines for the two different size pile specimens are shown in Fig. 5.12. Based on the graphs, the shrinkage growth for the small and large 12SM specimens were similar, with the larger shrinkage occurring within the smaller specimens. The small and large 18SM pile specimens show more difference in shrinkage growth, with the greater amount of shrinkage occurring within the larger specimens. The specimens that were moist cured demonstrated a very small difference in shrinkage between the two different sized samples. The small and large 24SM pile specimens displayed a large difference in shrinkage rates, with the larger shrinkage occurring within the smaller specimens.

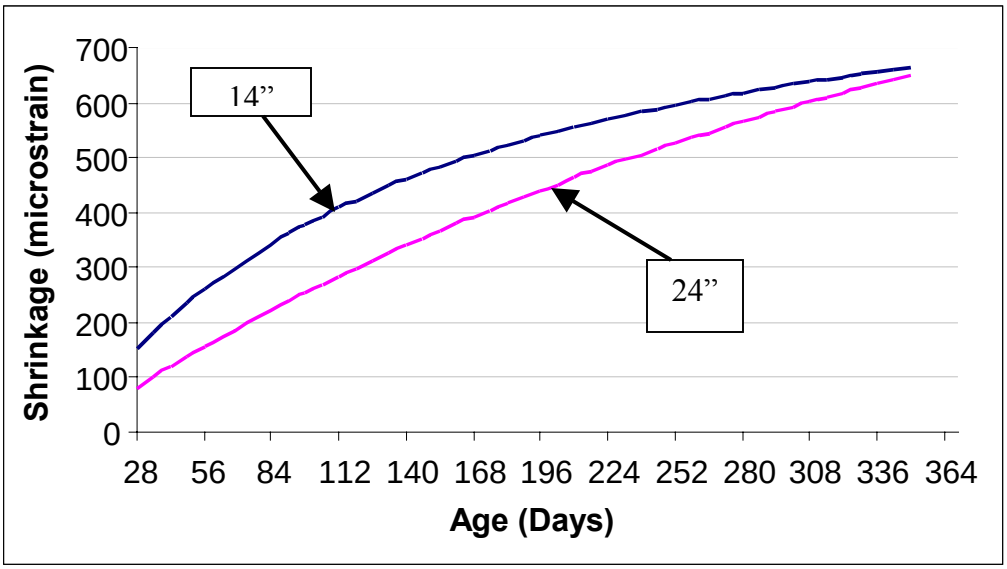

(a) 12SM Samples

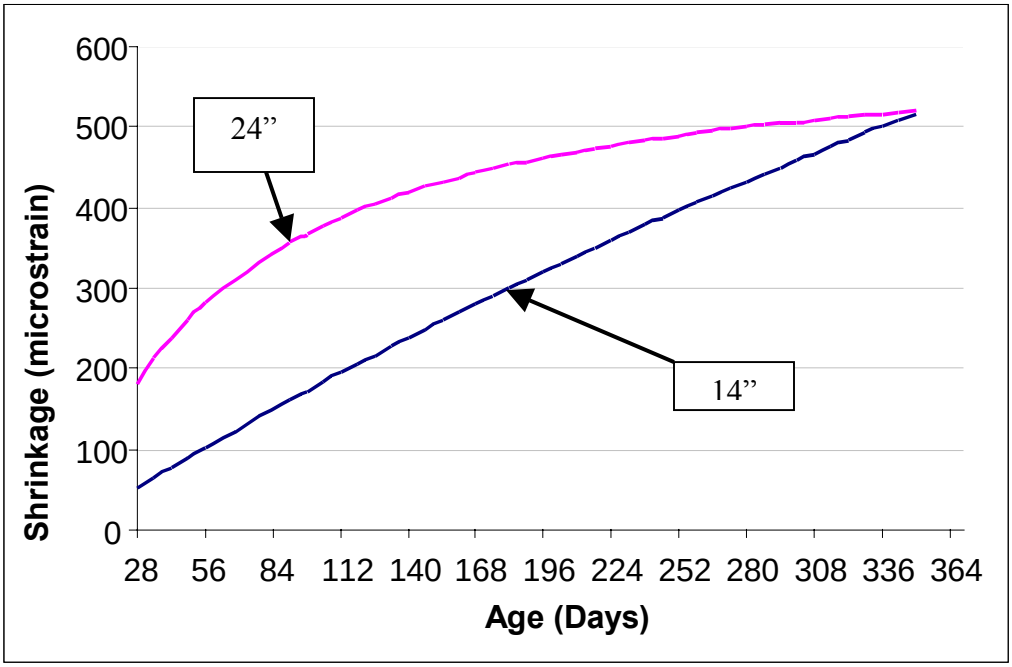

(b) 18SM Samples

Figure 5.12 Shrinkage Trendline Comparison for Small and Large Pile Specimens

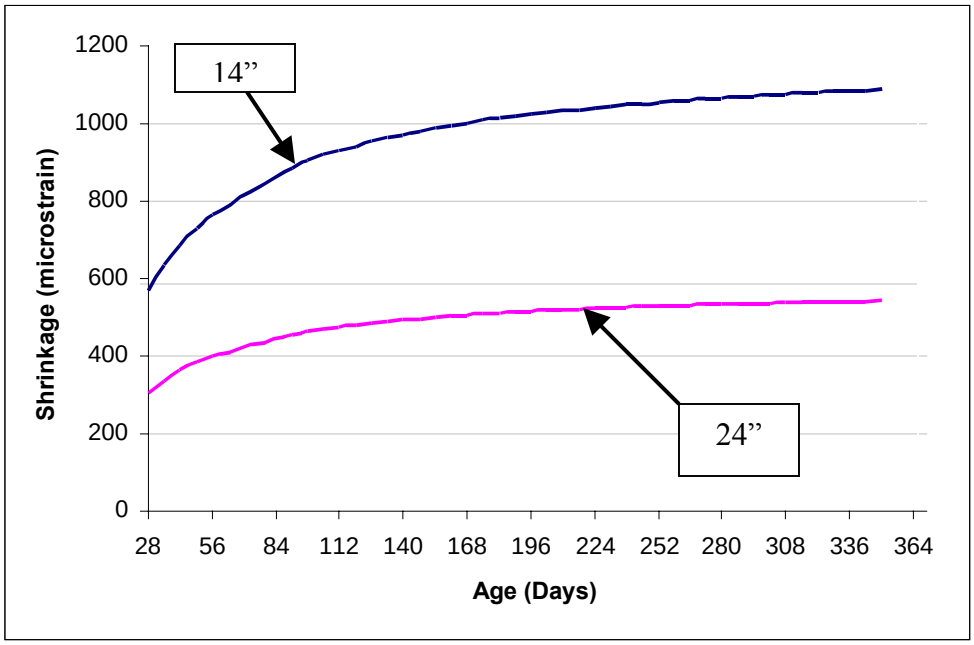

(c) 24SM Samples

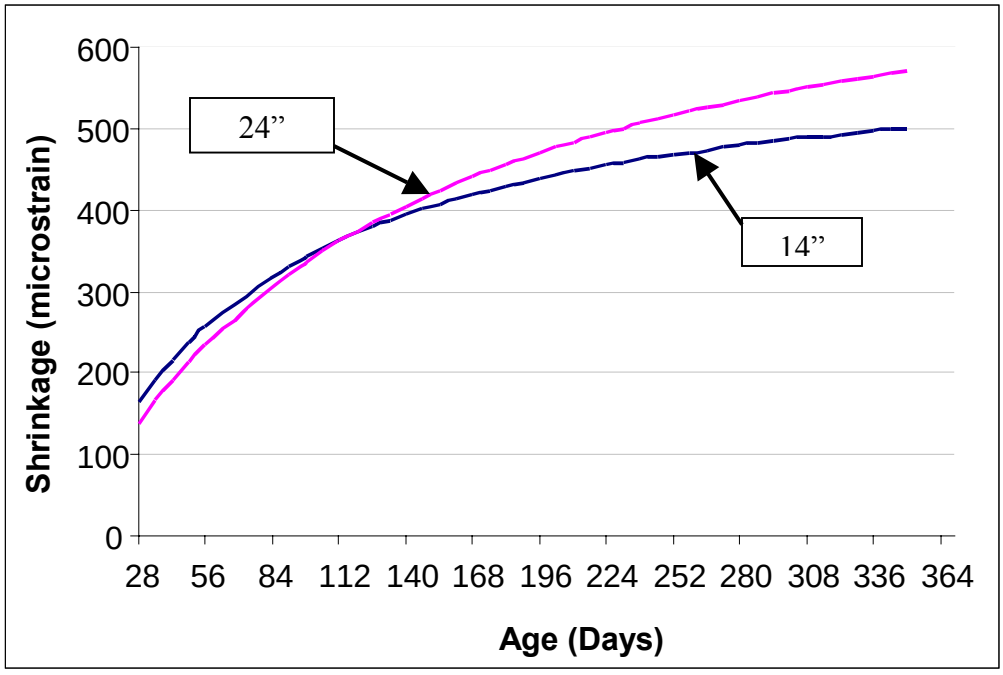

(d) MC Samples

Figure 5.12: Shrinkage Trendline Comparison for Small and Large Pile Specimens (cont.)

5.7 ACI Shrinkage Prediction

Due to the many variables among mix designs and several external factors that affect shrinkage within concrete, there is no current minimum or maximum amount of shrinkage that are allowable for design. As mentioned in Section 2.6, ACI adopted the Branson expression for shrinkage strain, Equations 2.1 and 2.2. The hyperbolic expression is based on several studies conducted under controlled environment. The ultimate shrinkage, $(\varepsilon_{sh})_u$, with a value of 800 x 10^{-6} mm/mm (in/in) at 40% humidity, is based on the Branson ultimate shrinkage strain at five years (Branson 1977).

A comparison of the shrinkage growth curve for the laboratory and pile data from this study and the ACI shrinkage curve was conducted herein. ACI Eqs. 2.1 and 2.2 were calculated at various concrete ages, as shown in Table D.6. ACI supplies only one generic shrinkage curve for all steam curing durations. Figure 5.13 displays the comparison of the ACI shrinkage strain prediction to shrinkage trendlines for the laboratory specimens. The shrinkage curve for the 12SM specimens remained well below the ACI curve. The shrinkage curve for the control MC specimens remained below the ACI curve, approaching it near the 365-day age. Both the 18SM and 24SM shrinkage curves surpassed the ACI curve, while the 24SD specimens showed lower shrinkage growth than the ACI prediction.

The pile specimens were stored in a non-controlled environment with varying humidity. To properly compare the ACI shrinkage relationships to the pile shrinkage, humidity correction factors were applied to the ACI equations. A regression analysis was performed on the actual shrinkage values to find the best-fit trend for the data. The ACI and the large pile modified shrinkage trendlines are plotted in Figs. 5.14 and 5.15.

It is obvious from Fig. 5.14 that the ACI shrinkage model at 365-day age predicts a shrinkage of about 534 x 10^{-6} and 565 x 10^{-6} for steam curing and moist curing, respectively, as expected. Most of the 356 mm (14 in) pile specimens displayed a shrinkage strain between 500-1000 x 10^{-6}, well above the ACI prediction. The 356 mm (14 in.) moist cured specimens showed a strain of about 500 x 10^{-6} at 365 days, slightly less than the ACI prediction. For the 610 mm (24 in.) piles, the 365-day shrinkage was 550-650 x 10^{-6}, close to the ACI prediction. The moist cured 610 mm (24 in.) pile samples showed 365-day shrinkage that were very close to the ACI prediction.

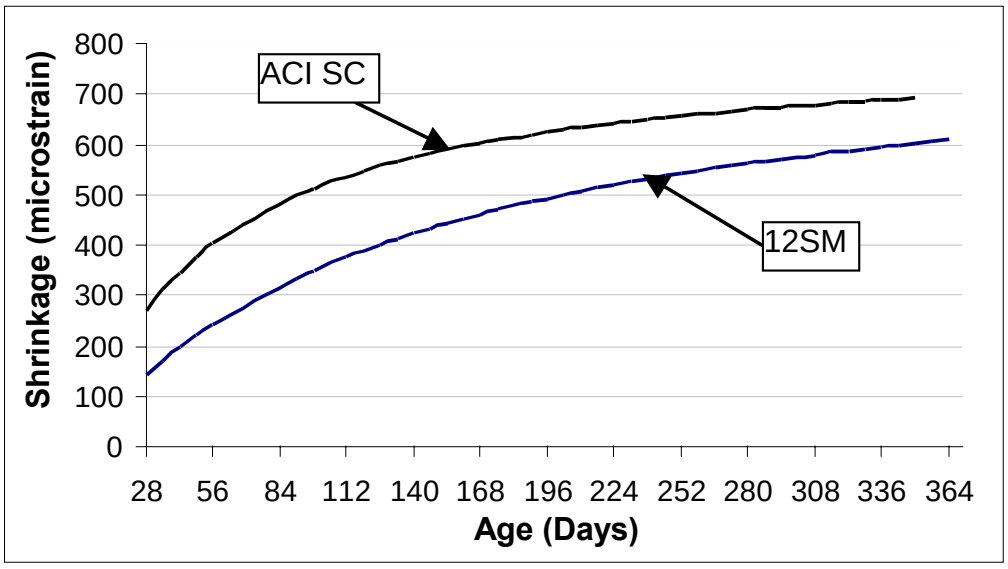

(a) ACI and 12SM

Figure 5.13: Comparison of ACI Shrinkage Predication to Laboratory Shrinkage Results

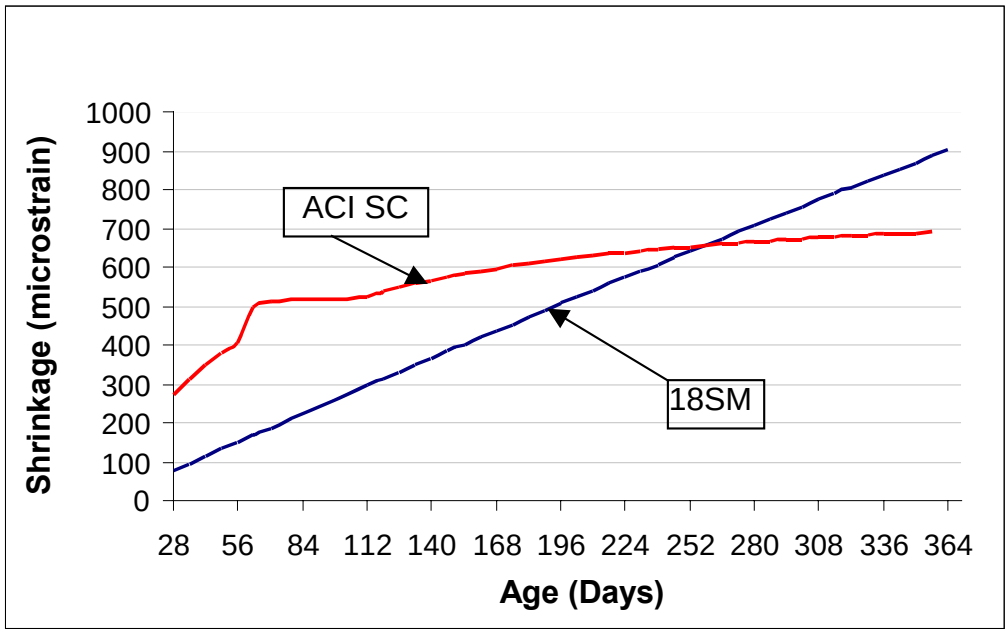

(b) ACI and 18SM

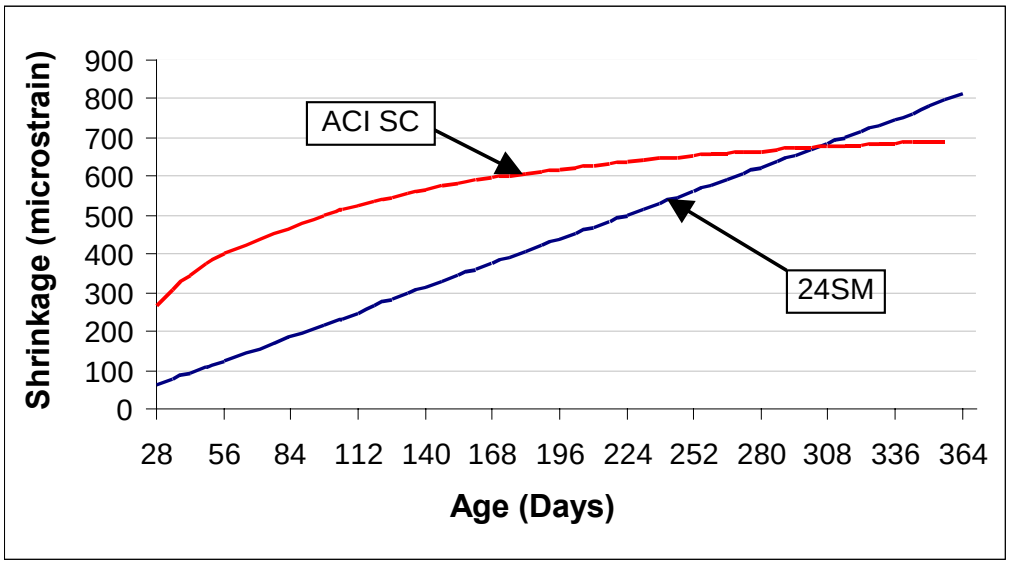

(c) ACI and 24SM

Figure 5.13: Comparison of ACI Shrinkage Predication to Laboratory Shrinkage Results (cont.)

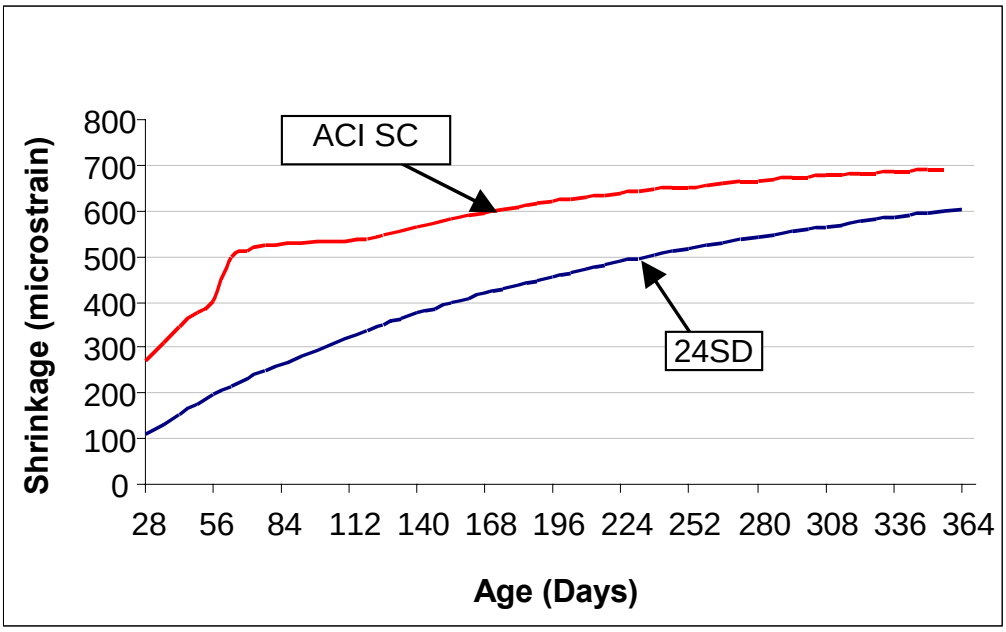

(d) ACI and 24SD

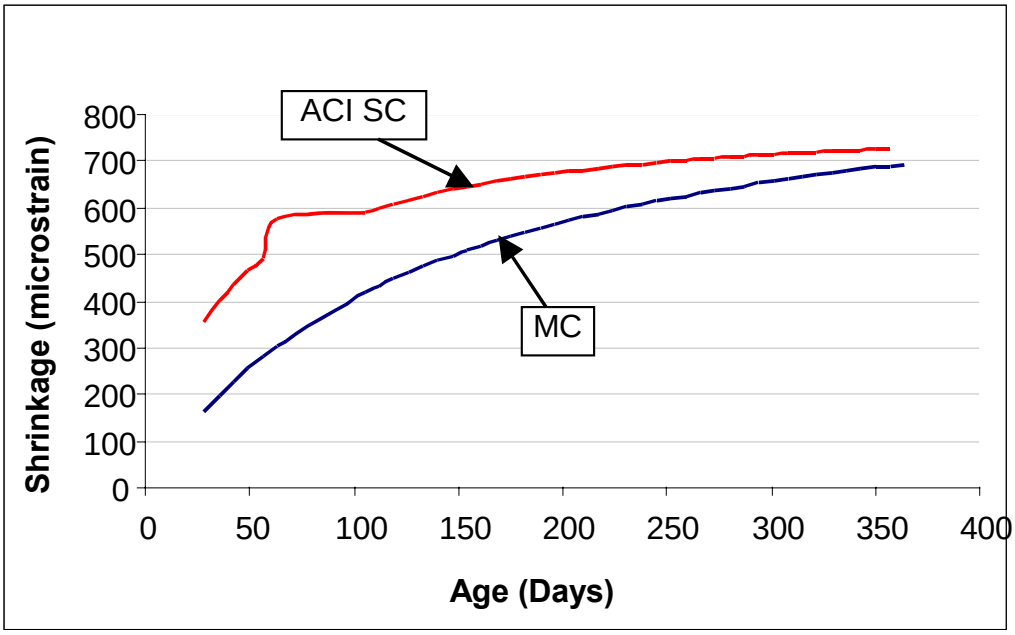

(e) ACI and MC

Figure 5.13: Comparison of ACI Shrinkage Predication to Laboratory Shrinkage Results (cont.)

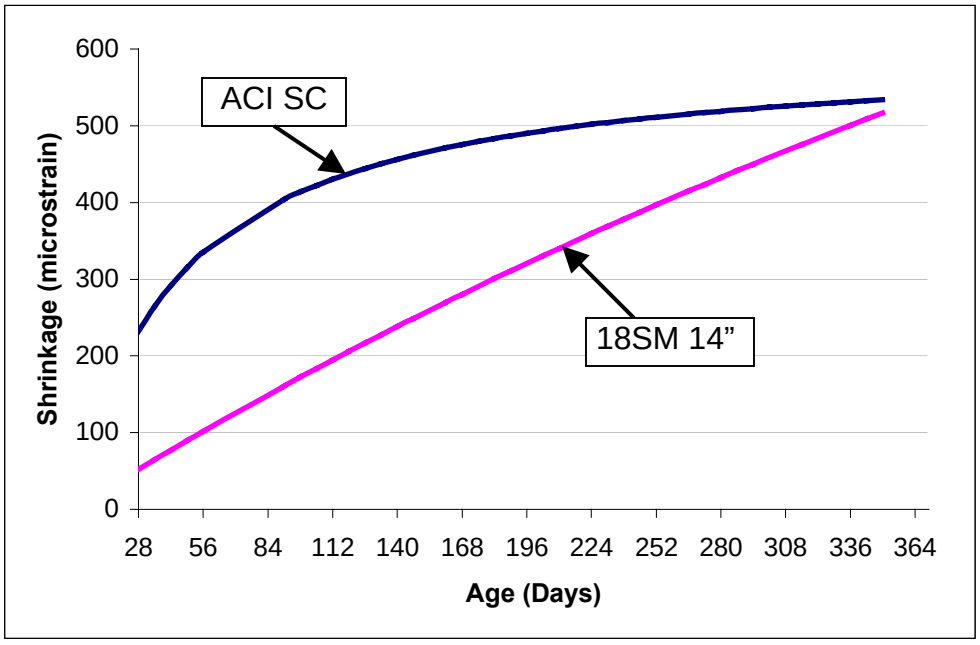

(a) 18SM

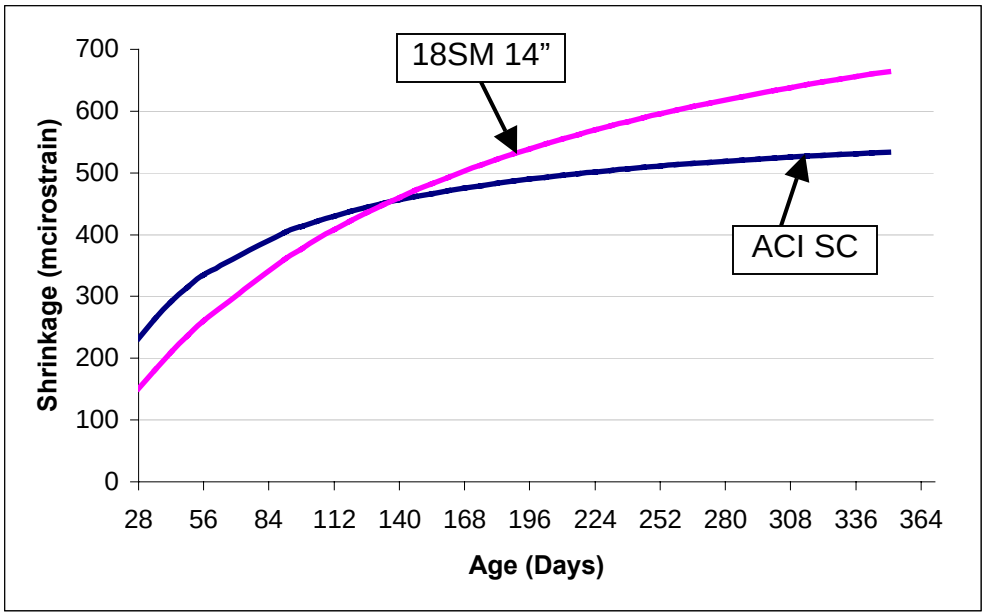

(b) 12SM

Figure 5.14: ACI and Large Pile Shrinkage Trendlines

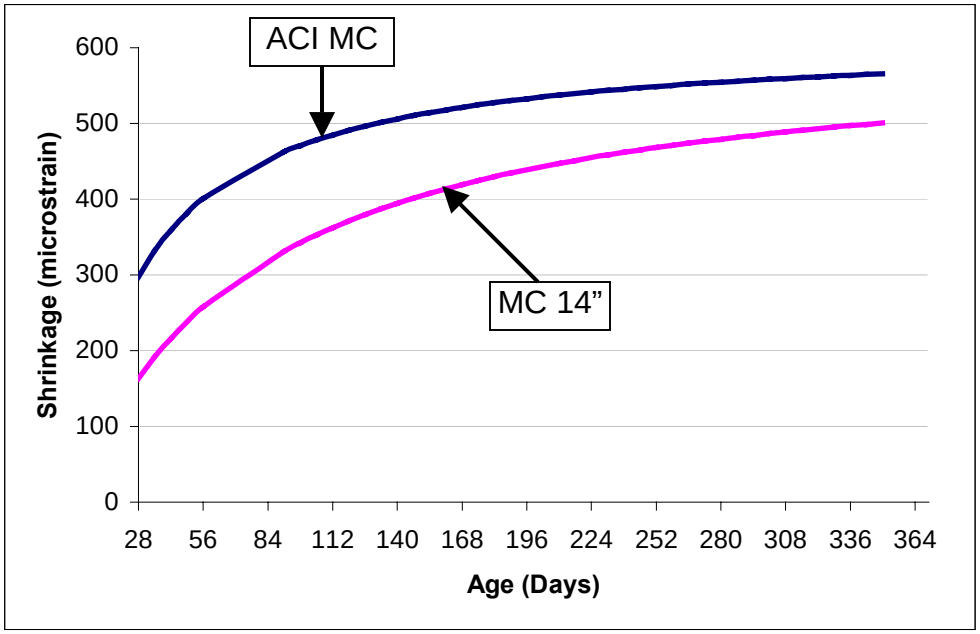

(c) MC

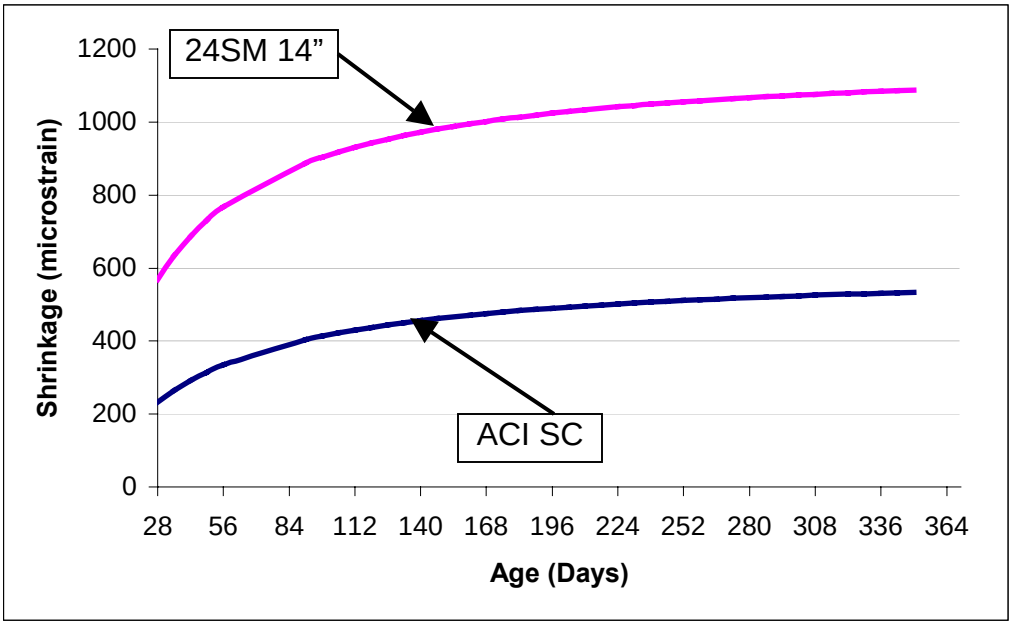

(d) 24SM

Figure 5.14: ACI and Large Pile Shrinkage Trendlines (cont.)

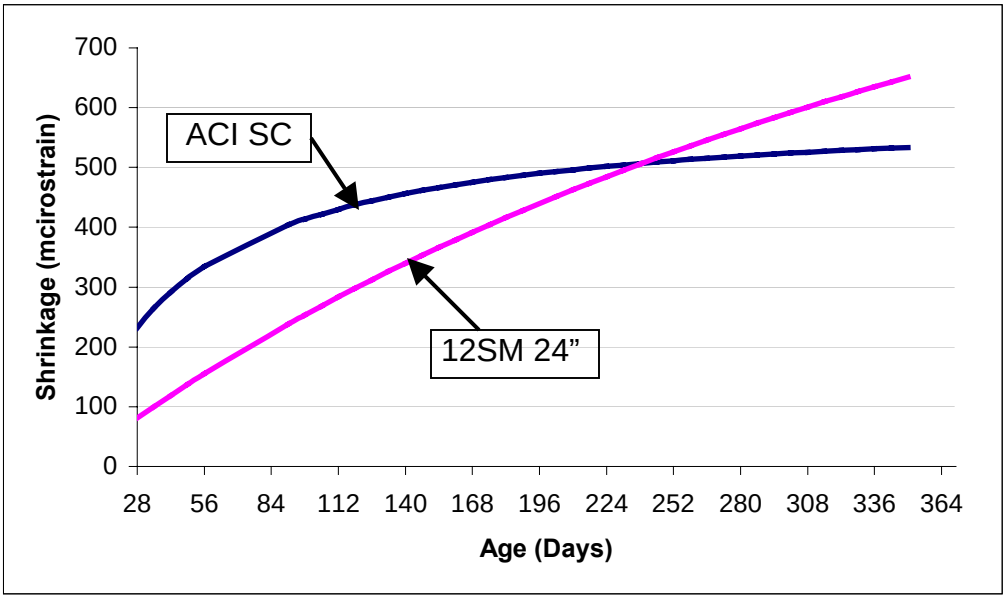

(a) 12SM

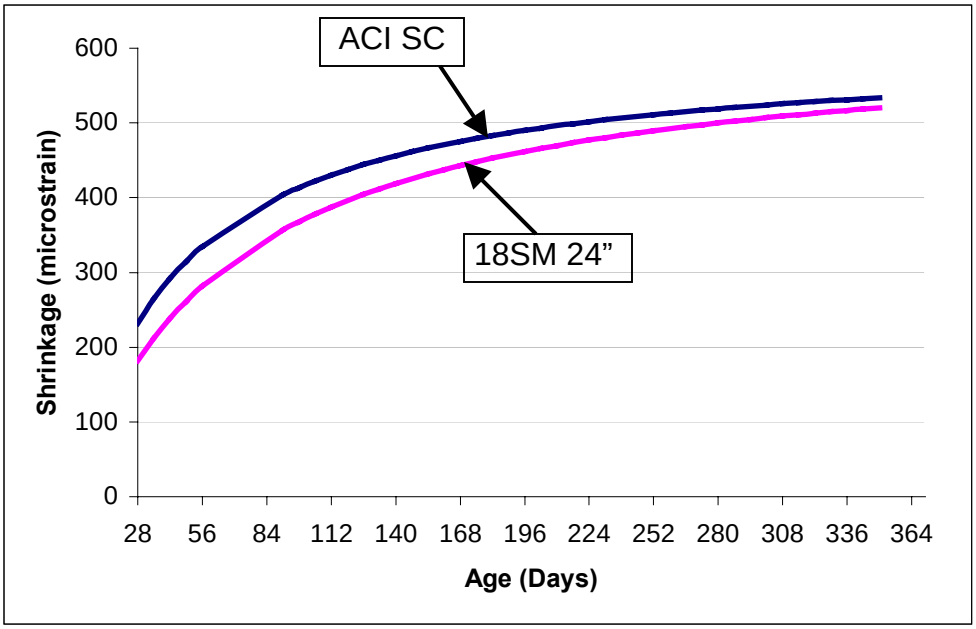

(b) 18SM

Figure 5.15: ACI and 24” Large Pile Shrinkage Trendlines

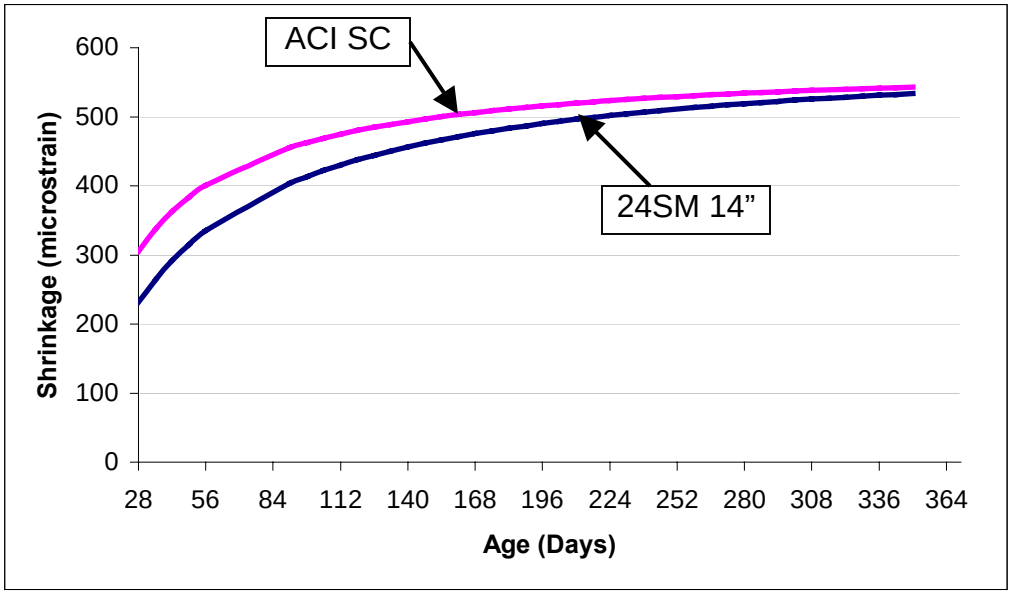

(c) 24SM

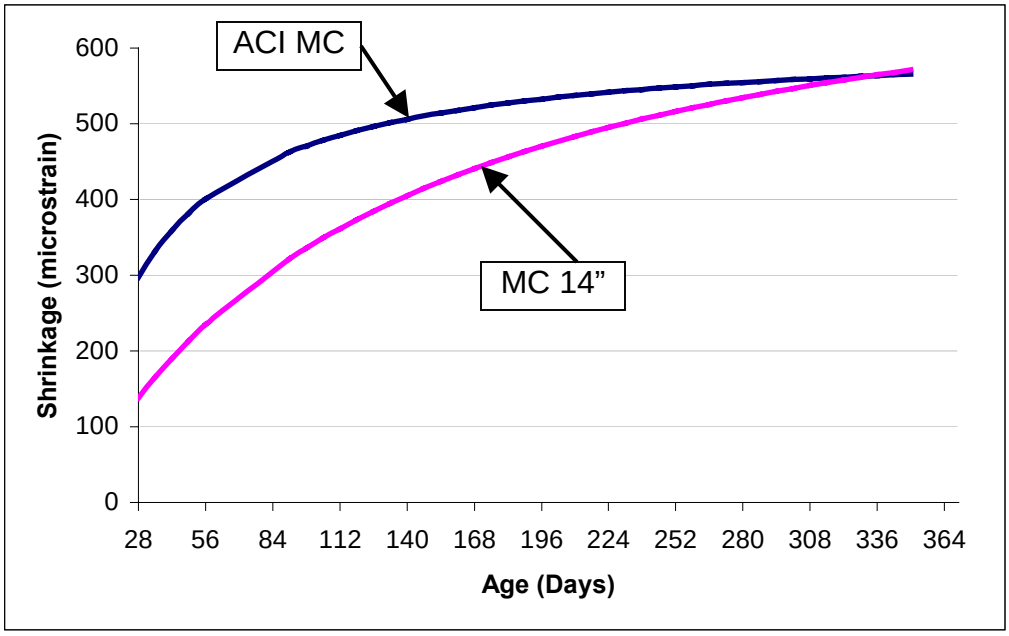

(d) MC

Figure 5.15: ACI and 24” Large Pile Shrinkage Trendlines (cont.)

Chapter 6

Conclusions and Recommendations

The following conclusions may be made based on the findings of this study:

1. Steam curing of silica fume precast concrete elements can be conveniently achieved with the present day technology and facilities available in large precast yards. This study has shown that it is easily possible to meet and even exceed the FDOT specifications regarding the temperature regimens during steam curing.
2. The steam curing temperature attainable in full-scale pile specimens is influenced by the specimen size. Larger pile specimens displayed higher maximum temperature gains (about 10 deg. C) as compared to the smaller pile specimens.
3. Steam cured silica fume concrete can achieve the target minimum compressive strengths, as specified in the FDOT specifications. In this study, most steam cured laboratory specimens and all field pile specimens reached the 28-day target strength of 41.37 MPa (6,000 psi) for the Class V mixes. All steam cured samples continued to gain in strength with time. At 365 day age, both the laboratory and field pile sample concrete displayed significantly higher compressive strengths than the 28-day strengths.
4. The steam cured samples displayed lower compressive strengths at all ages than their moist cured counterparts. This is consistent with previous research finding on silica fume concrete.
5. Steam curing times of 12, 18 and 24 hours do not seem to play a major role in controlling concrete compressive strengths. There was no consistent pattern of maximum strength displayed by samples from a single source of stem cured duration.

6. The surface resistivity of all samples increased significantly with time. The moist cured specimens gained surface resistivity at a much higher rate than the steam cured specimens, and at 365-day age, the moist cured samples displayed the greatest resistivity.
7. With previously published information as a comparative basis, the steam cured specimens displayed low-very low permeability and very low permeability at 28 and 364 day ages, respectively. Greater surface resistivity indicates lower permeability and increased long-term durability of concrete.
8. All steam cured and moist cured specimens showed a general increase in shrinkage with time. The steam curing duration did not seem to play a major role in affecting the shrinkage rates. At later stages, such as 364 day age, the longer steam curing periods such as 18 and 24 hours accelerate the shrinkage growth for the laboratory specimens.
9. The pile specimens underwent similar shrinkage trends as the laboratory specimens. The moist cured pile specimens showed lower shrinkage than the steam cured specimens in general. Again, the specimens with longer curing time showed more shrinkage, as compared to samples with shorter curing time.
10. Size of the pile specimens did not have a significant effect on the shrinkage rate. The larger and the smaller pile samples underwent similar shrinkage with time.
11. The ACI Banson model for shrinkage prediction under-predicts the shrinkage of steam cured specimens at 364 days, and over-predicts for the moist cured specimens.
12. During the 364 days of monitoring, no distress of the prestressed piles was observed due to shrinkage cracking. Visual inspections did not show any shrinkage cracks.

The following recommendations may be made based on the conclusions from this study:

1. It is recommended that FDOT allow steam curing of concrete with silica fume, as per the current FDOT specifications for steam curing of non-silica fume concrete. Such allowance will definitely be economical and efficient for precast yards. This recommendation is based on the fact that steam cured silica fume samples achieve the desired strength and durability levels, together with acceptable shrinkage rates and a lack of shrinkage related distress.
2. It is recommended that precast yards adopt a 12 – 24 hour period of steam curing for silica fume concrete elements. Typical current steam curing duration used by precasters is 10 – 18 hours.
3. It is recommended that FDOT continue the practice of 72 hours continuous total curing of silica fume concrete products. This means that the balance of the 72 hour requirement after the end of the steam curing time will be used for moist curing. The moist curing may be achieved through curing blankets or curing compound application.
4. Based on the results obtained in this study, it is recommended that Section 450-10.8 of the FDOT Specifications be modified as follows to allow steam curing as one of the options available to precast yards for the curing of FDOT bridge components produced with silica fume concrete:

   450-10.8 Curing Requirements for Silica Fume Concrete: Use either a 72 hour continuous moisture curing or a 12 – 24 hour duration low-pressure steam curing in accordance with 450-10.7. If the 72 hour continuous moist curing is used, begin curing silica fume concrete immediately after the finishing operation is complete, and keep a film of water on the surface by fogging until the curing blankets are in place. No

substitution of alternative methods nor reduction in the time period is allowed. After completion of the 72 hour curing period, apply a membrane curing compound to all concrete surfaces. Apply curing compound according to 450-10.6.

APPENDIX A

Mix Designs

Table A.1: Small Sample Mix Design

Issued	:	C.R. Davis
Reviewed	:	B. Ivery
Date	:	8/26/98
	:	

Concrete Mix Design

Class Concrete: V Special 41 MPa (6000 psi)

Coarse Aggregate	:		Grade	:	67 S.G. (SSD) : 2.50
Fine Aggreagete	:		F.M.	:	2.19 S.G. (SSD) : 2.63
Pit No. (Coarse)	:		Type	:	Crushed Limestone
Pit No. (Fine)	:		Type	:	Silica Sand
Cement	:		Spec	:	AASHTO M-85 Type II
Air Entr. Admix	:		Spec	:	AASHTO M-154
1st Admix	:		Spec	:	AASHTO M-194
2nd Admix	:		Spec	:	ASTM C-494 Type F
3rd Admix	:		Spec	:	ASTM C-1240
Fly Ash	:		Spec	:	ASTM C-618 Class F

Hot Weather Mix Design -------- Aggregate C.F. (0.8) -------- MBSF-110 has 28.9 (63.9) kg (lbs) of dry powder and contains 31.6 (69.7) kg (lbs) of water to include in w/c ratio

Cement kg (lbs)	:	251 (553)	Slump Range	:	140 to 216 (5.5 to 8.5) mm (in)
Coarse Agg. kg (lbs)	:	798 (1760)	Air Content	:	1.0 % to 5.0 %
Fine Agg. kg (lbs)	:	488 (1075)	Unit Weight (wet)	:	2275 (142) kg/m^3 (pcf)
Air Entr. Admix mL (oz)	:	166 (5.6)	W/C Ratio (Plant)	:	0.35 kg/kg (lbs/lb)
1st Admixture mL (oz)	:	444 (15.0)	W/C Ratio (Field)	:	0.35 kg/kg (lbs/lb)
2nd Admixture mL (oz)	:	1334 (45.1)	Theo Yield	:	0.78 m^3 (ft^3)
3rd Admixture mL (oz)	:	43976 (1487.0)			
Water kg (lbs)	:	87 (195.5)			
Fly Ash	:	61 (135)			

Producer Test Data

Chloride Cont	:	0.002 (0.221) kg/m^3 (pcf)
Slump	:	152.4 (6.00) mm (in)
Air Content	:	2.75%
Temperature	:	38 (100) DEG C (F)

Compressive Strength Mpa (psi)
28 -Day- 61 (8870)

Table A.2: GCP Pile Mix Design

Issued	:	F.C. Johns
Reviewed	:	B. Goldent
Date	:	10/27/95

Concrete Mix Design

Class Concrete: V Special 41 MPa (6000 psi)

Coarse Aggregate	:		Grade	:	67 S.G. (SSD) : 2.52
Fine Aggreagete	:		F.M.	:	2.57 S.G. (SSD) : 2.62
Pit No. (Coarse)	:		Type	:	River Gravel
Pit No. (Fine)	:		Type	:	Silica Sand
Cement	:		Spec	:	AASHTO M-85 Type II
Air Entr. Admix	:		Spec	:	AASHTO M-154
1st Admix	:		Spec	:	AASHTO M-194
2nd Admix	:		Spec	:	ASTM C-494 Type F
3rd Admix	:		Spec	:	ASTM C-1240
Fly Ash	:		Spec	:	ASTM C-618 Class F

Hot Weather Mix Design -------- W/C Contains 27.9 (61.7) kg (lbs) of water in Force 10000 and 27.3 (60.2) kg (lbs) of dry Microsilica. This mix cancel and supercedes mix no. 03-0269

Cement kg (lbs)	:	251 (553)	Slump Range	:	140 to 216 (5.5 to 8.5) mm (in)
Coarse Agg. kg (lbs)	:	798 (1760)	Air Content	:	1.0 % to 5.0 %
Fine Agg. kg (lbs)	:	488 (1075)	Unit Weight (wet)	:	2275 (142) kg/m^3 (pcf)
Air Entr. Admix mL (oz)	:	166 (5.6)	W/C Ratio (Plant)	:	0.35 kg/kg (lbs/lb)
1st Admixture mL (oz)	:	444 (15.0)	W/C Ratio (Field)	:	0.35 kg/kg (lbs/lb)
2nd Admixture mL (oz)	:	1334 (45.1)	Theo Yield	:	0.78 m^3 (ft^3)
3rd Admixture mL (oz)	:	43976 (1487.0)			
Water kg (lbs)	:	87 (195.5)			
Fly Ash	:	61 (135)			

Producer Test Data

Chloride Cont	:	0.002 (0.221) kg/m^3 (pcf)
Slump	:	152.4 (6.00) mm (in)
Air Content	:	2.75%
Temperature	:	38 (100) DEG C (F)

Compressive Strength MPa (psi)
28 -Day- 61 (8870)

APPENDIX B

Temperature Data

Table B.1: Temperature Log for 12SM Curing Cycle

Time	Ambient Temperature (°C)	Enclosure Temperature (°C)		Concrete Temperature (°C)					
20:28:06	26	60	62	35	43	32	41	36	40
21:28:06	26	62	63	59	63	57	64	59	62
22:28:06	26	66	67	69	68	69	68	68	69
23:28:06	26	68	68	71	69	72	69	70	71
0:28:06	26	70	69	72	70	73	70	71	71
1:28:06	26	70	69	73	71	73	70	72	72
2:28:06	25	71	69	72	71	73	70	71	72
3:28:06	25	70	69	72	71	73	70	71	72
4:28:06	25	70	69	72	71	73	70	71	71
5:28:06	25	70	69	72	71	72	70	71	71
6:28:06	25	70	68	71	70	72	70	70	71
7:28:06	25	70	69	71	70	71	70	70	70
8:28:06	25	69	68	70	69	71	69	69	70
9:28:06	25	66	65	69	68	70	69	68	69
10:28:06	25	60	59	65	64	67	65	64	65
11:28:06	25	54	52	60	59	63	60	60	60
12:28:06	25	51	49	56	56	59	55	57	55
13:28:06	25	49	47	53	53	56	51	54	52
14:28:06	25	47	46	51	50	53	49	52	50
15:28:06	25	46	44	49	49	51	48	50	48
16:28:06	25	44	43	47	47	49	45	48	46
17:28:06	24	41	42	45	45	48	44	46	45
18:28:06	24	39	40	44	41	46	41	45	44
19:28:06	24	38	39	43	39	45	39	43	42
20:28:06	24	36	37	41	38	43	38	42	41
21:28:06	24	34	36	40	36	40	37	40	39
22:28:06	24	33	35	39	35	39	35	39	38
23:28:06	24	32	33	37	34	38	34	37	37
0:28:06	24	31	30	35	31	36	31	36	35
1:28:06	24	29	27	34	29	33	29	34	34
2:28:06	24	28	26	33	28	31	28	33	32
3:28:06	24	26	24	30	27	30	27	31	31

Table B.2: Temperature Log for 18SM Curing Cycle

Time	Ambient Temperature (°C)	Enclosure Temperature (°C)		Concrete Temperature (°C)					
15:52:26	28	61	64	31	30	38	28	33	32
16:52:26	27	69	70	69	62	68	62	66	62
17:52:26	27	75	76	76	77	76	76	76	76
18:52:26	27	78	79	79	81	80	80	79	80
19:52:26	26	79	79	80	82	82	81	80	81
20:52:26	26	80	79	79	82	83	82	81	82
21:52:26	26	80	78	79	82	83	82	81	82
22:52:26	26	77	75	76	81	81	81	80	81
23:52:26	26	74	72	74	78	79	79	77	79
0:52:26	26	72	70	71	76	76	76	75	76
1:52:26	25	70	69	68	73	73	73	72	73
2:52:26	25	68	68	66	71	71	71	70	71
3:52:26	25	66	66	65	69	69	69	68	69
4:52:26	25	65	65	63	68	67	67	66	67
5:52:26	25	63	64	62	66	65	66	65	66
6:52:26	24	62	63	61	65	64	65	63	64
7:52:26	24	61	62	60	64	63	63	62	63
8:52:26	23	60	62	59	63	62	62	61	62
9:52:26	24	58	59	58	62	61	61	60	61
10:52:26	24	52	52	56	59	58	59	58	59
11:52:26	25	49	48	52	56	55	56	54	55
12:52:26	25	45	45	49	53	51	53	51	52
13:52:26	25	44	43	46	50	48	50	47	49
14:52:26	25	46	46	45	48	46	49	46	48
15:52:26	25	45	44	45	47	46	47	45	47
16:52:26	26	45	44	45	46	45	47	45	46
17:52:26	27	44	43	45	46	45	46	45	45
18:52:26	27	43	42	44	45	44	45	44	45
19:52:26	27	40	39	43	43	43	44	43	43
20:52:26	26	37	36	40	41	40	42	40	41
21:52:26	26	35	34	38	39	38	40	38	41
22:52:26	26	33	32	36	37	36	38	36	39
23:52:26	26	25	22	31	33	31	34	31	37
0:52:26	26	22	20	27	29	27	30	27	32
1:52:26	25	22	19	24	26	24	27	24	26

Table B.3: Temperature Log for 24SM Curing Cycle

Time	Ambient Temperature (°C)	Enclosure Temperature (°C)		Concrete Temperature (°C)					
15:49:14	26	62	62	38	26	29	29	34	32
16:49:14	26	65	65	62	64	56	55	58	62
17:49:14	26	68	68	70	71	70	68	69	71
18:49:14	26	70	70	73	72	74	74	73	74
19:49:14	26	70	70	74	69	76	77	75	75
20:49:14	25	71	69	73	69	75	77	74	74
21:49:14	25	73	69	72	68	75	76	73	73
22:49:14	24	73	70	72	68	74	75	73	72
23:49:14	24	73	69	72	67	73	74	72	72
0:49:14	24	73	70	71	68	73	74	72	72
1:49:14	24	73	71	71	67	72	74	71	71
2:39:14	24	68	68	70	65	72	73	70	71
2:49:14	24	67	67	70	64	71	73	70	70
3:49:14	24	65	66	68	63	70	71	68	69
4:49:14	24	64	65	66	61	68	70	66	67
5:49:14	23	62	64	65	60	66	68	64	66
6:49:14	23	61	63	63	59	65	67	63	64
7:49:14	23	59	62	62	58	63	65	61	63
8:49:14	23	59	61	61	56	62	64	60	62
9:49:14	23	58	62	60	55	61	63	60	61
10:49:14	23	58	62	60	52	61	63	59	61
11:49:14	23	58	62	60	55	60	63	59	61
12:49:14	24	58	63	60	55	60	63	59	61
13:49:14	24	60	64	60	52	60	63	60	62
14:49:14	24	65	69	62	56	62	64	62	63
15:49:14	25	69	73	66	59	65	66	65	66
16:49:14	26	62	62	65	63	65	67	65	66
17:49:14	26	57	57	63	64	64	65	62	64
18:49:14	27	52	52	59	60	61	62	60	60
19:49:14	26	47	46	55	55	57	58	56	56
20:49:14	25	43	42	50	50	53	54	52	51
21:49:14	25	40	38	46	46	49	50	48	47
22:49:14	25	37	36	42	42	45	46	44	43
23:49:14	25	35	33	39	39	42	43	41	40
2:49:14	24	30	28	32	32	34	35	34	33

Table B.4: Temperature Log for 24SD Curing Cycle

Time	Ambient Temperature (°C)	Enclosure Temperature (°C)		Concrete Temperature (°C)					
16:08:11	32	61	62	28	26	34	25	26	25
17:08:11	28	68	68	62	58	64	54	65	53
18:08:11	28	74	75	75	75	75	75	75	74
19:08:11	28	78	79	80	80	79	81	79	80
20:08:11	27	78	79	81	81	80	83	79	82
21:08:11	27	78	79	81	81	80	84	78	83
22:08:11	26	79	78	81	81	80	84	78	83
23:08:11	26	79	79	81	81	79	83	77	82
0:08:11	26	77	76	81	80	78	82	76	81
1:08:11	26	76	76	80	78	77	81	75	80
2:08:11	26	75	74	79	77	75	80	74	79
3:08:11	26	74	73	77	75	74	78	73	77
4:08:11	26	73	73	76	74	73	77	72	76
5:08:11	25	72	72	75	73	72	76	71	74
6:08:11	25	71	71	75	72	71	75	71	73
7:08:11	25	70	70	74	71	70	74	70	72
8:08:11	25	69	70	73	70	69	73	70	71
9:08:11	25	68	70	73	69	68	72	69	70
10:08:11	25	68	70	72	68	67	71	69	69
11:08:11	25	68	71	72	68	67	71	70	69
12:08:11	25	68	70	72	68	67	71	70	68
13:08:11	25	68	71	72	68	67	70	70	68
14:08:11	25	72	73	72	68	69	70	71	68
15:08:11	26	75	76	74	72	72	72	74	71
16:08:11	26	74	75	76	74	74	74	76	74
17:08:11	27	52	52	72	65	62	71	70	68
18:08:11	27	49	51	64	59	55	66	61	62
19:08:11	27	44	45	58	54	51	62	55	57
20:08:11	27	40	41	52	50	46	56	49	52
21:08:11	27	32	28	46	45	40	50	43	47
22:08:11	26	34	32	37	39	34	43	36	40
23:08:11	26	33	32	32	35	31	38	32	36
0:08:11	26	32	31	30	33	29	35	30	33
1:08:11	26	31	30	28	31	28	32	29	31

Table B.5: Thermal Log for the GPC Curing Cycle

Time	Concrete Temperature (°C)			
14:23:39	34	33	33	33
15:23:23	38	37	36	36
16:23:23	44	42	41	41
17:23:23	54	52	50	50
18:23:23	59	57	54	54
19:23:23	61	60	56	56
20:23:23	62	61	57	56
21:23:23	62	62	57	56
22:23:23	64	63	58	57
23:23:23	66	65	59	57
00:23:23	68	67	60	58
01:23:23	68	69	61	59
02:23:23	68	69	61	60
03:23:23	68	69	61	60
04:23:23	68	69	61	60
05:23:23	67	69	60	60
06:23:23	67	69	60	60
07:23:23	67	69	60	60
08:23:23	67	69	59	60
09:23:23	67	70	60	60
10:23:23	67	70	60	61
11:23:23	64	67	59	60
12:23:23	61	64	57	60
13:23:23	58	60	56	59
14:23:23	56	58	55	58

APPENDIX C

Surface Resistivity Data

Table C.1: Surface Resistivity Data, 12SM

14 Day Test	Angle								
SAMPLE	**0**	**90**	**180**	**270**	**0**	**90**	**180**	**270**	**Average**
A	12.9	15.6	14.7	15.8	12.3	15.6	14.3	14.5	14.5
B	19.0	18.8	17.4	18.5	18.2	18.8	17.5	18.2	18.3
C	16.4	16.6	16.1	16.7	16.4	16.5	15.9	17.6	16.5
D	15.5	16.9	15.6	15.4	15.5	16.8	16.1	16.1	16.0
E	16.7	15.8	14.9	15.5	16.2	15.7	16.3	15.4	15.8
	Overall								**16.2**
28 Day Test									
A	21.9	27.1	24.5	25.1	22.0	25.9	24.0	25.1	24.5
B	29.2	28.0	28.2	28.1	29.4	27.2	28.6	28.6	28.4
C	24.5	25.8	25.3	24.8	24.3	25.8	24.2	25.2	25.0
D	24.9	27.6	26.6	26.3	25.7	27.3	27.1	26.6	26.5
E	24.5	24.1	23.2	23.8	24.8	24.3	23.2	23.8	24.0
	Overall								**25.7**
56 Day Test									
A	39.1	45.0	43.8	43.4	39.2	46.5	43.8	44.7	43.2
B	50.9	49.5	52.4	46.5	51.7	50.0	50.5	48.2	50.0
C	45.0	41.6	44.7	44.5	44.7	42.8	42.5	43.5	43.7
D	44.7	44.9	48.8	53.6	48.1	46.2	48.6	53.3	48.5
E	42.7	43.2	42.1	41.5	43.1	42.9	42.5	41.6	42.5
	Overall								**45.6**
91 Day Test									
A	53.9	61.0	62.8	61.1	53.0	64.5	59.7	62.7	59.8
B	65.5	64.4	68.6	60.7	67.3	65.8	68.8	61.4	65.3
C	60.6	57.1	60.5	64.0	60.6	360.5	58.9	58.4	97.6
D	64.4	64.1	66.4	70.1	65.5	62.0	63.4	74.4	66.3
E	59.8	60.0	60.1	57.4	61.6	58.8	61.0	56.2	59.4
	Overall								**69.7**
182 Day Test									
A	70.6	78.4	85.1	82.7	70.2	77.9	81.6	78.9	78.2
B	83.3	84.1	88.7	79.6	84.2	84.7	87.5	81.7	84.2
C	74.5	70.4	77.2	79.0	75.0	71.4	76.8	79.8	75.5
D	84.2	82.4	83.7	87.3	83.7	79.6	84.7	85.7	83.9
E	73.0	76.0	75.8	77.0	74.0	76.9	75.9	75.0	75.5
	Overall								**79.5**
364 Day Test									
A	109.6	111.4	98.0	102.4	105.4	112.7	93.6	103.4	104.6
B	125.9	114.3	107.6	105.8	126.5	120.5	111.2	107.4	114.9
C	100.4	93.9	90.7	100.8	103.0	97.3	91.7	90.4	96.0
D	98.2	102.8	105.3	108.5	99.3	100.8	108.5	105.8	103.7
E	81.7	94.7	90.7	86.5	80.0	92.5	93.3	88.8	88.5
	Overall								**101.5**

Table C.2: Surface Resistivity Data, 18SM

14 Day Test	Angle								
SAMPLE	**0**	**90**	**180**	**270**	**0**	**90**	**180**	**270**	**Average**
A	26.7	24.6	26.0	26.5	27.0	24.4	27.3	26.7	26.2
B	26.1	26.8	27.0	28.4	25.2	27.4	23.8	29.0	26.7
C	26.3	28.3	27.0	26.3	26.2	25.5	27.0	25.6	26.5
D	27.4	27.6	25.3	27.5	27.7	27.1	26.8	27.9	27.2
E	32.2	32.8	30.6	32.7	32.8	34.1	31.5	32.5	32.4
	Overall								**27.8**
28 Day Test									
A	35.6	31.3	34.7	33.7	36.3	31.8	36.1	35.5	34.4
B	31.2	31.8	32.7	38.5	32.4	33.1	34.2	38.2	34.0
C	32.3	37.9	33.4	35.5	33.7	38.3	35.6	34.3	35.1
D	36.1	34.8	34.9	35.4	36.8	35.2	36.8	33.0	35.4
E	38.5	40.9	38.7	39.5	39.8	41.1	36.3	39.1	39.2
	Overall								**35.6**
56 Day Test									
A	53.4	45.6	53.5	52.2	55.3	48.2	56.0	56.5	52.6
B	47.4	48.1	52.2	52.5	46.7	46.5	47.0	53.6	49.3
C	44.1	45.9	47.6	49.0	45.1	53.2	48.1	48.6	47.7
D	50.6	49.7	50.9	50.4	53.8	50.0	51.3	51.1	51.0
E	57.2	58.8	55.1	56.9	58.5	57.9	55.6	56.3	57.0
	Overall								**51.5**
91 Day Test									
A	37.9	39.9	39.9	36.8	36.1	36.0	36.5	35.6	37.3
B	53.7	54.3	61.8	59.6	53.5	53.9	58.7	55.6	56.4
C	50.5	58.7	53.8	59.8	51.1	54.5	59.7	51.5	55.0
D	58.0	57.0	57.2	56.4	56.0	58.6	56.2	55.9	56.9
E	64.0	65.0	64.5	67.1	61.9	65.8	63.0	67.3	64.8
	Overall								**54.1**
182 Day Test									
A	86.6	84.3	91.0	95.2	86.6	85.2	93.7	93.8	89.6
B	86.1	88.2	90.2	93.8	86.8	85.1	82.5	88.6	87.7
C	74.9	73.2	74.2	82.2	73.7	76.6	75.2	82.3	76.5
D	84.6	86.0	88.8	90.7	88.3	83.1	88.8	89.1	87.4
E	82.8	89.5	92.0	84.0	79.4	85.5	89.9	83.9	85.9
	Overall								**85.4**
364 Day Test									
A	103.3	112.1	101.8	103.3	105.2	114.0	103.8	103.4	105.9
B	106.2	98.1	92.6	96.4	105.8	96.3	91.3	99.6	98.3
C	103.3	105.6	103.4	103.3	103.1	102.0	103.4	103.1	103.4
D	107.6	115.2	104.9	107.6	111.6	113.6	102.1	105.9	108.6
E	94.0	110.0	102.0	97.6	88.7	113.1	99.6	96.1	100.1
	Overall								**103.3**

Table C.3: Surface Resistivity Data, 24SM

14 Day Test	Angle								
SAMPLE	**0**	**90**	**180**	**270**	**0**	**90**	**180**	**270**	**Average**
A	21.5	23.5	24.0	22.5	22.5	23.1	22.7	24.9	23.1
B	21.5	23.2	23.1	20.8	21.6	24.0	23.3	21.4	22.4
C	19.5	18.8	19.0	20.5	19.6	18.9	19.5	20.4	19.5
D	21.1	20.7	19.8	18.6	19.1	20.1	20.7	18.7	19.9
E	16.6	16.2	17.1	18.0	16.6	15.3	17.7	16.9	16.8
	Overall								**20.3**
28 Day Test									
A	37.1	34.6	34.2	34.6	36.4	35.6	34.0	35.6	35.3
B	33.2	34.4	35.1	34.3	32.0	34.8	34.0	34.2	34.0
C	30.5	28.6	31.8	31.2	30.3	29.0	31.3	32.6	30.7
D	35.1	32.8	34.0	32.3	35.0	33.0	33.6	31.9	33.5
E	29.3	28.2	31.2	31.3	29.7	30.0	32.1	31.8	30.5
	Overall								**32.8**
56 Day Test									
A	55.3	52.3	48.2	50.2	53.8	53.1	48.6	52.8	51.8
B	47.5	52.8	50.4	50.3	47.2	54.3	50.3	50.3	50.4
C	42.8	40.6	44.5	48.2	42.7	42.2	45.0	45.9	44.0
D	51.3	48.5	50.0	47.7	51.7	48.2	49.1	47.6	49.3
E	43.4	38.5	46.6	48.0	42.8	49.3	46.9	47.5	45.4
	Overall								**48.2**
91 Day Test									
A	64.0	64.3	56.8	59.6	66.8	62.6	57.9	63.7	62.0
B	59.5	67.6	66.4	63.8	59.1	66.7	64.9	62.5	63.8
C	54.8	51.6	55.1	57.0	54.9	53.9	57.9	56.5	55.2
D	62.4	62.7	63.1	59.3	63.3	60.3	61.1	60.2	61.6
E	54.4	47.6	57.6	56.2	54.1	52.6	56.9	59.4	54.9
	Overall								**59.5**
182 Day Test									
A	74.4	75.6	75.7	83.2	75.6	74.4	79.3	83.6	77.7
B	81.2	68.8	75.0	79.1	77.5	74.4	74.1	79.8	76.2
C	85.5	84.0	85.7	85.1	84.2	83.8	85.4	84.3	84.8
D	85.9	88.5	74.9	78.4	80.7	89.2	75.4	77.3	81.3
E	86.4	86.4	88.5	85.3	86.5	89.1	88.2	90.3	87.6
	Overall								**81.5**
364 Day Test									
A	127.9	138.2	125.6	124.8	127.1	134.2	124.8	120.8	127.9
B	115.6	108.2	102.6	106.6	118.9	109.6	100.3	108.4	108.8
C	35.0	88.0	96.4	97.1	96.4	89.4	91.6	98.2	86.5
D	126.8	121.8	119.6	128.3	131.1	120.1	120.0	128.8	124.6
E	117.7	130.8	113.9	111.1	117.3	132.4	111.5	111.4	118.3
	Overall								**113.2**

Table C.4: Surface Resistivity Data, 24SD

14 Day Test	Angle								
Sample	**0**	**90**	**180**	**270**	**0**	**90**	**180**	**270**	**Average**
A	28.7	30.3	26.6	29.6	27.9	28.5	26.0	29.4	28.4
B	30.3	29.1	29.5	33.1	30.2	29.4	29.2	33.3	30.5
C	31.7	30.9	30.9	30.9	30.6	30.9	31.0	30.3	30.9
D	26.1	30.9	27.0	32.0	26.2	31.2	26.5	31.0	28.9
E	33.6	33.1	32.1	29.3	33.4	32.7	32.3	29.3	32.0
	Overall								**30.1**
28 Day Test									
A	33.9	32.9	31.9	32.0	33.1	33.4	30.5	32.4	32.5
B	35.2	36.5	33.5	32.3	33.7	36.4	34.3	33.2	34.4
C	30.5	34.0	35.9	36.1	33.2	33.4	36.5	37.3	34.6
D	30.8	35.1	30.2	35.4	30.4	34.8	30.5	35.7	32.9
E	36.0	31.9	35.8	36.5	35.7	32.4	35.9	35.3	34.9
	Overall								**33.9**
56 Day Test									
A	45.3	43.5	41.2	45.3	43.8	43.0	40.2	43.0	43.2
B	42.9	41.9	47.7	47.2	43.2	41.8	46.9	47.2	44.9
C	43.7	44.5	47.1	42.4	44.3	44.8	47.4	42.6	44.6
D	41.7	48.7	40.4	45.3	41.2	46.9	39.9	46.6	43.8
E	44.3	44.9	43.5	42.1	44.6	45.7	44.1	42.0	43.9
	Overall								**44.1**
91 Day Test									
A	59.6	61.4	60.0	57.4	60.9	58.7	59.2	62.8	60.0
B	57.4	64.0	60.5	55.4	58.8	64.9	56.4	54.5	59.0
C	59.1	60.4	64.5	53.4	63.8	66.0	63.3	64.6	61.9
D	55.4	54.8	54.6	67.2	56.6	61.0	55.2	64.7	58.7
E	59.5	56.3	60.0	63.3	61.6	56.2	61.2	64.3	60.3
	Overall								**60.0**
182 Day Test									
A	79.6	75.0	81.2	78.5	72.7	78.1	73.2	80.1	77.3
B	72.0	83.9	73.8	70.6	72.2	83.8	77.2	70.9	75.6
C	71.0	84.3	82.2	84.5	75.7	84.7	82.9	86.0	81.4
D	67.8	77.5	71.1	81.2	67.3	78.5	69.1	89.8	75.3
E	93.3	94.3	97.1	96.5	94.4	92.0	93.1	96.6	94.7
	Overall								**80.8**
364 Day Test									
A	86.8	92.4	93.3	88.3	85.7	90.4	99.1	86.2	90.3
B	111.4	120.0	126.0	103.0	117.3	123.2	122.4	110.0	116.7
C	100.0	102.5	94.5	92.9	98.6	106.7	91.2	91.9	97.3
D	84.6	82.8	99.5	86.5	82.2	77.4	99.7	96.2	88.6
E	116.2	136.7	123.6	123.4	116.3	120.1	116.8	128.8	122.7
	Overall								**103.1**

Table C.5: Surface Resistivity Data, MC

14 Day Test	Angle								
SAMPLE	**0**	**90**	**180**	**270**	**0**	**90**	**180**	**270**	**Average**
A	7.9	7.4	8.1	7.4	8.1	7.4	7.9	7.5	7.7
B	7.3	8.0	6.8	7.5	7.5	7.3	6.8	7.5	7.3
C	8.2	8.6	8.8	8.3	8.0	8.3	8.8	8.1	8.4
D	8.2	8.3	7.3	7.3	8.5	8.8	7.5	7.3	7.9
E	7.3	7.9	8.1	7.8	7.4	8.2	8.2	7.7	7.8
	Overall								**7.8**
28 Day Test									
A	20.8	19.8	21.2	19.1	20.6	19.9	20.9	19.2	20.2
B	19.4	21.0	18.4	20.4	20.0	19.7	18.7	20.0	19.7
C	21.7	21.8	23.7	22.0	21.3	21.8	22.7	20.9	22.0
D	20.9	21.6	20.1	18.7	21.2	22.9	19.1	19.2	20.5
E	20.7	21.4	20.6	21.5	20.5	21.0	21.3	21.2	21.0
	Overall								**20.7**
56 Day Test									
A	48.3	47.6	43.8	41.7	45.7	44.7	41.6	41.7	44.4
B	41.0	39.9	41.1	41.6	41.2	49.0	39.8	42.3	42.0
C	39.2	43.2	39.3	39.8	39.4	44.4	40.1	41.8	40.9
D	43.8	45.6	49.8	46.3	44.9	45.9	46.9	50.1	46.7
E	42.4	45.8	45.7	43.6	44.1	45.8	45.4	45.9	44.8
	Overall								**43.8**
91 Day Test									
A	59.8	60.9	58.0	52.9	62.2	60.8	52.4	52.6	57.5
B	51.0	53.5	53.8	55.8	51.7	51.0	52.6	54.7	53.0
C	49.8	54.5	51.6	50.8	22.2	54.4	50.6	54.9	48.6
D	57.7	59.1	59.5	61.4	57.8	58.3	61.5	61.0	59.5
E	55.4	59.8	58.9	59.9	55.8	59.9	58.3	57.7	58.2
	Overall								**55.4**
182 Day Test									
A	102.4	98.5	90.8	91.7	105.1	98.7	90.6	92.1	96.2
B	87.2	82.7	84.3	87.3	86.1	80.4	84.6	87.6	85.0
C	74.2	82.3	78.4	80.8	74.2	84.0	80.8	85.7	80.1
D	96.2	94.2	93.7	97.0	93.6	97.4	91.6	97.2	95.1
E	94.3	98.8	90.2	96.3	94.9	94.7	89.8	95.3	94.3
	Overall								**90.1**
364 Day Test									
A	134.8	148.6	159.3	161.2	137.9	144.6	148.9	156.1	148.9
B	161.1	157.4	156.9	157.0	154.9	163.4	157.4	158.4	158.3
C	97.9	98.9	103.3	121.7	104.3	102.9	102.8	123.6	106.9
D	148.9	139.2	148.6	144.0	146.1	135.0	149.2	139.3	143.8
E	165.6	160.2	155.4	158.0	163.9	146.9	150.9	163.0	158.0
	Overall								**143.2**

APPENDIX D

Shrinkage Readings

Table D.1 Small Prism Sample Shrinkage Results

Specimen Age (Days)	Shrinkage (%)				
	Curing Types				
	12SM	18SM	24SM	24SD*	MC
28	0.0041	0.0055	0.0014	0.0089	0.0010
35	0.0050	0.0093	0.0024	0.0105	0.0013
42	0.0071	0.0106	0.0027	0.0124	0.0041
49	0.0094	0.0183	0.0038	0.0151	0.0141
56	0.0216	0.0280	0.0049	0.0179	0.0183
63	****	0.0291	****	0.0188	0.0265
70	****	0.0294	****	0.0197	****
77	****	****	****	0.0196	****
84	****	****	****	****	****
91	0.0310	****	****	****	****
98	0.0331	****	0.0149	****	****
105	0.0351	****	0.0120	****	0.0272
112	0.0419	0.0303	0.0110	****	0.0409
119	0.0443	0.0366	0.0093	0.0217	0.0470
126	0.0484	0.0377	0.0131	0.0265	0.0558
133	0.0495	0.0274	0.0172	0.0306	0.0521
140	0.0515	0.0305	0.0202	0.0374	0.0541
147	0.0413	0.0326	0.0264	0.0408	0.0572
154	0.0474	0.0366	0.0295	0.0429	0.0562
161	0.0525	0.0387	0.0336	0.0470	0.0582
168	0.0556	0.0417	0.0377	0.0490	0.0613
175	0.0576	0.0458	0.0397	0.0521	0.0654
182	0.0566	0.0479	0.0418	0.0541	0.0674
189	0.0607	0.0509	0.0469	0.0572	0.0695
196	0.0505	0.0469	0.0489	0.0593	0.0725

Table D.1: Small Prism Sample Shrinkage Results (cont.)

Specimen Age (Days)	Shrinkage (%)				
	Curing Types				
	12SM	18SM	24SM	24SD*	MC
203	0.0474	0.0571	0.0418	0.0623	0.0766
210	0.0495	0.0601	0.0448	0.0603	0.0725
217	0.0417	0.0642	0.0500	0.0685	0.0594
224	0.0484	0.0581	0.0520	0.0726	0.0562
231	0.0578	0.0540	0.0541	0.0521	0.0671
238	0.0372	0.0509	0.0561	0.0278	0.0644
245	0.0556	0.0612	0.0582	0.0316	0.0623
252	0.0437	0.0581	0.0551	0.0254	0.0509
259	0.0514	0.0755	0.0592	0.0378	0.0489
266	0.0546	0.0724	0.0612	0.0490	0.0511
273	0.0587	0.0663	0.0653	0.0313	0.0633
280	0.0535	0.0571	0.0582	0.0483	0.0654
287	0.0566	0.0673	0.0602	0.0511	0.0664
294	0.0550	0.0683	0.0643	0.0541	0.0653
301	0.0587	0.0734	0.0684	0.0572	0.0623
308	0.0617	0.0775	0.0715	0.0552	0.0633
315	0.0524	0.0816	0.0694	0.0534	0.0641
322	0.0556	0.0775	0.0725	0.0562	0.0674
329	0.0607	0.0816	0.0766	0.0603	0.0664
336	0.0575	0.0795	0.0797	0.0582	0.0572
343	0.0597	0.0898	0.0828	0.0674	0.0593
350	0.0587	0.0949	0.0807	0.0695	0.0562
357	0.0604	0.0979	0.0838	0.0648	0.0613
364	0.0607	0.0938	0.0889	0.0682	0.0602

Table D.2 Predicted Shrinkage for Small Prism Samples

	Predicted Shrinkage (microstrain)				
Age (Days)	**12SM**	**18SM**	**24SM**	**24SD**	**MC**
28	142	75	62	109	165
35	170	94	78	132	197
42	196	113	94	154	227
49	220	131	109	175	255
56	243	150	125	195	280
91	334	168	218	214	304
98	349	186	234	233	418
105	363	295	249	250	433
112	376	313	265	339	447
119	389	331	281	351	461
126	401	348	296	364	474
133	412	366	312	375	486
140	423	384	327	387	497
147	433	401	343	398	508
154	443	419	358	408	519
161	452	436	374	418	529
168	461	454	390	428	538
175	470	471	405	438	547
182	478	488	421	447	556
189	486	505	436	456	564
196	493	523	452	464	572
203	500	540	468	472	580
210	507	557	483	480	587
217	514	574	499	488	594
224	520	591	514	496	601
231	526	607	530	503	608
238	532	624	545	510	614
245	537	641	561	517	620
252	543	658	577	523	626
259	548	674	592	530	632
266	553	691	608	536	637
273	558	707	623	542	642
280	563	724	639	548	647
287	567	740	655	554	652
294	572	756	670	559	657
301	576	773	686	565	662
308	580	789	701	570	666
315	584	805	717	575	671
322	588	821	732	581	675
329	592	837	748	585	679
336	596	853	764	590	683
343	599	869	779	595	687
350	603	885	795	600	690
357	606	901	810	604	694
364	609				

Table D.3: Actual Shrinkage for Small and Large Piles (microstrain)

	14"x14"x6' Pile				24"x24"x6' Pile			
Age (Days)	MC	12SM	18SM	24SM	MC	12SM	18SM	24SM
28	33	41	67	20	34	26	73	110
35	80	72	131	445	104	89	87	183
42	178	194	165	721	148	111	189	279
49	230	369	292	972	375	238	315	488
56	128	307	110	837	248	193	202	446
91	404	418	256	1026	303	234	232	530
98	379	332	197	795	268	232	400	440
105	430	404	296	947	370	355	516	556
112	459	556	402	1236	523	514	665	698
119	468	585	374	1193	516	422	564	707
126	239	278	185	577	265	183	267	333
133	439	512	258	1072	438	285	415	589
140	565	621	354	1376	557	549	535	769
147	344	371	170	816	393	244	326	462
154	526	631	310	1376	648	426	730	744
161	480	542	352	1204	542	388	568	613
168	530	495	352	1094	459	350	557	602
175	678	597	439	1271	513	433	600	674
182	399	402	285	1180	483	349	630	568
189	313	496	276	1084	395	388	372	474
196	432	616	214	1069	458	387	536	401
203	309	335	167	643	246	243	240	377
210	452	501	244	1045	403	393	345	588
217	483	423	192	1043	401	444	206	525
224	400	535	219	1096	511	543	334	386
231	518	667	354	1081	315	641	476	343
238	501	570	262	922	232	558	426	215
245	454	457	195	946	261	433	470	234
252	339	523	345	861	316	396	410	384
259	397	386	202	849	472	442	304	371
266	376	469	345	808	464	439	290	383
273	459	573	389	973	553	529	353	453
280	424	628	423	996	579	583	412	491
287	304	486	328	748	443	484	301	393
294	426	646	451	986	606	638	432	522
301	435	654	452	992	707	683	488	559
308	373	535	388	799	576	550	415	484
315	483	679	510	1056	617	623	565	630
322	524	718	554	1110	654	661	656	599
329	558	751	598	1137	609	630	634	622
336	555	749	610	1145	603	632	643	624
343	604	855	729	1308	717	751	754	725
350	612	863	681	1313	729	755	774	746

Table D.4: Predicted Shrinkage for Small Piles (microstrain)

Age (Days)	12S	18S	24S	MC
28	151	52	568	163
35	182	65	634	191
42	210	77	687	216
49	236	89	731	238
56	261	102	767	258
91	361	161	887	331
98	378	172	903	342
105	393	184	918	353
112	408	195	931	362
119	422	206	942	371
126	436	217	953	379
133	448	228	963	387
140	460	238	972	394
147	472	249	980	401
154	483	260	988	407
161	493	270	995	413
168	503	280	1002	419
175	513	291	1008	424
182	522	301	1014	429
189	531	311	1019	434
196	539	321	1024	439
203	547	330	1029	443
210	555	340	1033	447
217	562	350	1037	451
224	569	359	1041	455
231	576	369	1045	458
238	583	378	1049	462
245	589	387	1052	465
252	596	397	1055	468
259	602	406	1058	471
266	607	415	1061	474
273	613	424	1064	477
280	618	433	1067	479
287	624	441	1069	482
294	629	450	1072	484
301	633	459	1074	486
308	638	467	1076	489
315	643	476	1079	491
322	647	484	1081	493
329	652	492	1083	495
336	656	500	1084	497
343	660	509	1086	499
350	664	517	1088	501

Table D.5: Predicted Shrinkage for Large Piles (microstrain)

Age (Days)	12SM	18SM	24SM	MC
28	81	182	305	138
35	100	212	337	165
42	119	238	363	190
49	137	261	384	214
56	155	282	401	235
91	238	356	455	322
98	253	368	463	336
105	269	378	469	349
112	283	387	475	362
119	298	396	480	373
126	312	404	485	385
133	326	412	489	395
140	340	419	493	405
147	353	425	497	415
154	366	432	500	424
161	379	437	503	433
168	392	443	506	441
175	404	448	509	449
182	416	453	511	456
189	428	457	513	463
196	440	462	516	470
203	451	466	518	477
210	463	470	520	483
217	474	473	521	489
224	485	477	523	495
231	495	480	525	501
238	506	484	526	506
245	516	487	528	511
252	526	490	529	516
259	536	492	530	521
266	546	495	532	526
273	555	498	533	530
280	565	500	534	534
287	574	502	535	539
294	583	505	536	543
301	592	507	537	547
308	601	509	538	550
315	610	511	539	554
322	618	513	540	558
329	627	515	541	561
336	635	517	542	564
343	643	519	542	568
350	651	520	543	571

Table D.6: ACI Shrinkage Strain Prediction (Eqs. 2.1 and 2.2), microstrain

Without Humidity Correction				With Humidity Correction		
Age (Days)	Moist Curing	Steam Curing	Humidity Factor	Age (Days)	Moist Curing	Steam Curing
28	356	270	0.63	28	224	170
35	400	311	0.68	35	274	213
42	436	346	0.81	42	354	281
49	467	377	1.00	49	467	377
56	492	404	0.73	56	358	293
91	578	499	0.82	91	472	407
98	589	512	0.62	98	366	318
105	600	525	0.80	105	480	420
112	610	537	1.00	112	610	537
119	618	547	0.97	119	602	533
126	626	557	0.45	126	280	249
133	633	566	0.78	133	492	440
140	640	574	1.00	140	640	574
147	646	582	0.56	147	364	328
154	652	589	1.00	154	652	589
161	657	596	0.88	161	580	526
168	662	603	0.83	168	549	499
175	667	609	1.00	175	667	609
182	671	614	0.94	182	632	579
189	675	620	0.86	189	581	533
196	679	625	0.89	196	606	558
203	682	629	0.56	203	382	353
210	686	634	0.99	210	676	625
217	689	638	0.75	217	518	480
224	692	642	0.78	224	540	501
231	695	646	0.86	231	596	554
238	697	650	0.74	238	516	480
245	700	653	0.77	245	536	500
252	702	657	0.79	252	552	516
259	705	660	0.74	259	521	488
266	707	663	0.69	266	486	455
273	709	666	0.79	273	562	527
280	711	669	0.79	280	562	528
287	713	671	0.59	287	420	395
294	715	674	0.76	294	546	515
301	717	676	0.74	301	529	499
308	718	679	0.59	308	424	400
315	720	681	0.74	315	532	504
322	722	683	0.77	322	552	523
329	723	685	0.77	329	555	526
336	725	687	0.74	336	537	510
343	726	689	0.83	343	602	572
350	727	691	0.81	350	586	557
357	729	693				
364	730	695				

REFERENCES

AASHTO T 277. "Standard Method of Test for Rapid Determination of the Chloride Permeability of Concrete." American Association of State Highway and Transportation Officials, Washington, DC (1983).

ACI Committee 234 Report. "Guide for the Use of Silica Fume in Concrete," *ACI Manual of Concrete Practice: Materials and General Properties of Concrete (Part 1)*: 234R1 - 234R51 (1997). American Concrete Institute. Farmington Hills, MI.

ACI Committee 308 Report. "Standard Practice for Curing of Concrete," *ACI Manual of Concrete Practice: Construction Practices and Inspection Pavements (Part 2):* 308-1 - 308-11 (2000). American Concrete Institute, Farmington Hills, MI.

ACI Committee 363 Report. "High Strength Concrete," *ACI Manual of Concrete Practice: Materials and General Properties of Concrete (Part 1):* 363R1 - 363R55 (1997). American Concrete Institute, Farmington Hills, MI.

ACI Committee 517.2 Report. "Accelerated Curing of Concrete at Atmospheric Pressure - State of the Art." *ACI Manual of Concrete Practice*. American Concrete Institute (1992). Farmington Hills, MI.

Alampalli, S. and Owens, F. "In-Service Performance of High-Performance Concrete Bridge Decks." *New York State Department of Transportation Research Record* No. 580121 (1996): 193 - 196.

Alexander, M.G. and Magee B. J. "Durability Performance of Concrete Containing Condensed Silica Fume." *Cement and Concrete Research* 29 (1999): 917-922,

ASTM. *Designation*: C 39. *Standard Test Method for Compressive Strength of Cylindrical Concrete Specimens*. Philadelphia, PA (2003).

ASTM. *Designation:* C 127. *Standard Test Method for Density, Relative Density (Specific Gravity), and Absorption of Coarse Aggregate.* Philadelphia, PA (2001)

ASTM. *Designation*: C 128. *Standard Test Method for Density, Relative Density (Specific Gravity), and Absorption of Fine Aggregate.* Philadelphia, PA (1997)

ASTM. *Designation*: C 143. *Standard Test Method for Slump of Portland Cement Concrete*. Philadelphia, PA (2003).

ASTM. *Designation*: C 157. *Standard Test Method for Length Change of Hardened Hydraulic Cement Mortar and Concrete*. Philadelphia, PA (2003).

ASTM. Designation: C 173. *Standard Test Method for Air Content of Freshly Mixed Concrete by the Volumetric Method.* Philadelphia, PA (2003).

ASTM. *Designation*: C 192. *Standard Practice for Making and Curing Concrete Test Specimens in the Laboratory.* Philadelphia, PA (2001).

ASTM. *Designation*: C 231. *Standard Test Method for Air Content of Freshly Mixed Concrete by the Pressure Method.* Philadelphia, PA (2003).

ASTM. *Designation*: C 403. *Standard Test Method for Time of Setting of Concrete Mixtures by Penetration Resistance.* Philadelphia, PA (1999).

ASTM. *Designation*: C 490. *Standard Practice for Use of Apparatus for the Determination of Length Change of Hardened Cement Paste, Mortar, and Concrete*. Philadelphia, PA (2000).

ASTM. *Designation*: C 167. *Standard Practice for Capping Cylindrical Concrete Specimens*. Philadelphia, PA (1998).

ASTM. *Designation*: C 684. *Standard Test Method for Making, Accelerated Curing, and Testing Concrete Compression Test Specimens*. Philadelphia, PA (1999).

ASTM. *Designation*: C 1064. *Standard Test Method for Temperature of Freshly Mixed Portland Cement Concrete.* Philadelphia, PA (1999).

ASTM. *Designation*: C 1202. *Standard Test Method for Electrical Indication of Concrete's Ability to Resist Chloride Ion Penetration*. Philadelphia, PA (1997).

ASTM. *Designation*: C 1240. *Standard Specification for Silica Fume for Use as a Mineral Admixture in Hydraulic Cement Concrete, Mortar, and Grout.* Philadelphia, PA (2003).

Ayers, M.E. and Khan, M.S. "Overview of Fly Ash and Silica Fume Concrete: The Need for Rational Curing Standards." *Proceedings* of V. Mohan Malhotra Symposium, "Concrete Technology: Past, Present, and Future," SP-144, pp. 605-622. Farmington Hills, MI (1994)

Barr, B., Hoseinian, S.B., and Beygi, M.A. "Shrinkage of Concrete Stored in Natural Environments." *Cement and Concrete Composites* 25 (2003): 19 - 29.

Bhanja, S. and Sengupta B. "Modified Water-cement Ratio Law for Silica Fume Concretes." *Cement and Concrete Research* 33 (2003): 447 - 450.

Branson, D.E. *Deformation of Concrete Structures*. New York: McGraw-Hill International Book Co. (1977).

Broomfield, J. and Millard, S. "Measuring Concrete Resistivity to Assess Corrosion Rates." *Concrete* 36.2 (2002): 37-39.

Byfors, K. "Influence of Silica Fume and 114 sh on Chloride Diffusion and pH Values in Cement Pastes." *Cement and Concrete Research* 17 (1987): 115-130.

Cement Association of Canada. "Autoclave Steam Curing and Atmospheric Steam Curing." (2004).

Chini, A.R., Muszynski, L.C., and Hicks, J. and "Determination of Acceptance Permeability Characteristics for Performance-Related Specifications for Portland Cement Concrete." *Florida Department of Transportation Research* No. BC 354-41. Florida: University of Florida (2003).

Ewins, A.J. "Resistivity Measurements in Concrete." *British Journal of Non-Destructive Testing* 32.3 (1990): 120-126

Florida Department of Transportation. "Standard Specifications for Road and Bridge Construction." Tallahassee, Florida. (2004)

Holland, T.C. "Working with Silica Fume in Ready-Mixed Concrete: U.S.A Experience." *Proceedings*, 3rd International Conference, Fly Ash, Silica Fume, Slag, and Natural Pozzolans in Concrete, SP-114, Vol. 2, pp. 763-781. Farmington Hills, MI (1989).

Holland, T.C. "Benefits of Silica Fume in HPC." *Silica Fume Association* 16 July/August 2001: 5.

Hooton, R.D. "Influences of Silica Fume Replacement of Cement on Physical Properties and Resistance to Sulfate Attack, Freezing and Thawing and Alkali-Silica Reactivity." *ACI Materials Journal* 90 (1993): 143-151.

Huang, C. and Feldman, R.F. "Influence of Silica Fume on the Microstructural Development in Cement Mortars." *Cement and Concrete Research* 15 (1985): 285 - 294.

Kojundic, T. "High Performance (HP) Concrete Flexes its Muscles." *Roads and Bridges Magazine* April 1997.

Kosmatka, S.H. and Panarese, W.C. Design and Control of Concrete Mixtures. 13th e.d. Portland Cement Association, 1994.

Langan, B.W., Weng K., and Ward, M.A. “Effect of Silica Fume and Fly Ash on Heat of Hydration of Portland Cement.” *Cement and Concrete Research* 32 (2002): 1045-1051

Mazloom, M., Ramezanianpour, A.A., Brooks, J.J. “Effect of Silica Fume On Mechanical Properties of High Strength Concrete.” *Cement & Concrete Composites* 26 (2003): 347-357

Mehta, P.K. and Gjørv, O.E. “Properties of Portland Cement on Concrete Containing Fly Ash and Condensed Silica fume.” *Cement and Concrete Research* 12 (1982): 587 - 595.

Millard, S.G. “Reinforced Concrete Resistivity Measurements Techniques.” Proc. Instn. Civ. Engrs, Part 2 91.3 (1991): 71-88.

Morris, W., Moreno, E.I., and Sagues, A.A. “Pratical Evaluation of Resistivity of Concrete in Test Cylinders Using a Wenner Array Probe.” *Cement and Concrete Research* 26 (1996): 1779-1787.

Nawy, E.G. *Prestressed Concrete: A Fundamental Approach*. 4th ed. New Jersey: Prentice Hall, 2002.

Ozyildirim, C. “Concrete Bridge-Deck Overlays Containing Silica Fume,” CANMET/ACI International Workshop on the Use of Silica Fume in Concrete, April 7- 9, 1991, Washington, DC, V.M. Malhotra, Ed., pp. 305-312.

PCI Committee on Durability. “Guide to Using Silica Fume in Precast/Prestressed Concrete Products.” *PCI Journal* 39 (1994): 36-46

Pennsylvania State University. Department of Civil and Environmental Engineering and Instructional Systems Concrete Clinic. “Curing Concrete in Normal, Hot, and Cold Weather.” (1999).

Polder, R.B. “Test Methods of on Site Measurement of Resistivity of Concrete - a RILEM TC-154 Technical Recommendation.” *Construction and Building Materials* 15 (2001): 125-131.

Rocole, L. “Silica Fume Concrete Proves to be and Economical Alternative.” *Concrete Construction*. The Aberdeen Group, June 1993.

Savas, B.Z. “Effects of Microstructure on Durability of Concrete.” Raleigh, NC: North Carolina Sate University Department of Civil Engineering. (1999)

Scali, M.J., Chin, D., and Berke, N.S. "Effect of Microsilica and Fly Ash upon the Microstructure and Permeability of Concrete." *Proceedings*, 9th International Conference on Cement Microscopy, pp. 375-387. Duncanville, TX: International Cement Microscopy Association (1987).

Sellevold, E. J. and Nilsen, T. "Condensed Silica Fume in Concrete: A World Review." *Supplementary Cementing Materials for Concrete* 1987: 165-243.

Shannag, M.J. "High Strength Concrete Containing Natural Pozzolan and Silica Fume." *Cement and Concrete Composites* 22 (2000): 399-406.

Wee, T.H., Suryavanshi, A.K., and Tin, S.S. "Evaluation of Rapid Chloride Permeability Test (RCP) Results for Concrete Containing Mineral Admixtures." *American Concrete Institute Materials Journal* 97 (2000): 221-232.

Thelend, D. "The Make-or-Break Process: With and Eye on the Bottom Line, the Producer Increasingly is Trying to Optimize the Curing Process." *The Concrete Producer* July 2003.

Toutanji, H.A. and Bayasi, Z. "Effect of Curing Procedures on Properties of Silica Fume Concrete." *Cement and Concrete Research* 29 (1999): 497-501.

Toutanji, H. A. and El-Korchi, T. "Tensile and Compressive Strength of Silica Fume Cement Pastes and Mortars." *Cement, Concrete, and Aggregates* 18 (1996): 78-84.

Vieira, M., de Almeida, I.R., and Gonclaves, A.F. "Influence of Moisture Curing on Durability of Fly Ash Concrete for Road Pavement." In V.M. Malhorta (Ed.), *Durability of Concrete* (2000): 91-102

Wang, C.K. and Salmon, C.G. *Reinforced Concrete Design.* 6th ed. New Jersey: Wiley Textbooks, 1998.

Yazdani, N., "Time Dependent Strength and Elasticity Development in Florida Concrete." Final Report, FDOT Contract No. BD-221, *FAMU-FSU College of Engineering.* Tallahassee, FL. (2001).

Zhang, M.H., Tam, C.T., and Leow, M.P. "Effect of Water-to-Cementitious Materials Ratio and Silica Fume on the Autogenous Shrinkage of Concrete." *Cement and Concrete Research* 33 (2003): 1687-1694.